Accretion Discs around Magnetised Stars, in particular Neutron Stars

by

Solomon Belay Tessema

A Dissertation Submitted to the
Department of Physics Addis
Ababa University

in partial fulfillment of
the requirements of for the Degree of
Doctor of Philosophy in Physics

February, 2010
Addis Ababa, Ethiopia

ADDIS ABABA UNIVERSITY

DEPARTMENT OF PHYSICS

Accretion Discs around Magnetised Stars, in particular Neutron Stars

by

Solomon Belay Tessema

Approved by the Examination Committee:

Dr. Mulugeta Bekele Chairman ———————————

Prof. Jonathan Ferreira External Examiner ———————————

Prof. V.N. Malnev Internal Examiner ———————————

Dr. Ulf Torkelsson Research Advisor ———————————

Abstract

We develop a self-consistent theoretical model for the steady-state of an axisymmetric thin accretion disc with an internal dynamo around a magnetised stars. Starting from the vertically integrated equations of magnetohydrodynamics we derive a single ordinary differential equation for a thin accretion disc around a massive magnetic dipole and based on the analytical formulation we integrate this equation numerically from the outside inwards. Our numerical solution shows that the torque between the star and the accretion disc is dominated by the contribution from the dynamo in the disc. We extend this model for weak magnetic fields and we present millisecond x-ray pulsars have weak magnetic dipole moments of $\sim 10^{16}\,\mathrm{T\,m^3}$ compared to ordinary X-ray pulsars with dipole moments of $10^{20}\,\mathrm{T\,m^3}$. For this reason a surrounding accretion disc can extend closer to the neutron star, and thus reach a higher temperature, at which the opacity is dominated by electron scattering and radiation pressure is strong. We compute the self-similar structure of such a geometrically thin axisymmetric accretion disc with an internal dynamo for the three regions of the disc. For the outer disc region which corresponds to the gas pressure and Kramer's opacity dominated, in the middle region the gas pressure and electron scattering dominated , in the inner region the radiation pressure and electron scattering dominated accretion disc. Our numerical solution shows that the torque between the star and the accretion disc is dominated by the coupling between the stellar magnetic field and the dynamo in the disc. Finally, we have developed that the time-dependent equations for an accretion disc and linear stability analysis of steady-state disc solutions in the presence of a strong external magnetic field. The analytical and numerical analysis of the solutions to the stability properties and time evolution will tell us the observed behaviours of the torque between the disc and the star.

Key words: accretion, accretion discs - magnetohydrodynamics (MHD) - magnetic fields - stars: neutron X-rays: binaries- pulsars: general

Dedication

For the souls of all innocents of African people who were devoted their life, money and time to bring Universal Freedom, democracy, Justice and development in Africa.

Acknowledgments

I can say without exaggeration that the completion of this PhD has been the most difficult challenge that I have ever undertaken in my career. It would have not totally remotely possible without the support of my supervisor, collaborators, departments and my wonderful friends and families.

Firstly I would like to thank my supervisor, Ulf Torkelsson, for all of the encouragement, support, devotion of his time, energy and insight over the past four years, for guiding me the path of research that ultimately led to this thesis. Particularly for his immediate response and support while I was in miserable and obstaculum conditions of finding appropriate supervisor and continuous assistance.

I would like to thank Swedish Institute (SI) for one year research grant under the Guest scholarship program during my research work in Sweden at University of Gothenburg. I would also like to thank the University of Gothenburg, Department of Physics for its support in all facilities and the working conditions it provided me. But all these facilities and favorable working conditions have not been realized without kind hospitality, support and cooperation of the staff members of the department. I never for get my colleagues, particularly PhD students at the department of physics and the community at the University of Gothenburg.

I would like to thank Addis Ababa University, Department of Physics for this research opportunity it has provided me. I extend my thanks to the Head department of Physics, Dr. Gizaw Mengistu and other staff members in facilitating academic and administrative affairs for my thesis work. Many thanks to Ms Tselat, secretary of the Physics department, for kindness and cooperativeness.

I am also very grateful to my PhD Sponsorship, Kotebe College of Teacher Education.

I would like grateful to Tolu Biressa my PhD colleague at AAU, department of Physics, in Astrophysics. He is my true friend that I will never for get at any time any where. I never for get the ups and downs we have faced and passed in the last four years in our work. The frequent

discussions regarding our research, about our life, solving our daily problems, the dedication and commitment in popularizing Astronomy in Ethiopia remain memorable. I would like to extend my gratitude to AAU President's Office, Office of the Graduate Studies and Research.

I would like to thank Mr. Tefera Walwua, Minister of Capacity Building and Chairperson of Ethiopian Space Science Society Director's Board, Dr. Hirut W/mariam, Vice President of AAU, Dr. Hirut Terefe, Director, institute of Gender studies for their strong support and encouragements during my difficult time in finding my thesis supervisor.

Most of all, I would like to express my gratitude to my wife Yalemtesfa Nigat and my mother Yeshi Seyoum for their grate patience, continual encouragement and endless love and support through all the ups and downs of the last a few years. And finally, I have my deepest gratitude to all of my families and friends for constant and encouragement.

This research has made use of NASA's Astrophysics Data System.

Solomon Belay Tessema

Addis Ababa University,

Department of Physics,

Addis Ababa, Ethiopia.

List of Publications

This thesis is based on the following publications, which are referred to in the next by their Roman numerals.

I "The structure of thin accretion discs around magnetised stars"

S. B. Tessema, and **U. Torkelsson**, *Astronomy & Astrophysics*, 509, A45 (2010)

II "Thin accretion discs around millisecond X-ray pulsars"

S.,Tessema, and **U. Torkelsson**, submitted (and reviewed) to *Monthly Notices of the Royal Astronomical Society*, MN-10-0535-MJ, (2010)

III "Time-dependent accretion discs around magnetized stars"

S.,Tessema, and **U. Torkelsson**, in preparation for *The Monthly Notices of the Royal Astronomical Society Journal*

Contents

List of Figures

List of Tables

Chapter 1

General Introduction

1.1 X-ray binaries

One of the major developments in the mid-twentieth-century stellar astrophysics was the understanding that there is often a *third object* in a close binary star system, especially in a system undergoing mass transfer. Matter from one star swirls around the other forming a configuration known as an accretion disc. According to theoretical model, the gas will spiral in and fall to the surface of the compact object, creating a flow of matter in the shape of a disc-an accretion disc. Such discs were first recognized in the study of cataclysmic variables, close systems in which one of the stars is a white dwarf. With the advent of X-ray astronomy, it became clear that accretion discs play a prominent role in binary systems containing neutron stars or black holes. In many cases, the accretion disc is the primary source of radiation; in particular X-ray radiation; and sometimes, the disc channels matter into streams of outgoing material and energy, jets.

The matter in the accretion disc in general performs a Keplerian motion around the accreting object, that is it is held in place by the balance between gravity and the centrifugal force. If this was all there was, nothing would ever happen in an accretion disc, the matter would just go on revolving around the accreting star forever, but there is always some viscosity in the disc. The effect of the viscosity is to remove some angular momentum from each gas element and transfer it to a gas element further out. The first gas element will then move a bit closer to the accreting object, as its new angular momentum corresponds to a smaller orbit. Finally the gas element falls down, is accreted, onto the central object. During the process the accretion disc is heated by the release of potential energy, which it radiates away.

We can say accretion discs are ubiquitous in astrophysics. They appear in interacting binaries in which the tidal forces from one of the stars, usually a compact object such as a white dwarf, a neutron star or a black hole, forces matter to stream over from the surface of the companion star, but in general this matter has too much angular momentum to settle directly onto the surface of the accreting star, and it forms rather an accretion disc around the accreting star. The matter in this disc is supported against the gravitational field by its Keplerian rotation, but some form of anomalous viscosity acts in the disc, and transports the angular momentum outwards such that the disc material gradually drifts inwards and eventually settles onto the accreting star. During this process half of the potential energy of the matter goes into heating the accretion disc. An accretion disc around a neutron star or a stellar-mass black hole reaches a temperature of several million degrees and becomes an X-ray emitter. As a matter of fact, in these cases the accretion disc is more efficient in converting rest-mass to energy than nuclear fusion. Accretion discs appear also around newly forming stars and around the super-massive black holes in active galactic nuclei. The reason for this is that also in those cases do we have a central gravitating mass which is accreting surrounding gas that has a net angular momentum.

The understanding of accretion discs is still in a somewhat crude state. The situation is analogous to the early days of stellar evolution when there was an understanding of the balance between pressure and gravity, but the power source of stars was not known.

The central problem in accretion disc theory has been to explain the anomalous viscosity, which is usually attributed to turbulence in the disc, but it is trivial to show that a hydrodynamic disc in Keplerian rotation is stable towards axisymmetric perturbations, and there does not appear to be any form of linear instability that could develop into turbulence (Balbus & Hawley 1991; Balbus & Hawley 1998) showed though that a disc with a vertical magnetic field is linearly unstable and subsequent numerical simulations (e.g. Hawley, Gammie & Balbus 1995, Brandenburg et al. 1995) showed that this turbulence can transport the angular momentum outwards, and it is now commonly accepted that the accretion is driven by magnetohydrodynamic turbulence. The magnetic field derives energy from the rotation of the accretion disc, and feeds this energy into the turbulence. The turbulence in its turn is heating the disc, but it is also re-generating the magnetic field. A self-consistent solution of the disc equations requires that the turbulent viscosity is related to the physical state of the disc.

1.2 Standard model of accretion disc

The modern theory of accretion discs can be traced back more or less directly to Kuiper's remarkable paper (1941) on contact binary systems (two stars sharing a common gaseous envelope). Kuiper studied the properties of the gas stream that was induced by the tidal forces to flow from one star to the other. He was particularly intrigued by the "curious result" that it seemed to form a ring around the accreting star. This makes accretion discs one of a handful of astrophysical objects whose existence was deduced theoretically well in advance of observational discovery. Some other examples of objects that were predicted theoretically before they were discovered neutrons and black holes. Several important papers from this era (Crawford and Kraft, 1956) show an understanding of Kuiper's results and appeal to them as support for what would now be referred to as disc-based accretion. Yet, when compact X-ray sources were discovered in the 1960s and were identified with binary stars, the realization that a disc must form during the mass transfer process required renewed appreciation(Prendergast and Burbidge, 1968). Thus the detailed study of the physics of accretion did not begin in earnest until later in that decade,when Lynden-Bell put forth his disc/black-hole model as the central power source for quasars (1969). In turn, this laid the ground work for the accretion discs formulated by Shakura and Sunyaev (1973) and Lynden-Bell and Pringle(1974).

The well known and most widely used standard model of the accretion disc was proposed and formulated by Shakura and Sunyaev (1973). The disc is thin, the scale height of the disc being much less than its radial length scale. The self-gravity of the disc was ignored and the radial component of the pressure gradient is small relative to the stellar radial gravity; the angular velocity is therefore Keplerian, except close to the stellar surface where a boundary layer forms; turbulent viscosity is invoked in the Shakura - Sunyaev model to explain the angular momentum transfer required by the accretion flow. They were able to obtain an analytical solution of the height integrated hydrodynamic equations, after having introduced the α-prescription for the turbulent stress, which transports the angular momentum outwards through the disc. Their model has acted as a basis for subsequent disc investigations. The central problem of accretion disc theory has been to understand how the discs accrete. In principle, the presence of shear viscosity allows the transfer of angular momentum from one fluid element to another, but, the needed accretion rates are orders of magnitude higher than the standard microscopic viscosities (Spitzer, 1962) could provide. If, on the other hand, the disc was for some reason turbulent, the effective viscosity due to interacting eddies could be large enough to provide the needed viscosity.

Since the fluid shear viscosity is small, the Reynolds number of astrophysical discs is very high. Ordinarily one would then expect the discs to be turbulent, but according to Rayleigh's criterion a fluid in Keplerian rotation, as it would be in a thin, disc is stable, and there is no obvious mechanism that would make the flow unstable. Rather Balbus and Hawley (1991) showed that it is unstable if there is a weak magnetic field in the disc. Subsequent numerical simulations (e.g. Hawley, Gammie and Balbus 1995 ; Balbus and Hawley 1998) confirmed that this instability generates turbulence and that the resulting turbulent stresses transport angular momentum outwards. As originally pointed out in Lynden-Bell (1969) and Shakura and Sunyaev (1973) a magnetic field can also contribute to the angular momentum transport. The Balbus- Hawley (magnetorotational) instability (Velikhov 1959; Chandrasekhar 1961) of weak magnetic fields in accretion discs drives MHD turbulence which transports angular momentum radially outwards (Balbus & Hawley 1991; Hawley & Balbus 1991; Stone et al. 1996), and is thought to play an important role in the evolution and dynamics of astrophysical accretion discs. The instability has also been invoked as a component of a disc dynamo model, in which the instability creates radial field from vertical field, the shear in the disc creates azimuthal field from the radial component, and the Parker instability creates vertical from azimuthal field and expels flux from the disc (Tout & Pringle 1992). A robust mechanism of the excitation of magnetohydrodynamic (MHD) turbulence was shown to operate in accretion discs due to the magneto-rotational (MRI) instability (Balbus & Hawley 1998). The growth of the MRI leads to the excitation of turbulent magnetic fields and self-sustained MHD turbulence. The contribution of Maxwell stresses to the transport of angular momentum is usually larger than Reynolds stresses. However, the magnetic energy observed in many numerical experiments was smaller than the thermal energy of the gas in the disc (Brandenburg, 1998). The magnetorotational instability (MRI) is believed to be responsible for turbulent motion and angular momentum transport in accretion discs, at least those that are sufficiently ionized (Balbus & Hawley 1991, 1998). In its simplest version it appears as a linear instability of a rotating shear flow in the presence of a uniform magnetic field (Velikhov 1959). The nonlinear outcome, at sufficiently large Reynolds and magnetic Reynolds numbers, is magnetohydrodynamic (MHD) turbulence (Hawley et al.1995). More importantly, the MRI is also believed to act as a dynamo in the accretion discs, meaning that the inductive effect of the motions driven by the instability is able to sustain the magnetic field against resistive decay and so to perpetuate, here we will not discuss more about MRI in this thesis.

1.2.1 X-Ray Pulsars

Accretion disc occur around strong magnetic stars in X-ray binary pulsars, magnetic white dwarfs, in cataclysmic variables, and T Tauri stars. The magnetic fields are important to angular momentum transport with in the disc. The interaction between a magnetized, rotating star and a surrounding accretion disc has been of continued interest since the discovery of X-ray pulsars in binary systems (Giacconi et al.1971). X-ray pulsars are rotating strongly magnetized neutron stars which accrete gas from a stellar companion. The gas is preferentially accreted at the magnetic poles of the neutron star, where most of the X-ray emission is consequently generated. Thus the observed X-ray flux is modulated on the spin period of the neutron star as the magnetic poles rotate into and out of our line of sight. Most importantly, this qualitative picture has become the paradigm for accretion onto other types of magnetic stars, such as magnetic CVs and T Tauri stars (Warner 1990, *Königl* 1991). In some sources, such as Her X-1, SMC X-1, and Cen X-3, it is clear that the in falling matter processed through an accretion disc around the pulsar (Nagase, F., 1989; Tjemkes et al 1986). In the case of accreting white dwarfs, there is direct observational evidence that the accretion disc it truncated in magnetised stars; in weakly magnetised systems such as DQ Her the disc extends inwards to a boundary layer, while in AM Her systems in which the white dwarf is known.
The Burst and Transient Source Experiment(BATSE) was a high energy astrophysics experiment on NASA satellite Compton Gamma-Ray Observatory. The primary objective of BATSE was to study gamma-ray bursts, although the detectors also recorded data from pulsars, terrestrial gamma-ray flashes, soft gamma-ray repeaters, black holes, and other transient exotic astrophysical objects. BATSE detected more than 50 outbursts from 12 transient X-ray pulsars in the first five years of operation (Bildsten et al. 1997).

The continuous monitoring of accretion-powered pulsars with BATSE/CGRO has also been used to obtain essentially daily measurements of spin frequencies of a number of the brightest X-ray pulsars. Some of these systems are known to possess accretion discs, although other objects in the group are accreting directly from a stellar wind.

The BATSE recorded the neutron star spin history over timescales from days to years. These timing observations are some of the best sources of information on, the interaction between an accretion disc and a magnetic accretor. Such time series are much easier to produce for neutron stars than for protostars or white dwarfs, because the neutron stars have comparatively small moments of inertia, and an X-ray pulsar can be timed accurately, thus the changes in spin

frequency are a good measure of the torque.

The most commonly studied systems are the Be/X-ray transients, which consist of a neutron star on an elliptic orbit around a Be-star. The neutron star can pick up a temporary accretion disc, which is gradually accreted onto the neutron star, as it gets close to the Be-star. One does find a correlation between the spin up of the X-ray pulsar and its X-ray flux, which is a measure of the accretion rate, as is expected from the Ghosh and Lamb model in these systems.

The BATSE experiment on the Compton Gamma-Ray Observatory made it possible to follow the spin evolutions of a large number of X-ray pulsars (Bildsten et al.1997), most of which were either Be/X-ray transients or wind-fed X-ray pulsars, that do not have any accretion discs at all, but there was also a small number of X-ray pulsars with permanent accretion discs. Most notably it was found that four of these sources 4U1626-67, GX 1+4, Cen X-3 and OAO 1657-415 are oscillating between spin-up and spin-down phases without any significant change in the X-ray flux. This behaviour is difficult to explain within the framework of the Ghosh and Lamb model, and different modifications of the standard model were suggested. Torkelsson (1998) pointed out that the Ghosh and Lamb model ignores the possibility of an internal dynamo in the accretion disc. Such a dynamo is a natural consequence of the magnetohydrodynamic turbulence in the accretion disc and would generate an extra magnetic field in the accretion disc. Since the co-rotation radius does not play a role in such a dynamo this magnetic could extert either a spin-up or a spin-down torque on the neutron star irrespective of the accretion rate, the torque reversals can be interpreted in terms of field reversals analogous to the magnetic field reversals that we see on the sun. He showed that the torque between an accretion disc and an accreting star can be enhanced by the presence of a dynamo-generated magnetic field in the accretion disc. He suggested that torque reversals can be explained by reversals of the magnetic field generated by a disc dynamo. However, Torkelsson did not construct a self-consistent model of the accretion disc. The aim of this thesis is therefore be to construct such a theoretical model which can be used as the basis for further analytical and numerical investigations. The model is be based on the standard assumptions for thin accretion discs, that is that $H(R) \ll R$, which leads to that $V_R \ll V_\phi$ and $V_\phi = V_{\rm Kepl}(R)$, where $V_{\rm Kepl}$ is the Keplerian velocity. Firstly I develop a stationary thin disc model of the accretion disc around a magnetized star including the effect of the magnetic field generated by an internal dynamo in the disk. I then develop a theory for the time-dependent behaviour of such discs. This theory gives us the tools to start exploring the stability properties of the disc, we analysis the time dependent equation of the disc in order

to understand the torque reversals of the X-ray pulsars and set mathematical frameworks for further numerical study.

1.2.2 Millisecond X-ray pulsars

Accreting millisecond pulsars (AMSPs) are a subset of neutron stars in low-mass X-ray binaries (LMXBs) that exhibit persistent X-ray pulsations with periods less than 10 ms (Alpar et al. 1982; Radhkrishnan and Srinivasan 1982) and weak magnetic field. It was first discovered ten years ago, which was a good confirmation of the theory of the production of millisecond radio-pulsars in the course of accretion. The discoveries of the Rossi X-ray Timing Explorer over past decade have greatly enhanced over understanding of low-mass-Xray binary. This growing class of objects provides a laboratory for an array of physics inaccessible anywhere else in the universe. Here we study the accretion discs around magnetised millisecond X-ray pulsars in the presence the magnetic field generated due to internal dynamo.

1.2.3 The magnetic field - disc interaction

The qualitative features of disc accretion by rotating magnetic neutron stars were first described by Pringle and Rees(1972) and Lamb, Pethick, and Pines(1973). These authors argued that a slowly rotating neutron star accreting matter from a Keplerian disk should spin up as a consequence of the torque exerted on the star by the accreting matter.

In spite of the early progress, interaction of the accretion disc with in the stellar magnetosphere is not yet well understood (Spruit and Taam, 1993). From a theoretical point of view, two kinds of models have been investigated. If the disc plasma is infinitely conductive, the surface currents on the disc will exclude the stellar magnetic field (Anzer and Börner,1980,1993; Arons et al., 1984; Aly,1986). However, Ghosh and Lamb (1979) pointed out that the stellar field is not completely excluded even from a disc with an infinite conductivity because of turbulent diffusion, magnetic field reconnection and Kelvin-Helmholz instabilities. This leads us to the second class of models, accretion disks with a finite resistivity so that the stellar magnetic field can diffuse into them. Only the later models have been developed in detail for comparison with observations. Ghosh and Lamb(1979a) showed that the stellar magnetic field penetrates a broad zone of the accretion disc. They presented solutions for the boundary layer, but instead of solving for the magnetic field in the disc given a certain magnetic diffusivity they assumed a magnetic field and solved for the diffusivity. Heptinstall and Campbell(1998) and Brandenburg

and Campbell(1998) obtained solutions for the magnetic, and velocity field in the disc given a certain model for the magnetic diffusivity.

Ghosh and Lamb(1979b) calculated the magnetic torque acting on the star by integrating over the surface of the disc. This is the most convenient approach, but it does not provide any information on how the torque is transferred to the star. The co-rotation radius, where the angular velocities of the disk and the star are the same, plays a key role in this model. The magnetic field that penetrates the disc inside the co-rotation radius, spin up the star, whilst that penetrating the accretion disc outside the co-rotation radius brakes the star. The spin evolution of the star is therefore the result of a balance between the angular momentum carried by the accreted matter from the disc to the star, the magnetic spin-up torque from the accretion disk inside the co-rotation radius, and the magnetic spin-down torque from the accretion disc outside the co-rotation radius. The position of the inner edge of the accretion disc varies with the accretion rate such that it moves closer to the star when the accretion rate increases. Thus we expect the star to spin up, the most rapidly, when the accretion rate, or equivalently the luminosity, is high.

Angular momentum that the gas possesses at the magnetospheric boundary is advected with the gas to the star (Pringle and Rees 1972, Rappaport and Joss 1977b), the accreting pulsar will experience a spin-up torque

$$N \approx \dot{M}\sqrt{GMR_m}, \tag{1.1}$$

where $R_m = \xi R_A$ is the magnetospheric radius with the Alfvén radius expressed as a fraction of

$$R_A = \left(\frac{\mu^4}{2GM_x\dot{M}^2}\right)^{1/7}$$

$$\simeq 6.8 \times 10^6 \left(\frac{\mu}{10^{20}\mathrm{T\,m^3}}\right)^{4/7} \left(\frac{10^{-10}M_\odot}{M}\right)^{2/7} \left(\frac{1.4M_\odot}{M}\right)^{1/7} \mathrm{m} \tag{1.2}$$

which is the characteristic radius given by equating magnetic and fluid stress for a neutron star with magnetic moment μ. ξ ranges from 0.52 (Ghosh and Lamb 1979) to ≈ 1(Arons 1993: Ostriker and Shu 1995; Wang 1996) and $R_m \sim 10^6$m. Accretion will be inhibited by a centrifugal barrier if the pulsar magnetosphere rotates faster than the Kepler frequency at the inner disk boundary. For accretion to occur, the magnetospheric radius should thus lie inside the corotation radius

$$R_{co} = \left(\frac{GMP^2}{4\pi^2}\right)^{1/3} \simeq 1.7 \times 10^6 \left(\frac{P}{1s}\right)^{2/3} \left(\frac{M}{1.4M\odot}\right)^{1/3} \mathrm{m} \tag{1.3}$$

where P is spin period. It is convenient to express the torque in terms of

$$N_o \equiv \dot{M}\sqrt{GMR_{co}}. \tag{1.4}$$

Which only depends on the observable spin period of the pulsar and the inferred accretion rate. The actual torque might be significantly smaller though. A pulsar subject to the torque in (1.4) spins up at a rate

$$\dot{\nu} = \frac{N}{2\pi I} \simeq 1.6 \times 10^{-13} s^{-2} \left(\frac{\dot{M}}{10^{-10} M_{\odot} yrs^{-1}} \right) \left(\frac{P}{1s} \right)^{1/3} \left(\frac{R_m}{R_{co}} \right)^{1/2} \tag{1.5}$$

where $I \simeq 0.4MR^2$ is the neutron star's moment of inertia and $M = 1.4M_{\odot}$. The time scale for the spinning up the neutron star is then

$$t_{spinup} \equiv \frac{\nu}{\dot{\nu}} \simeq 2 \times 10^5 yrs \left(\frac{10^{-10} M_{\odot} yrs^{-1}}{\dot{M}} \right) \left(\frac{1s}{P} \right)^{4/3} \left(\frac{R_{co}}{R_m} \right)^{1/2} \tag{1.6}$$

which is much shorter than the ages of most X-ray binaries (Easer, Ghosh and Lamb 1980). Hence in this simple picture, the neutron star spins up until the spin frequency matches the Keplerian frequency at the magnetosphere that is until (or where $R_{mm} = R_{mco}$).

$$P_{\text{equilibrium}} \simeq 8s \left(\frac{10 \times^{-10} M_{\odot}}{\dot{M} yr^{-1}} \right)^{3/7} \left(\frac{\mu}{10 \times^{20} Tm^3} \right)^{6/7} \tag{1.7}$$

In this case $\dot{M}$ is an appropriately averaged mass accretion rate. Most likely, neutron stars with shorter periods than $P_{\text{equilibrium}}$ cannot accrete easily, and may experience a strong spin-down torque as they expel matter through the so called "propeller effect" (Illarionov and Sunyaev 1975).

Some pulsars show secular spin-down behaviour while continuing to accurate (4U 1626-67, GX 1 + 4, 1E1048-1-5937,1E2259 + 586, E1145.1-614, 4U1538-52), while others show more erratic variations in spin period (Cen X-3, Vela X-1, X per). More sophisticated theories of accretion torque were developed to explain these observations, which take into account the magnetic interaction between the inner magnetosphere (Ghosh and Lamb 1979, Anzer and Borner 1980, Arons et al. 1984). However, the continuous monitoring of accreting pulsars by the BATSE instrument has now substantially changed over view of many of these systems.

The BATSE instrument on the Compton Gamma Ray Observatory(CGRO) has produced in accurate timing observations of the rotational modulation of the X-ray emission from a number of accreting neutron stars(Bildsten et al.1997, Nelson et al.1997, Chakrabarty et al. 1997). Data from a system such as Cen X-3 that accretes gas from a surrounding accretion disc ($P = 4.83s$) shows that the torque on short time-scales is much larger than the mean spin-up torque, and that the torque changes its sign suddenly without a significant change in the magnitude of the torque. The flip in the sign of the torque is quite stochastic. Some other systems such as 4U

1626-67 ($P = 7.6s$) and GX 1+4 ($P =\simeq 120s$) show much more extended spin-up and spin-down episodes than Cen X-3, but the inferred positive and negative torques are still of comparable magnitudes. These observations provide strict constraints on models of the accretion torque, and Nelson et al. (1997) proposed that they are inconsistent with the standard Ghosh and Lamb model. The problems raised by Nelson et al.(1997) were:

1. The observed torques appear to switch rapidly between two states of opposite sign. This requires step-function-like changes in the accretion rate for the standard picture to apply.

2. The two states of opposite sign have torque of comparable magnitudes. To use the standard torque formulation, one has to assume that the accretion rate is finely tuned to two, different values in between which it is oscillating

3. For GX 1+4($P \simeq 120s$), there exists an extended spin-down state with a persistent high luminosity, the opposite of what would be expected with the standard formulation.

4. The standard model for explaining GX 1+4 requires a stellar dipole surface field $B_d \sim 10^{10}T$.

5. It is not clear why systems like GX 1+4 and 4U 1626-67 are stable for years between transitions from spin-up to spin-down.

The most significant problem is that the torque-luminosity relation in the standard model does not fit the observations, as demonstrated by point 3 above since spin-down would be associated with a reduction in the accretion rate and hence of the luminosity.However, BATSE was only sensitive to the pulsed X-ray flux from the X-ray pulsars, and thus one cannot completely exclude a variation of the steady X-ray flux in accordance with the standard model.

On the other hand the neutron stars in Be/X-ray transients sometimes pick up an accretion disc at the time of their periastron passage, which leads to an outburst of X-rays. The observations of transient X-ray pulsars, such as EXO 2030+375(Reig and Coe 1998) and A0535+262 give some support to the Ghosh and Lamb model as the spin- up rate of the X-ray pulsar decreases as the X-ray flux goes down, though the relation between the observed X-ray flux and the accretion rate is uncertain also for these system (Bildsten et al. 1997).

1.3 Organization of the thesis

This thesis presents studies of an accretion disc with an internal dynamo around magnetized stars, in particular neutron stars. General equations used to solve many thin accretion disc problems are derived in chapter 2.

In Chapter 3 we will develop a steady state, a thin, axisymmetric model of the structure of an accretion disc around magnetized star with an internal dynamo that is interacting with the magnetic field of the accretor. The equations for the thin accretion disc with an internal dynamo can be reduced to a single ordinary differential equation for dynamical viscosity ($\nu\Sigma$), which we solve by integrating it numerically starting from the boundary condition and we construct a one-dimensional solution for the structure of a steady thin accretion disc that can be expressed in a self-similar form similar to the classical solution by Shakura and Sunyaev(1973). We calculate detail structure of the thin accretion disc in terms of magnetic moment μ, r, M and $\dot{M}$. Using this model we have investigated the relation between the structure of the accretion disc and the torque acting on the neutron star. Result and discussions, and conclusion are given at end of the chapter.

In Chapter 4 we extend our model for the accretion disc with an internal dynamo around magnetized millisecond X-ray pulsars. We calculate the detail structure of accretion disc for different region of the disc starting from mathematics formulated in Chapter 3. Result and discussions, and conclusion are given at end of this chapter.

In Chapter 5 we develop a theory for time-dependent behaviour of a stationary thin accretion disc with an internal dynamo around a magnetized stars, and we determine the stability properties of our disc model and a linear stability analysis of our steady disc solutions in the presence of a strong external magnetic field. Results and discussion, and conclusion are given at the end of this Chapter, summaries of the present work and a brief look forward can be found in Chapter 6. Finally list of references are given at last and this work has been published in Astronomy and Astrophysics Journal (one of the most reputable international Journal).

Chapter 2

Accretion Discs

2.1 Introduction

In this chapter we derive general mathematical equations which will be used to solve many problems concerning thin accretion disc starting from Navier-Stokes equation this equation can be reduced into standard disc equation in the absence of Lorentz force.

2.2 Basic Equations

The equations of the standard disc accretion theory were first formulated by Shakura(1972) and Shakura and Sunyaev (1973). These equations were using standard disc equations. Now let us derive general equations for accretion disc, starting from Navier stokes equation in the presence of magnetic field (Landau and Lifshitz 1987, 1959)

$$\rho\frac{\partial \mathbf{v}}{\partial t} + \rho(\mathbf{v}.\nabla\mathbf{v}) = \mathbf{J}\times\mathbf{B} - \nabla P - \rho\nabla\Phi + \eta\Delta\mathbf{v}, \tag{2.1}$$

where the ratio of $\frac{\eta}{\rho}$ is the kinematic viscosity and η itself is the dynamic viscosity, ρ the mass density, $\mathbf{v}$ the velocity, P the pressure and Φ the gravitational potential of the central star, $\mathbf{J}\times\mathbf{B}$ the Lorentz force. Before we derive for specific case we have to put the general Navier stokes equation which is applicable for any accretion disc.

Now in general form the Navier-Stokes equations in cartesian coordinates system, describing the motion of a viscous fluid with variable dynamic viscosity η and bulk viscosity η coefficients

(Chapman and Cowling, 1939; Landau and Lifshitz, 1959) can be written as:

$$\rho\left(\frac{\partial v_\imath}{\partial t}+v_k\frac{\partial v_\imath}{\partial x_k}\right)=\mathbf{J}\times\mathbf{B}-\frac{\partial P}{\partial x_\imath}+\rho g_\imath+\frac{\partial}{\partial x_k}\left[\eta\left(\frac{\partial v_\imath}{\partial x_k}+\frac{\partial v_\imath}{\partial x_k}+\frac{\partial v_k}{\partial x_i}-\frac{2}{3}\frac{\partial v_\ell}{\partial x_\ell}\delta_{\imath k}\right)+\eta_B\frac{\partial v_\ell}{\partial x_\ell}\delta_{\imath k}\right], \tag{2.2}$$

or in vector notation,

$$\rho\left(\frac{\partial\mathbf{v}}{\partial t}+(\mathbf{v}.\nabla)\mathbf{v}\right)=\mathbf{J}\times\mathbf{B}-\nabla P+\rho\mathbf{g}+\nabla_k\left[\eta\left(\nabla_\mathbf{k}\mathbf{v}+\nabla_\mathbf{k}\mathbf{v_k}-\frac{2}{3}(\nabla.\mathbf{v})\delta\right)+\eta_B(\nabla.\mathbf{v})\delta\right]. \tag{2.3}$$

Here, the usual tensor definitions are used with $\delta_{\imath k}$ the Kronecker delta, and δ the unit tensor; $g_\imath$ is the gravitational acceleration. Summation over repeated indices is assumed. The last term in Eq. (2.2) is the divergence of the viscosity stress tensor $\sigma_{\imath k}$, which is related to the symmetric and divergent.

$$T_{\imath k}=\frac{1}{2}(\nabla_\mathbf{k}\mathbf{v}+\nabla\mathbf{v_k}-\frac{1}{3}(\nabla.\mathbf{v})\delta, \tag{2.4}$$

where

$$\begin{aligned}2T_{\imath k}=&\frac{4}{3}\frac{\partial v_R}{\partial R}-\frac{2}{3}\left(\frac{v_R}{R}+\frac{1}{R}\frac{\partial v_\phi}{\partial\phi}+\frac{\partial v_z}{\partial z}\right)\frac{\partial v_\phi}{\partial R}+\frac{1}{R}\frac{\partial v_R}{\partial\phi}-\frac{v_\phi}{R}\\
&\frac{\partial v_\phi}{\partial R}+\frac{1}{R}\frac{\partial v_R}{\partial\phi}-\frac{v_\phi}{R}\frac{4}{3}\left(\frac{1}{R}\frac{\partial v_\phi}{\partial\phi}+\frac{v_r}{R}\right)-\frac{2}{3}\left(\frac{\partial v_R}{\partial R}+\frac{\partial v_z}{\partial z}\right)\\
&\frac{\partial v_z}{\partial R}+\frac{\partial v_R}{\partial z}\frac{1}{R}\frac{\partial v_z}{\partial\phi}+\frac{\partial v_\phi}{\partial z}\\
&\frac{\partial v_z}{\partial R}+\frac{\partial v_R}{\partial z}\\
&\frac{1}{R}\frac{\partial v_z}{\partial\phi}+\frac{\partial v_\phi}{\partial z}\\
&\frac{4}{3}\frac{\partial v_z}{\partial z}-\frac{2}{3}\left(\frac{\partial v_R}{\partial R}+\frac{1}{R}\frac{\partial v_\phi}{\partial\phi}+\frac{v_R}{R}\right)\end{aligned} \tag{2.5}$$

The second term in the brackets on the left-hand side of Eq.(2.3) is a scalar product of the vector $\mathbf{v}$ and tensor $\nabla\mathbf{v}$, which is the same in cartesian and curvilinear coordinates. The last term on the right- hand side of Eq.(2.3) is the divergence of the tensor $2\eta T_{\imath k}$, which is calculated using Eqs.(appendix A) and (2.5). As a result we obtain the components of Eq.(2.3) in the cylindrical coordinates:

$$\begin{aligned}\rho\left(\frac{\partial v_R}{\partial t}+v_R\frac{\partial v_R}{\partial R}+\frac{v_\phi}{R}\frac{\partial v_R}{\partial\phi}+v_z\frac{\partial v_R}{\partial z}-\frac{{v_\phi}^2}{R}\right)=&(\mathbf{J}\times\mathbf{B})\hat{R}-\frac{\partial P}{\partial R}+\rho g_R\\
&+\frac{2}{3}\frac{\partial}{\partial R}\left[\eta\left(\frac{2}{R}\frac{\partial(Rv_R)}{\partial R}-\frac{1}{R}\frac{\partial v_\phi}{\partial\phi}-\frac{\partial v_z}{\partial z}\right)\right]\\
&-2\frac{v_R}{R}\frac{\partial\eta}{\partial R}+\frac{1}{R}\frac{\partial}{\partial\phi}\left[\eta\left(\frac{\partial v_\phi}{\partial R}+\frac{1}{R}\frac{\partial v_R}{\partial\phi}-\frac{v_\phi}{R}\right)\right]\\
&-2\frac{\eta}{R^2}\frac{\partial v_\phi}{\partial\phi}+\frac{\partial}{\partial z}\left[\eta\left(\frac{\partial v_\phi}{\partial R}+\frac{\partial v_R}{\partial z}\right)\right].\end{aligned} \tag{2.6}$$

$$\rho\left(\frac{\partial v_\phi}{\partial t}+v_R\frac{\partial v_\phi}{\partial R}+\frac{v_\phi}{R}\frac{\partial v_R}{\partial \phi}+v_z\frac{\partial v_\phi}{\partial z}-\frac{v_R v_\phi}{R}\right)=(\mathbf{J}\times\mathbf{B})\hat{\phi}-\frac{1}{R}\frac{\partial P}{\partial \phi}+\rho g_\phi$$
$$+\frac{1}{R^2}\frac{\partial}{\partial R}\left[\eta R^3\frac{\partial}{\partial R}\left(\frac{v_\phi}{R}\right)\right]+\frac{\partial}{\partial R}\left(\frac{\eta}{R}\frac{\partial v_R}{\partial \phi}\right)$$
$$+\frac{2}{3R}\frac{\partial}{\partial \phi}\left[\eta\left(2\left(\frac{1}{R}\frac{\partial v_\phi}{\partial \phi}+\frac{v_R}{R}\right)-\frac{\partial v_R}{\partial R}-\frac{\partial v_z}{\partial z}\right)\right]$$
$$+\frac{\partial}{\partial z}\left[\eta\left(\frac{1}{R}\frac{\partial v_z}{\partial \phi}+\frac{\partial v_\phi}{\partial z}\right)\right]+\frac{2\eta}{R^2}\frac{\partial v_R}{\partial \phi}. \tag{2.7}$$

$$\rho\left(\frac{\partial v_z}{\partial t}+v_R\frac{\partial v_z}{\partial z}+\frac{v_\phi}{R}\frac{\partial v_z}{\partial \phi}+v_z\frac{\partial v_z}{\partial z}\right)=(\mathbf{J}\times\mathbf{B})\hat{z}-\frac{\partial P}{\partial z}+\rho g_z$$
$$+\frac{1}{R}\frac{\partial}{\partial R}\left[\eta R\left(\frac{\partial v_z}{\partial R}+\frac{\partial v_R}{\partial z}\right)\right]+\frac{1}{R}\frac{\partial}{\partial \phi}\left[\eta\left(\frac{1}{R}\frac{\partial v_z}{\partial \phi}+\frac{\partial v_\phi}{\partial z}\right)\right]$$
$$+\frac{2}{3}\frac{\partial}{\partial z}\left[\eta\left(2\frac{\partial v_z}{\partial z}-\frac{\partial v_R}{\partial R}-\frac{1}{R}\frac{\partial v_\phi}{\partial \phi}-\frac{v_R}{R}\right)\right]. \tag{2.8}$$

The continuity equation for the disc flow in general

$$\frac{\partial \rho}{\partial t}+\frac{\partial(\rho v_\imath)}{\partial x_\imath}=0 \text{ or } \frac{\partial \rho}{\partial \mathrm{t}}+\nabla\cdot(\rho\mathbf{v})=0. \tag{2.9}$$

Now in cylindrical coordinates the continuity equation yields

$$\frac{\partial \rho}{\partial t}+\frac{\partial(R\rho v_R)}{R\partial R}+\frac{\partial(\rho v_\phi)}{r\partial \phi}+\frac{\partial(\rho v_z)}{\partial z}=0. \tag{2.10}$$

2.3 Thin Disc Equations

For axisymmetric disc flow the ϕ- partial derivatives vanish so that the above equations become

$$\rho\left(\frac{\partial v_R}{\partial t}+v_R\frac{\partial v_R}{\partial R}+v_z\frac{\partial v_R}{\partial z}-\frac{v_\phi^2}{R}\right)=(\mathbf{J}\times\mathbf{B})\hat{R}-\frac{\partial P}{\partial R}+\rho g_R$$
$$+\frac{2}{3}\frac{\partial}{\partial R}\left[\eta\left(\frac{2}{R}\frac{\partial(Rv)}{\partial R}-\frac{\partial v_z}{\partial z}\right)\right]-2\frac{v_R}{R}\frac{\partial \eta}{\partial R}+\frac{\partial}{\partial z}\left[\eta\left(\frac{\partial v_z}{\partial R}+\frac{\partial v_R}{\partial z}\right)\right], \tag{2.11}$$

$$\rho\left(\frac{\partial v_\phi}{\partial t}+v_R\frac{\partial v_\phi}{\partial R}+v_z\frac{\partial v_\phi}{\partial z}+\frac{v_R v_\phi}{R}\right)=(\mathbf{J}\times\mathbf{B})\hat{\phi}+\frac{1}{R^2}\frac{\partial}{\partial R}\left[\rho\nu R^3\frac{\partial}{\partial R}(\frac{v_\phi}{R})\right]+\frac{\partial}{\partial z}\left(\eta\frac{\partial v_\phi}{\partial z}\right), \tag{2.12}$$

$$\rho\left(\frac{\partial v_z}{\partial t}+v_R\frac{\partial v_z}{\partial R}+v_z\frac{\partial v_z}{\partial z}\right)=(\mathbf{J}\times\mathbf{B})\hat{z}-\frac{\partial P}{\partial z}+\rho g_z$$
$$+\frac{1}{R}\frac{\partial}{\partial R}\left[\eta R\left(\frac{\partial v_z}{\partial R}+\frac{\partial v_R}{\partial z}\right)\right]+\frac{2}{3}\frac{\partial}{\partial z}\left[\rho\nu\left(2\frac{\partial v_z}{\partial z}-\frac{\partial v_R}{\partial R}-\frac{v_R}{R}\right)\right]. \tag{2.13}$$

The continuity equation(2.10) takes the form

$$\frac{\partial\rho}{\partial t}+\frac{1}{R}\frac{\partial(R\rho v_R)}{\partial R}+\frac{\partial(\rho v_z)}{\partial z}=0. \tag{2.14}$$

The vertical structure of the disc is determined by the equilibrium of the pressure gradient and the vertical gravitational force g_z. Neglecting v_z, and all z derivatives, we obtain the approximate equations

$$\rho\left(\frac{\partial v_R}{\partial t}+v_R\frac{\partial v_R}{\partial R}-\frac{v_\phi^2}{R}\right)=(\mathbf{J}\times\mathbf{B})\hat{R}-\frac{\partial P}{\partial R}+\rho g_R+\frac{4}{3}\frac{\partial}{\partial R}\Big[\frac{\rho\nu}{R}\frac{\partial(Rv_R)}{\partial R}\Big]-2\frac{v_R}{R}\frac{\partial(\rho\nu)}{\partial R}, \tag{2.15}$$

$$\rho R\left(\frac{\partial Rv_\phi}{\partial t}+v_R\frac{\partial Rv_\phi}{\partial R}\right)=(\mathbf{J}\times\mathbf{B})\hat{R}+\frac{\partial}{\partial R}\left[\rho\nu R^3\frac{\partial}{\partial R}\left(\frac{v_\phi}{R}\right)\right], \tag{2.16}$$

Neglecting v_z it follows from (2.13) that the hydrostatic equilibrium gives

$$\rho g_z=\frac{\partial P}{\partial z}, \tag{2.17}$$

The components of the gravitational acceleration are given by

$$g_i=-\frac{\partial\Phi}{\partial x_i}=\left(-\frac{GMR}{(R^2+z^2)^{3/2}},0,-\frac{GMz}{(R^2+z^2)^{3/2}}\right). \tag{2.18}$$

In Eq.(2.15) we assume that the last two terms on the right-hand-side are very small and neglected (or neglecting viscosity in the radial equation), then we get the general equation which describes the thin accretion disc

$$\rho\left(\frac{\partial v_R}{\partial t}+v_R\frac{\partial(v_R)}{\partial R}\right)-\rho(\Omega^2R+g_R)+\frac{\partial P}{\partial R}=0, \tag{2.19}$$

Then the continuity equation reduces to

$$\frac{\partial\rho}{\partial t}+\frac{1}{R}\frac{\partial(R\rho v_R)}{\partial R}=0. \tag{2.20}$$

Integrating the continuity equation vertically over the thickness of the disc we get another set of thin disc equations

$$\frac{\partial\Sigma}{\partial t}+\frac{1}{2\pi R}\frac{\partial\dot{M}}{\partial R}=0. \tag{2.21}$$

Therefore, for steady-state disc we define

$$\Sigma = \int_{-H}^{+H} \rho dz, \quad \dot{M} = -2\pi \int_{-H}^{+H} \rho v_R dz = -2\pi R \Sigma v_R, \quad \Omega = \frac{v_\phi}{R}, \quad \ell = R v_\phi \tag{2.22}$$

The radial motion in the disc is due to the friction between adjacent layers and the exchange of the angular momentum between in a disc along the R-coordinates is associated with the moment of viscous force. The particles spiral inward to the compact objects (black holes or neutron stars) which leads to the loss of the angular momentum of the particles. Thus the radial component of velocity appears and the particles spiral inward to compact objects which can be expressed as

$$v_R = \frac{\dot{M}}{2\pi R \Sigma} = \frac{\dot{M}}{4\pi R H \rho} \tag{2.23}$$

Thus the structure of the thin disc solutions are related using the above set of equations.

2.4 Conclusion

According to the standard disc model accretion disk structure is defined by a set of differential equations essentially describing the flow of mass, energy and angular momentum within the disk. With a few simplifying assumptions the structure equations can be solved analytically. One such analytical solution, originally derived by Shakura & Sunyaev (1973), is the classical or Shakura-Sunyaev disk model. The assumptions leading to the Shakura-Sunyaev-solution are:Steady state (all time derivatives set to zero), Vertical hydrostatic equilibrium, the disk is thin ($r \gg H$), orbits of gas particles are nearly Keplerian, the efficiency of angular momentum transport is described by the α-parameter in which physics related to the viscosity is hidden in the α-parameter. Some of the assumptions, like vertical hydrostatic equilibrium and near-Keplerian orbits are relatively hard to constrain from observations. The Shakura-Sunyaev solution also divides the disk into regions depending on equation of state (pressure is dominated either by radiation pressure or ideal gas pressure) and main opacity source (electron scattering or Kramer's opacity). In transition regions, where the dominant source of pressure or opacity changes, solutions are more complex and require numerical methods. The assumptions of near-keplerian orbits and thinness are critical as the whole solution collapses without them.

The Shakura-Sunyaev model assumes vertical hydrostatic equilibrium. For disk region dominated by gas pressure, this means predicts Gaussian vertical density structure near the disk plane and exponential structure further away. The classical model assumes the scale height is

small. However, observations have shown that the vertical structure of accretion disks is complex. Deviations from axial symmetry and very extended vertical structure have been observed.

Thus our equation can reduced into the Shakura-Sunyaev equation in the absence of magnetic field and other approximations. In the standard disc model the equations for thin disc approximation have been solved in the absence of magnetic field- disc interaction, that is the effect of Lorentz was not included. But here we have derived the fundamental equations which are used to solve many problems related to thin accretion discs including the effect of magnetic field. These solutions can be described by the basic equations of viscous fluid dynamics: the continuity equation and Navier-Stokes equations, given by the geometry of the problem. The solutions can be found using equations derived in this chapter in the equatorial plane integrated over the thickness of the disc. The vertical structure of the disc has been determined by the hydrostatic equilibrium by neglecting the dynamical flow along the vertical direction.

Chapter 3

Accretion disc around magnetised stars

This chapter is adapted from the paper "The Structure of Thin Accretion Discs Around Magnetised Star" by S.B Tessema and U. Torkelsson has been published in **Astronomy and Astrophysics Journal, 2010, 509, A45**.

3.1 Introduction

In chapter two we have derived that the general equations used to solve many problems concerning thin accretion discs. Here we develop a model of an accretion with an internal dynamo around magnetised stars in a steady state. We work in the spirit of Shakura & Sunyaev (1973) and assume that the dynamics of a thin disc, which assuming cylindrical polar coordinates (R, ϕ, z)) is located in the equatorial plane z = 0. To a first approximation, the matter in the disc is rotating in circular Keplerian orbits. With the standard assumptions for thin accretion discs, that is $\frac{H(R)}{R} \ll 1$, thereby implies $c_s \gg v_R$, for $V_\phi = V_{\rm Kepl}(R)$ which will lead us to $V_R \ll V_\phi$ for a reasonable viscous stress, where $V_{\rm Kepl}$ is the Keplerian velocity, which is equal to $\Omega_k R$. We start from the equations of magnetohydrodynamics and derive a single ordinary differential equation for the radial structure of the accretion disc, we present numerical solutions of this equation. Finally, discuss the properties of these solutions and we summarize our conclusions at the end of this chapter.

3.2 Basic Equations of Magnetohydrodynamics

In stars and galaxies, and indeed in many other astrophysical settings, the gas is partially or fully ionized and can carry electric currents that, in turn, produce a magnetic field. The associated Lorentz force exerted on plasma might be included in the momentum equation for the fluid. In the magnetohydrodynamic approximation the behaviour of a continuous plasma is governed by a simplified form of Maxwell's equations, together with Ohm's law, and the equations of hydrodynamics to which one adds the effect of the Lorentz force. The Maxwell's equations in MKS units can be written in the form

$$\nabla \times \mathbf{E} = -\frac{\partial \mathbf{B}}{\partial t} \tag{3.1}$$

where $\mathbf{E}$ is electric field and $\mathbf{B}$ is the magnetic field. We also assume that the net charge density $\rho_e = 0 \Longrightarrow \nabla \cdot \mathbf{E} = 0$ other wise you have that $\nabla \cdot \mathbf{E} = \frac{\rho_e}{\varepsilon_0}$

$$\nabla \cdot \mathbf{B} = 0 \tag{3.2}$$

$$\nabla \times \mathbf{B} = \frac{1}{c^2}\frac{\partial E}{\partial t} + \mu_0 \mathbf{J} \tag{3.3}$$

where $\mathbf{J}$ is the current density, c is the speed of light, μ_0 is permeability of free space. This shows that either currents or time- varying electric fields may produce magnetic fields. A fundamental assumption of magnetohydrodynamics is that the velocities are non-relativistic that is

$$v_0 \ll c, \tag{3.4}$$

where $v_0 = \frac{l}{\tau}$ is a characteristic electromagnetic(or plasma) speed, while l and τ are a typical length and time scales, respectively. In addition, Eq. (3.1) shows that

$$\frac{E_0}{l} \approx \frac{B_0}{\tau}, \tag{3.5}$$

but in a moving medium we have that

$$\mathbf{E} \approx -\mathbf{v} \times \mathbf{B}$$

so that the first term on the RHS of Eq. (3.3) (the displacement current) has a magnitude

$$\frac{E_0}{c^2\tau} \approx \frac{B_0 l}{c^2\tau^2} = \frac{v_0^2 B_0}{c^2 l} \approx v_0^2 \ll |\nabla \times \mathbf{B_0}| \approx \frac{B_0}{L} \tag{3.6}$$

Taking the divergence of equation (3.3), we get $\nabla \cdot \mathbf{J} = 0$; which implies that local accumulations of charge are negligible.

Thus Eq. (3.3) can be reduced to Ampere's law

$$\nabla \times \mathbf{B} = \mu_0 \mathbf{J}. \tag{3.7}$$

According to Ohm's law the current density is proportional to the total electric field of the fluid in its local frame of reference moving with the plasma and it can be written as

$$\mathbf{J} = \sigma \left(\mathbf{E} + \mathbf{v} \times \mathbf{B} \right) \tag{3.8}$$

where σ is the electric conductivity, $\mathbf{E}$ the electric field in the laboratory frame, which is at rest, $\mathbf{v}$ the velocity of the fluid in the laboratory frame and $\mathbf{B}$ the magnetic field in the laboratory frame.

Solving for $\mathbf{E}$ and substituting it into Faraday's law of induction, one obtains the induction equation

$$\frac{\partial \mathbf{B}}{\partial t} = \nabla \times \left(\mathbf{v} \times \mathbf{B} - (\mu_0 \sigma)^{-1} \mathbf{J} \right) \tag{3.9}$$

$$\frac{\partial \mathbf{B}}{\partial t} = \nabla \times (\mathbf{v} \times \mathbf{B}) - \nabla \left(\eta \nabla \times \mathbf{B} \right), \tag{3.10}$$

where in the second step we have used Ampere's law to eliminate $\mathbf{J}$ and have introduced the magnetic diffusivity $\eta = \frac{1}{\mu_0 \sigma}$. The behaviour of the magnetic field is coupled to that of the plasma by the presence of the velocity term in Eq. (3.10). The plasma motion is in turn given by the Navier-Stokes's equations and the equation of continuity (conservation of mass)

$$\frac{\partial \rho}{\partial t} + \nabla \cdot (\rho \mathbf{v}) = 0, \tag{3.11}$$

If ρ is independent of time t then we have that $\nabla \cdot (\rho \mathbf{v}) = 0$ if in addition ρ is independent of $\mathbf{r}$. The momentum equation is the ordinary Navier- Stokes equation supplemented by the Lorentz force, $\mathbf{J} \times \mathbf{B}$ is

$$\rho \frac{\partial \mathbf{v}}{\partial t} + \rho \left(\mathbf{v} \cdot \nabla \mathbf{v} \right) = -\nabla P + \mathbf{J} \times \mathbf{B} + \mathbf{f} + \mathbf{F}_\nu, \tag{3.12}$$

where $\mathbf{v}$ is the velocity of fluid, ρ the density, P the pressure, $\mathbf{F}_\nu$ the viscous force and $\mathbf{f}$ is all other body forces acting on the fluid including gravity, and in a rotating system also the Coriolis and centrifugal forces. The magnetohydrodynamic equations form the basis for our work.

3.3 Mathematical Formulation

We study a steady thin axisymmetric Keplerian disc around a star with a magnetic dipole field. This field is interacting with the accretion disc and can transfer angular momentum between the

disc and the star (Ghosh and Lamb 1979). The basic equations describing the structure of the thin accretion disc can be derived from the equations of magnetohydrodynamics. We assume that the accretion disc is around magnetized star, and there is some viscosity that transport angular momentum. And we consider the accreting system in which the central object interacts, through the magnetic field, with the disc that surrounds it. First we have the dipole field from the star (the neutron star), and there is an interaction of a dipole magnetic field and the accretion disc. Secondly the different magnitudes of the Keplerian angular velocity and the stellar angular velocity of the dipole field (the central star and the disc) creates or generates a radial current and thereby, toroidal component of the magnetic field is created with in the disc as well as the toroidal magnetic field produces a Lorentz force that expands the disc. Therefore accretion through successive Keplerian orbits towards the central mass is possible only if the fluid can constantly lose angular momentum because of some viscous torque.

3.3.1 Conservation of Mass

In steady state the continuity equation can be written as:

$$\nabla\cdot(\rho\mathbf{v}) = 0 \tag{3.13}$$

When only the radial advection is dominant, Eq.(3.13) yields

$$\frac{1}{R}\frac{\partial}{\partial R}(R\Sigma v_R) = 0, \tag{3.14}$$

where Σ is the surface density and defined by

$$\Sigma = \int_{-H}^{H} \rho dz \simeq 2\rho H, \tag{3.15}$$

where H is the half thickness of the disc. For steady-state and thin discs the integral of Eq.(3.14) gives

$$\dot{M} = -2\pi R \int_{-H}^{H} \rho v_R dz = -2\pi R\Sigma v_R = \text{constant}, \tag{3.16}$$

which is the accretion rate.

3.3.2 Conservation of Momentum

Assuming a steady state the Navier-Stoke's equation can be written as:

$$\begin{aligned}\rho(\mathbf{v}\cdot\nabla)\mathbf{v} = &-\nabla P + \rho\nabla\Phi + \mathbf{J}\times\mathbf{B}\\ &+\nabla\cdot\left(\rho\nu\left(\nabla\mathbf{v} - \frac{2}{3}(\nabla\cdot\mathbf{v})\right)\right).\end{aligned} \tag{3.17}$$

where P is pressure, ν kinematic viscosity, Φ the gravitational potential $\mathbf{J} = \frac{1}{\mu_0}(\nabla \times \mathbf{B}) = (J_R, J_\phi, J_z)$ the current density and $\mathbf{B} = (B_R, B_\phi, B_z)$ the magnetic field. Then the current density for axisymmetric case gives

$$\mathbf{J} = \mathbf{J_z} + \mathbf{J_r} \tag{3.18}$$

The viscosity is in general small, and we will only retain it where it plays a crucial role.
The radial component of Navier-Stoke's equation is :

$$\rho\left[v_R\frac{\partial v_R}{\partial R} - \frac{v_\phi^2}{R} + \frac{GM}{(R^2+z^2)^{3/2}}\right] = \left[\frac{B_z}{\mu_0}\left(\frac{\partial B_R}{\partial z} - \frac{\partial B_z}{\partial R}\right) - \frac{B_\phi}{\mu_0}\left(\frac{1}{R}\frac{\partial}{\partial R}(RB_\phi)\right)\right] - \frac{\partial P}{\partial R} + \frac{4}{3R^{3/2}}\frac{\partial}{\partial R}\left(R^{3/2}\nu\rho\frac{\partial v_R}{\partial R}\right) - \frac{2}{3R^3}\frac{\partial(R^2\nu\rho v_R)}{\partial R} \tag{3.19}$$

We assume that $v_R \ll v_\phi$ and also assume that for a thin accretion disc v_ϕ is much larger than the speed of sound and the Alfvén speed . Thus the dominant terms of the equation (3.19) give us to lowest order when all the right-hand side of Eq.(3.19) go to zero

$$\Omega^2 R - \frac{GM}{R^2} = 0 \tag{3.20}$$

which shows that the disc rotates in a Keplerian fashion.
In similar manner the vertical component of momentum equation for a steady flow is

$$\rho\left[v_R\frac{\partial v_z}{\partial R} + v_z\frac{\partial v_z}{\partial z}\right] = -\frac{B_\phi}{\mu_0}\frac{\partial B_\phi}{\partial z} - \frac{B_R}{\mu_0}\frac{\partial B_R}{\partial z} + \frac{B_R}{\mu_0}\frac{\partial B_z}{\partial R}$$
$$-\frac{\partial P}{\partial z} - \frac{\rho GM}{R^2} + \frac{1}{R}\frac{\partial}{\partial R}\left[\rho\nu R\left(\frac{\partial v_z}{\partial R} + \frac{\partial v_R}{\partial z}\right)\right] + \frac{4}{3}\frac{\partial}{\partial z}\left[\rho\nu\frac{\partial v_z}{\partial z} - \frac{\partial v_R}{\partial R} - \frac{v_R}{R}\right] \tag{3.21}$$

Neglecting vertical outflows and assuming the magnetic field to be weak the equation reduces to the equation of hydrostatic equilibrium

$$\frac{1}{\rho}\frac{\partial P}{\partial z} = -\frac{GM}{R^2}\frac{Z}{R} \tag{3.22}$$

Using H as the half thickness of the disc, the total pressure at the midplane of the disc is

$$P = \frac{1}{2}\Sigma H\frac{GM}{R^3} \tag{3.23}$$

but the hydrostatic equilibrium can also be expressed as

$$\frac{H}{R} = \frac{c_s}{v_{kepl}} \tag{3.24}$$

where

$$c_s = \left(\frac{P}{\rho}\right)^{1/2} \tag{3.25}$$

is the isothermal speed of sound and

$$v_{kepl} = \sqrt{\frac{GM}{R}} \tag{3.26}$$

is the Keplerian speed.

This means that in a thin disc the Keplerian velocity is highly supersonic; which leads to the solution for the disc height H

$$H = c_s \frac{R^{3/2}}{\sqrt{GM}} \tag{3.27}$$

The azimuthal component of Navier- Stoke's equation for steady-state is:

$$\rho\left(\frac{v_R}{R}\frac{\partial}{\partial R}\left(Rv_\phi\right)\right) = \left[\frac{B_R}{\mu_0}\frac{1}{R}\frac{\partial}{\partial R}(RB_\phi) + \frac{B_z}{\mu_0}\frac{\partial B_\phi}{\partial z}\right] + \frac{1}{R^2}\frac{\partial}{\partial R}\left[R^3\rho\nu\frac{\partial}{\partial R}\left(\frac{v_\phi}{R}\right)\right], \tag{3.28}$$

We neglect $\frac{B_R}{R}\frac{\partial}{\partial R}(RB_\phi)$ because the the radial length scale is much longer than the vertical length scale in a thin accretion disc. We integrating Eq. (3.28) vertically across the disc

$$\int_{-H}^{+H} \rho\left[\frac{v_R}{R}\frac{\partial}{\partial R}\left(Rv_\phi\right)\right] dz = \int_{-H}^{+H} \frac{B_z}{\mu_0}\frac{dB_\phi}{dz}dz + \int_{-H}^{+H} \frac{1}{R^2}\frac{\partial}{\partial R}\left[R^3\rho\nu\frac{\partial}{\partial R}\left(\frac{v_\phi}{R}\right)dz\right] \tag{3.29}$$

We have

$$\Sigma\left[\frac{v_R}{R}\frac{\partial}{\partial R}\left(Rv_\phi\right)\right] = \frac{B_z}{\mu_0}\left[B_\phi(H) - B_\phi(-H)\right] + \frac{1}{R^2}\frac{\partial}{\partial R}\left[R^3\nu\Sigma\frac{\partial}{\partial R}\left(\frac{v_\phi}{R}\right)\right] \tag{3.30}$$

Now multiplying both sides of Eq. (3.30) by R we get

$$\Sigma\left(v_R\frac{\partial l}{\partial R}\right) = \left[\frac{B_z B_\phi}{\mu_0}\right]_{-H}^{H} R + \frac{1}{R}\frac{\partial}{\partial R}\left[R^3\nu\Sigma\frac{\partial}{\partial R}\left(\frac{l}{R^2}\right)\right], \tag{3.31}$$

where B_ϕ is the sum of toroidal magnetic fields due to the dynamo and the shear, respectively, ${B_\phi}^+(R) \equiv B_\phi(R, z = H) = -B_\phi(R, z = H)$ because of the field antisymmetry and $l = Rv_\phi \propto R^{1/2}$ is the specific angular momentum. The magnetic term describes the exchange of angular momentum between the disc and the star via the magnetosphere. This term vanishes if B_ϕ is an even function of z, but the shear between the disc and the stellar magnetosphere generates an odd B_ϕ whose value in the upper half of the disc is

$$B_{\phi,\mathrm{shear}} = -\gamma B_\mathrm{z}\frac{(\Omega_\mathrm{k} - \Omega_\mathrm{s})}{\Omega_\mathrm{k}}, \tag{3.32}$$

where $\Omega_k = v_\phi/R$, is the angular velocity of the star, γ is a dimensionless free parameter (Ghosh and Lamb 1979).

In this work we will consider the effect of adding a large scale toroidal field, that is generated by an internal dynamo in the accretion disc. Such a dynamo is a natural consequence of the magnetohydrodynamic turbulence in the accretion disc (Balbus and Hawley 1998), and the magnetic field that it generates could have either a positive or a negative parity or be of a mixed kind (e.g. Torkelsson and Brandenburg 1994). In order to estimate the size of $B_{\phi,\mathrm{dyn}}$ we will for the moment assume that the viscous stress in the accretion disc is due to the internal magnetic stress

$$f_{r\phi} = \frac{B_R B_{\phi_{dyn}}}{\mu_0} = \alpha_{ss} P(r) \tag{3.33}$$

where we use the Shakura and Sunyaev (1973) prescription for the viscosity in the last equality. Based on the results of numerical simulations of magnetohydrodynamic turbulence in accretion discs (e.g. Brandenburg et al. 1995; Torkelsson 1998) argued that

$$\gamma_{dyn} = \frac{B_\phi}{B_R} \sim \frac{B_\phi}{B_z} \tag{3.34}$$

where $\gamma_{\mathrm{dyn}} \sim 10$. However this B_ϕ is the sum of the large-scale field and a small-scale turbulent field, which is also contributing to the stress $f_{R\phi}$ through its correlation with a turbulent B_R-field. Since the large-scale field might be a small fraction of the total field we multiply B_ϕ with a factor ϵ to get an estimate for $B_{\phi,\mathrm{dyn}}$:

$$B_{\phi_d yn} = \epsilon \left(\alpha_{ss} \mu_0 \gamma_{dyn} P(r)\right)^{1/2}, \tag{3.35}$$

$-1 \leq \epsilon \leq 1$, and a negative value describes a magnetic field which is pointing in the negative ϕ-direction at the upper disc surface.

The stellar dipolar magnetic field, whose value in the stellar equatorial plane is

$$B_z = -\frac{\mu}{R^3} \tag{3.36}$$

Here μ is the magnetic dipole moment of the star.

Since the magnetic field B_ϕ can be generated through an internal dynamo and the shear through between the disc and magnetosphere, then we now expand the $\frac{B_z B_\phi}{\mu_0}$ term in Eq. (3.31)

$$\Sigma\left(v_R \frac{\mathrm{d}l}{\mathrm{d}R}\right) = 2\frac{B_z}{\mu_0}\epsilon\left(\alpha_{\mathrm{ss}}\mu_0\gamma_{\mathrm{dyn}}P\right)^{1/2} R - 2\gamma\frac{B_z^2}{\mu_0}\frac{\Omega_{\mathrm{k}} - \Omega_{\mathrm{s}}}{\Omega_{\mathrm{k}}}R + \frac{1}{R}\frac{\mathrm{d}}{\mathrm{d}R}\left[R^3\nu\Sigma\frac{\mathrm{d}}{\mathrm{d}R}\left(\frac{l}{R^2}\right)\right]. \tag{3.37}$$

3.3.3 Conservation of Energy

In many astrophysical settings one can distinguish four different energy reservoirs that are involved in magnetohydrodynamics such as magnetic, kinetic, thermal, and potential energy. In accretion discs any other form of energy comes ultimately from the potential energy. This is only possible by getting rid of angular momentum via Reynolds and/ or Maxwell stresses. Here we will restrict ourselves on derivations of energy equations related to thin accretion disc. The Navier- Stoke's equation for the conservation of internal energy can be written as:

$$\frac{\partial}{\partial t}(\rho e) + \nabla \cdot [(\rho e + P)\,\mathbf{v}] = \mathbf{v} \cdot \mathbf{f}_\nu + \frac{\mathbf{J^2}}{\sigma} - \nabla \cdot \mathbf{F_{rad}} - \nabla \cdot \mathbf{q}, \tag{3.38}$$

For steady state Eq. (3.38) becomes

$$\nabla \cdot [(\rho e + P) \cdot \mathbf{v}] = \mathbf{v} \cdot \mathbf{f}_\nu + \frac{\mathbf{J^2}}{\sigma} - \nabla \cdot \mathbf{F_{rad}} - \nabla \mathbf{q}, \tag{3.39}$$

where e is the internal energy, $\mathbf{f}_\nu$ the viscous force that covert kinetic energy to heat , the term $\frac{\mathbf{J^2}}{\sigma}$ is ohmic dissipation, $\nabla \mathbf{q}$ is heat conduction small because the radiative transport or convection will dominate, $\mathbf{F_{rad}}$ is radiative energy flux.

For a slow inflow of matter through an optically thick disc Eq.(3.39) reduces to a balance between the local viscous dissipation $\mathbf{v} \cdot \mathbf{f}_\nu$ and radiative losses $\nabla \cdot \mathbf{F_{rad}}$.

$$\mathbf{v} \cdot \mathbf{f}_\nu = \nabla \cdot \mathbf{F_{rad}}. \tag{3.40}$$

Integrating the viscous dissipation vertically we get the total dissipated power per unit surface area of the disc (Frank, King and Raine 2002)

$$W_\nu = -\frac{9}{8}\nu\Sigma\frac{GM}{R^3} \tag{3.41}$$

This is the dissipation rate as a function of M and R.

If the gas is optically thick, $\mathbf{F_{rad}}$ will approximate the black body flux and $-\nabla \cdot \mathbf{F_{rad}}$ will be given by the Rosseland approximation as.

$$\mathbf{F_{rad}} = -\left(\frac{16\sigma}{3\kappa_R\rho}\right) T^3 \nabla T \tag{3.42}$$

where κ_R is the Rosseland mean opacity. Integrating Eq. (3.42) vertically for an optically thick disc we get

$$\mathbf{F_{rad}} = -\int_0^H \frac{16\sigma T^3}{3\kappa_R\rho}\frac{dT}{dz}dz \simeq -\frac{4\sigma T_c^4}{3\tau}, \tag{3.43}$$

Finally the total dissipated power per unit surface area is now equal to the radiation flux, which is the required energy equation that can relate most of the physical quantities is

$$\frac{9}{8}\nu\Sigma\frac{GM}{R^3} = \frac{4\sigma T_c^4}{3\tau} \tag{3.44}$$

where T_c is the temperature at the midplane of the disc, σ the Stefan - Boltzmann constant and also the magnetic dissipation is negligible as long as $\eta \approx \nu$, where $\eta = 1/\sigma\mu_0$ (here σ is electric conductivity). For optically thick disc the optical depth, τ, of the disc is given by:

$$\tau = \rho H \kappa_{\mathrm{R}}(\rho, T_c) = \frac{1}{2}\Sigma\kappa_{\mathrm{R}} \tag{3.45}$$

and we assume that the opacity is given by Kramer's law

$$\kappa_{\mathrm{R}} = \kappa_0 \rho T_{\mathrm{c}}^{-7/2} \mathrm{m}^2\,\mathrm{kg}^{-1}, \tag{3.46}$$

where $\kappa_0 = 5 \times 10^{20}\,\mathrm{m}^5\ \mathrm{kg}^{-2}\,\mathrm{K}^{-7/2}$.

3.4 Structure equations

A solution for the structure of an accretion disc with an internal dynamo can be found after reducing Eq. (3.37) to a single ordinary differential equation for the radial structure of the accretion disc. First we assume that the disc is dominated by a gas pressure, then the equation of state for an ideal gas:

$$P = \frac{\rho k_B T_c}{m_p \bar{\mu}}, \tag{3.47}$$

where k_B is Boltzmann constant, $\bar{\mu}$ the mean molecular weight, and m_p the mass of a proton. Since the gas pressure is dominant compared to radiation pressure, then the total pressure is equal to the gas pressure. But the pressure can also be expressed using the equation of hydrostatic equilibrium which gives us

$$\frac{1}{2}\frac{\Sigma G M H}{R^3} = \frac{\rho k_B T_c}{\bar{\mu} m_p}, \tag{3.48}$$

which gives us a relation between H and T_c

$$H = \left(\frac{k_B}{m_p\bar{\mu}}\right)^{1/2}\left(\frac{R^3}{GM}\right)^{1/2} T_c^{1/2} \tag{3.49}$$

The viscous stress tensor gives us the equation

$$f_{R\phi} = \frac{3}{4}\Sigma\nu\left(\frac{GM}{R^3}\right)^{1/2} H^{-1} = \alpha_{ss} P(r) \tag{3.50}$$

which we solve for the density of the gas

$$\rho = \frac{3}{4}\alpha_{ss}^{-1}\left(\frac{m_p\bar{\mu}}{k_B}\right)^{3/2}\frac{\nu\Sigma}{T_c^{3/2}}\frac{GM}{R^3} \tag{3.51}$$

The optical depth of the disc is

$$\tau = \frac{9\kappa_0}{16}\alpha_{ss}^{-2}\left(\frac{m_p\bar{\mu}}{k_B}\right)^{5/2}\left(\frac{GM}{R^3}\right)^{3/2}(\nu\Sigma)^2 T_c^{-6} \tag{3.52}$$

where $\kappa_0 = 5\times10^{20}\,\mathrm{m^5\ kg^{-2}\,K^{-7/2}}$.

$$T_c = \alpha_{ss}^{-1/5}\left(\frac{243\kappa_0}{512\sigma}\right)^{1/10}\left(\frac{m_p\bar{\mu}}{k_B}\right)^{1/4}(GM)^{1/4}\,R^{-3/4}(\nu\Sigma)^{3/10} \tag{3.53}$$

Using Eqs.(3.52) and (3.44), and rearranging we have

$$T_c = \left(\frac{243\kappa_0}{512\sigma}\right)^{1/10}\left(\frac{m_p\bar{\mu}}{k_B}\right)^{1/4}\alpha_{ss}^{-1/5}\left(\frac{GM}{R^3}\right)^{1/4}y^{3/10}, \tag{3.54}$$

where $y = \nu\Sigma$. The central temperature depends on mass, radius, alpha and vertically integrated dynamical viscosity, y which is a function of radius. Using expression of temperature the scale height

$$H = \left(\frac{243\kappa_0}{512\sigma}\right)^{1/20}\left(\frac{m_p\bar{\mu}}{k_B}\right)^{-3/8}\alpha_{ss}^{-1/10}\left(\frac{GM}{R^3}\right)^{-3/8}y^{3/20} \tag{3.55}$$

We express the density as

$$\rho = \frac{3}{4}\left(\frac{243\kappa_0}{512\sigma}\right)^{-3/20}\left(\frac{m_p\bar{\mu}}{k_B}\right)^{9/8}\alpha_{ss}^{-7/10}\left(\frac{GM}{R^3}\right)^{5/8}y^{11/20} \tag{3.56}$$

The pressure is then given by

$$P(r) = \frac{3}{4}\left(\frac{243\kappa_0}{512\sigma}\right)^{-1/20}\left(\frac{m_p\bar{\mu}}{k_B}\right)^{3/8}(GM)^{7/8}\,\alpha_{ss}^{-9/10}(\nu\Sigma)^{17/20}R^{-21/8} \tag{3.57}$$

Then equation (3.57) gives

$$P(r) = \frac{3}{4}\left(\frac{243\kappa_0}{512\sigma}\right)^{-1/20}\left(\frac{m_p\bar{\mu}}{k_B}\right)^{3/8}\alpha_{ss}^{-9/10}\left(\frac{GM}{R^3}\right)^{7/8}y^{17/20} \tag{3.58}$$

We see that the total pressure depends on mass, radius, alpha and vertically integrated dynamical viscosity, y.

The ϕ-component of magnetic field generated by the internal dynamo can be expressed using Eqs. (3.58) and (3.35) as:

$$B_{\phi_{dyn}} = \left(\frac{3}{4}\right)^{1/2}\left(\frac{243\kappa_0}{512\sigma}\right)^{-1/40}\left(\frac{m_p\bar{\mu}}{k_B}\right)^{3/16}(GM)^{7/16}\,\alpha_{ss}^{1/20}(\gamma_{dy}\mu_0)^{1/2}y^{17/40}R^{-21/16} \tag{3.59}$$

Then the above equation becomes

$$B_{\phi_{dyn}} = C_1 \epsilon \alpha_{ss}^{1/20} \gamma_{dy}^{1/2} M^{7/16} y^{17/40} R^{-21/16} \tag{3.60}$$

where

$$C_1 = \left(\frac{3\mu_0}{4}\right)^{1/2} \left(\frac{243\kappa_0}{512\sigma}\right)^{-1/40} \left(\left(\frac{m_p \bar{\mu}}{k_B}\right)^3 G^7\right)^{1/16} \tag{3.61}$$

The magnetic field generated due to shear can be rewritten as:

$$B_{\phi,shear} = -\frac{\mu\gamma}{R^3}\left[1 - \left(\frac{R}{R_c}\right)^{3/2}\right], \tag{3.62}$$

where

$$R_c = \left(\frac{GMP^2}{4\pi^2}\right) \simeq 1.5 \times 10^6 P_{spin}^{2/3} \left(\frac{M}{M_\odot}\right)^{1/3} \text{ m}, \tag{3.63}$$

is the co-rotation radius, at which the Keplerian angular velocity is the same as the stellar angular velocity. Here $P_{\rm spin} = 2\pi/\Omega_{\rm s}$ is the spin period of the star, and $M_1 = M/M_\odot$. If the field is moving more rapidly than the disc, which occurs outside the co-rotation radius, then the disc gains angular momentum and is pushed out to greater radii. Inside the corotation radius the disc moves more rapidly than the field and hence loses angular momentum and is accreted more rapidly.

Eqs. (3.60) and (3.62) show that the magnetic field generated by the internal dynamo varies more slowly with radius $\sim R^{-1.3}$ than the magnetic field due to shear, $\sim R^{-3}$. Thus the dynamo component dominates at large radii.

The toroidal component of magnetic field in the disc gives us

$$B_\phi = C_1 \epsilon \alpha_{ss}^{1/20} \gamma_{dy}^{1/2} M^{7/16} y^{17/40} R^{-21/16} - \frac{\mu\gamma}{R^3}\left[1 - \left(\frac{R}{R_c}\right)^{3/2}\right] \tag{3.64}$$

The total magnetic torque is then

$$N_{\rm total,mag} = 4\pi \int_{R_0}^{\infty} \frac{B_z B_{\phi,\rm dyn}}{\mu_0} R^2 dR + 4\pi \int_{R_0}^{\infty} \frac{B_z B_{\phi,\rm shear}}{\mu_0} R^2 dR \tag{3.65}$$

where the first term is the magnetic torque generated due to the dynamo component of the magnetic field and the second term is due to the shear component of the magnetic field.

The shear is resulting from the difference between Ω_s and the Keplerian angular velocity in the disc Ω_k. The toroidal field B_ϕ changes sign about the midplane. At large radius the magnetic field due to dynamo is dominant and at low radius the magnetic field due to shear is dominant

and the resulting field is the sum of the two which shows the nature of magnetic field in the disc. Thus Eq. (3.65) can be rewritten as

$$N_{\rm total,mag} = 4\pi\epsilon \int_{R_0}^{R} \frac{C_1\mu}{\mu_0} y^{17/40} R^{-37/16} dR - 4\pi \int_{R_0}^{R} \frac{\mu^2\gamma}{\mu_0 R^4} \left[1 - \left(\frac{R}{R_c}\right)^{3/2}\right] dR \tag{3.66}$$

The first term is a steep function of radius ($\sim R^{-2.3}$) where as the second one varies with radius ($\sim R^{-4}$). So the first term is dominant at large radii.

Equation (3.37) gives us an ordinary differential equation for y given by

$$y' = \frac{\dot{M}}{6\pi R} - \frac{y}{2R} - C_2 y^{17/40} R^{-45/16} - C_3 R^{-9/2} \left[1 - \left(\frac{R}{R_c}\right)^{3/2}\right], \tag{3.67}$$

where

$$C_2 = \frac{4}{3\mu_0\sqrt{G}} C_1 \epsilon \gamma_{\rm dyn}^{1/2} \alpha_{\rm ss}^{1/20} M^{-1/16} \bar{\mu}^{3/16} \mu \tag{3.68}$$

and

$$C_3 = \frac{4\gamma}{3\mu_0\sqrt{G}} M^{-1/2} \mu^2. \tag{3.69}$$

The solution of Eq. (3.67) approaches the Shakura -Sunyaev solution at large radii, thus giving us the boundary condition $y \longrightarrow \frac{\dot{M}}{3\pi}$ as $R \longrightarrow \infty$.

Now let us introduce the dimensionless variable Λ through

$$y = \Lambda \dot{M}, \tag{3.70}$$

and a dimensionless radial coordinate through

$$R = r R_A, \tag{3.71}$$

where $R_{\rm A}$ is the Alfvén radius in the vicinity of the neutron star,

$$R_A = \left(\frac{2\pi^2\mu^4}{GM\dot{M}^2\mu_0^2}\right)^{1/7} = 5.1 \times 10^6 \dot{M}_{13}^{-2/7} M_1^{-1/7} \mu_{20}^{4/7} \,\mathrm{m}, \tag{3.72}$$

that is given by putting the magnetic pressure equal to the ram pressure of the accreting fluid (e.g. Frank, King & Raine 2002). Here $\dot{M}_{13}$ represents the mass transfer rate in units of $10^{13}\,\mathrm{kg\,s^{-1}}$, and μ_{20} is the stellar magnetic dipole moment in units of $10^{20}\,\mathrm{T\,m^3}$. The boundary condition is then $\Lambda \longrightarrow \frac{1}{3\pi}$ as $r \longrightarrow \infty$, and Eq. (3.67) can be written as

$$\Lambda' = -\frac{\Lambda}{2r} + \frac{1}{6\pi r} - C_4 \Lambda^{17/40} r^{-45/16} - C_5 r^{-9/2}(1 - \omega_s r^{3/2}), \tag{3.73}$$

Table 3.1: Spin parameters of the models

P (s)	$R_{\rm c}$ (m)	$\omega_{\rm s}$
7	6.1×10^6	0.71
18.7	1.2×10^7	0.26
100	3.6×10^7	0.05

where

$$C_4 = 4.9\epsilon\alpha_{\rm ss}^{1/20}\gamma_{\rm dyn}^{1/2}\bar{\mu}^{3/16}M_1^{11/56}\dot{M}_{13}^{-2/35}\mu_{20}^{-1/28}, \tag{3.74}$$

$$C_5 = 0.3\gamma,$$

and

$$\omega_{\rm s} = \left(\frac{R_{\rm A}}{R_{\rm c}}\right)^{3/2} = 6.3\,\dot{M}_{13}^{-3/7}M_1^{-5/7}\mu_{20}^{6/7}P^{-1} \tag{3.75}$$

is the fastness parameter.

3.5 Numerical solution

3.5.1 Global solutions

We integrate Eq. (3.73) inwards from a large radius, usually $100R_{\rm A}$, at which we impose the boundary condition that $\Lambda = \frac{1}{3\pi}$, which is similar to the approach by Brandenburg and Campbell (1998), but most studies of accretion discs have rather applied a boundary condition at the inner edge of the disc, and then integrated the equations outwards. (Paper I) argue that there are two possible boundary conditions that can be applied at the inner edge of the accretion disc, either that $\Lambda = 0$, which corresponds to that ρ and $T \to 0$ at the inner edge (case D), or that

$$\frac{\mathrm{d}}{\mathrm{d}r}\left(r^3\Lambda\frac{\mathrm{d}\Omega}{\mathrm{d}r}\right) = 0, \tag{3.76}$$

which means that the viscosity is not at all contributing to driving the accretion at this radius. Case D is the boundary condition that has been most widely used, and was adopted for instance by Shakura and Sunyaev (1973). In this case the density drops to zero because the inflow velocity becomes infinite, which is of course not realistic, and a more accurate treatment shows that the inflow becomes transonic close to this position Paczyński and Bisnovatyi-Kogan (1981). In case V the inflow at the inner edge of the accretion disc is driven completely by the transfer of excess angular momentum from the accreting matter to the stellar magnetic field (e.g. Wang

1995). For our fiducial model we take a neutron star of $M = 1.4M_{\odot}$ and a magnetic moment of $10^{20}\,\mathrm{T\,m^3}$, which is accreting at $10^{13}\,\mathrm{kg\,s^{-1}}$. The dimensionless parameters γ and $\gamma_{\rm dyn}$ are 1 and 10 respectively in our fiducial model, while $\alpha_{\rm ss} = 0.01$. The exact values of $\alpha_{\rm ss}$ and $\gamma_{\rm dyn}$ are unimportant, since we will vary the parameter ϵ below, but γ influences the solutions in its own way as will be shown at the end of this section. We consider three different spin periods with corresponding co-rotation radii and fastness parameters (see Table.1). Note that the system goes into the propeller regime for $\omega_s \geq 1$ (e.g. Illarionov & Sunyaev 1975, Ghosh & Lamb 1979). Firstly, for a spin period of 7 s and $\epsilon = 1$, 0.1, 0, -0.1, and -1 we get the solutions shown from the top to the bottom of Fig. 3.1. The $\epsilon = -1$ and -0.1 solutions have case D inner boundaries at approximately 5 and 2 $R_{\rm A}$, respectively, while the other three solutions have case V inner boundaries (Fig. 3.2). The inner boundary is close to $R_{\rm A}$ if $\epsilon = 0$, which corresponds to the absence of an internal disc dynamo, but moves outwards as $|\epsilon|$ increases. As we have seen in the Fig.1 as we ascend from the bottom to the top $\Lambda(r) \longrightarrow 0$ at radii which are about five times larger than the Alfvén radius for $\epsilon = 1$ and two times larger than the Alfvén radius for $\epsilon = 0.1$ for two lower solid and dotted lines, respectively. The reason for this is that the dynamo increases the magnetic field and stress in the inner part of the accretion disc but for the rest $\Lambda(r) \neq 0$. For $\epsilon = 0$ as indicated by dashed line in Fig.1 at the middle we have sharp minima at radii about equal to Alfvén radius the sharpness increases for the spin period of less than 7s and decreases as the spin period increases, for ϵ = - 0.1, - 1 we cannot find exactly the minima point of the graph because $\Lambda(r)$ grow with out limit at small radii and the graph becomes smooth curve which corresponds that the accretion is driven by small-scale stresses, which also produce a large-scale weak toroidal magnetic field that couples the accretion disc to the stellar magnetosphere. Notice that in case V the solution continues inside the inner edge of the accretion disc, but the viscosity is counteracting the accretion, which is rather driven by the magnetic stresses. This regime has been described by Campbell (1998), who discussed how the disc is disrupted in this region, and we will therefore assume that this region belongs to a boundary layer that we do not attempt to model in this thesis. On the other hand all solutions approach the Shakura-Sunyaev solution at large radii as required by our boundary condition.

By increasing the spin period to 100 s we see that also the $\epsilon = -0.1$ solution develops a case V inner boundary (Fig. 3.3), but there are only small quantitative changes for the $\epsilon = -1$ and 1 solutions. The dependence of the solution on the spin period can be better seen in Fig. 3.4, where we vary the spin period, when ϵ is fixed to 0. Λ has a local minimum for $P_{\rm s} = 7\,\mathrm{s}$, but

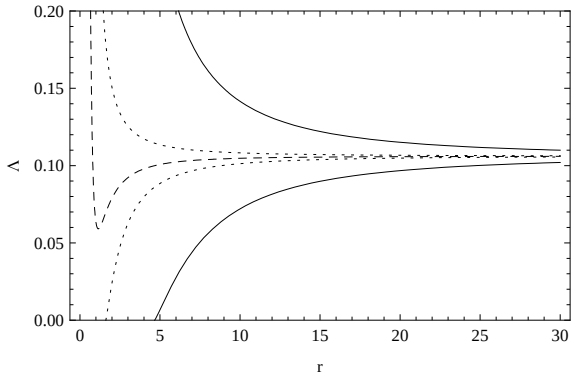

Figure 3.1: $\Lambda(r)$ for our fiducial neutron star with a spin period of 7 s and $\epsilon = 1, 0.1, 0, -0.1, -1$ from the top to the bottom. Note that $\Lambda(r) \to 0$ at $r \approx 4.67 R_{\rm A}$ for $\epsilon = -1$, and at $r \approx 1.62 R_{\rm A}$ for $\epsilon = -0.1$.

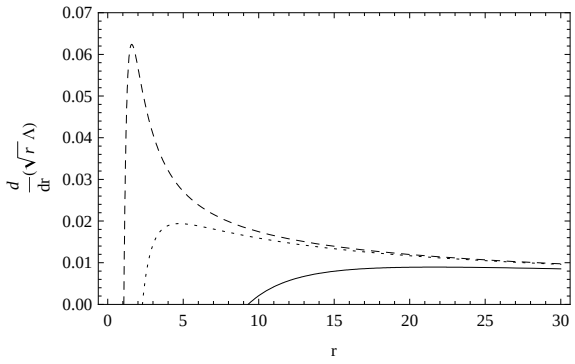

Figure 3.2: $\frac{d}{dr}(\sqrt{r}\Lambda)$, as a function of r for the fiducial neutron star with a spin period of 7 s and with $\epsilon = 1$, 0.1, and 0 from the bottom to the top.

this minimum weakens and disappear as the spin period is increased. This is similar to how Λ depends on ϵ. For $\epsilon = -1$, Λ has an un physical negative local minima at a small radius, such that the physical solution has a case D boundary at several Alfvén radii. As ϵ is increased the local minimum grows and the solution develops a case V inner boundary when the minimum becomes positive. Increasing ϵ further removes the local minimum and the solution becomes a strictly decreasing function of r, which asymptotically approaches $1/3\pi$ as required by our boundary condition. Increasing γ has a similar effect to decreasing ϵ (Fig 3.5).

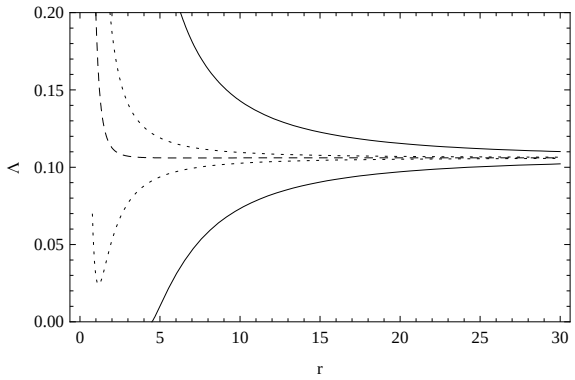

Figure 3.3: $\Lambda(r)$ for our fiducial neutron star with a spin period of 100 s and $\epsilon = 1$, 0.1, 0, -0.1, -1 from the top to the bottom. Note that $\Lambda(r) \to 0$ at $r \approx 4.4R_{\rm A}$ for $\epsilon = -1$, and grow without limit at small radii in all the other cases.

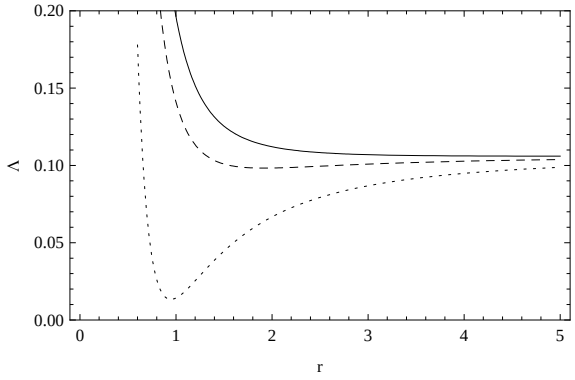

Figure 3.4: $\Lambda(r)$ for our fiducial neutron star with $\epsilon = 0$ and spin periods of 100, 18.7 and 7 s from the top to the bottom. Note that $\Lambda(r)$ develops a local minimum as the spin period decreases.

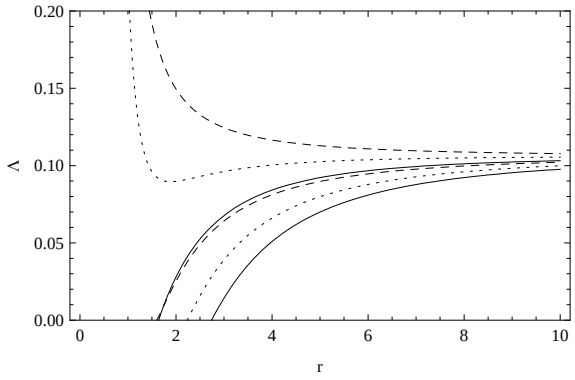

Figure 3.5: $\Lambda(r)$ for our fiducial neutron star with spin period of 7 s and $\epsilon = 0.1$ and $\gamma = 1$, 3 and 5 (upper dashed, dotted and solid lines, respectively), $\epsilon = -0.1$ and $\gamma = 1$, 3 and 5 (lower dashed, dotted and solid lines, respectively).

3.5.2 The structure of an accretion disc

The physical structure of the accretion disc can now be expressed using Λ and $r = R/R_A$. We have that

$$\Sigma = 3.7 \times 10^3 \alpha_{\rm ss}^{-4/5} M_1^{5/14} \dot{M}_{13}^{32/35} \mu_{20}^{-3/7} \Lambda(r)^{7/10} r^{-3/4} \,{\rm kg\,m^{-2}} \tag{3.77}$$

$$T_{\rm c} = 4.8 \times 10^5 \alpha_{\rm ss}^{-1/5} \bar{\mu}^{1/4} M_1^{5/14} \dot{M}_{13}^{18/35} \mu_{20}^{-3/7} \Lambda(r)^{3/10} r^{-3/4} \,{\rm K} \tag{3.78}$$

$$\frac{H}{R} = 0.012 \alpha_{\rm ss}^{-1/10} \bar{\mu}^{-3/8} M_1^{-11/28} \dot{M}_{13}^{4/35} \mu_{20}^{1/14} \Lambda(r)^{3/20} r^{1/8} \tag{3.79}$$

$$\rho = 3.0 \times 10^{-2} \alpha_{\rm ss}^{-7/10} \bar{\mu}^{9/8} M_1^{25/28} \dot{M}_{13}^{38/35} \mu_{20}^{-15/14} \Lambda(r)^{11/20} r^{-15/8} \,{\rm kg\,m^{-3}} \tag{3.80}$$

$$\tau = 370 \alpha_{\rm ss}^{-4/5} \bar{\mu} \dot{M}_{13}^{1/5} \Lambda(r)^{1/5} \tag{3.81}$$

$$\nu = 2.7 \times 10^9 \alpha_{\rm ss}^{4/5} \bar{\mu}^{-3/4} M_1^{-5/14} \dot{M}_{13}^{3/35} \mu_{20}^{3/7} \Lambda(r)^{3/10} r^{3/4} \,{\rm m^2\,s^{-1}} \tag{3.82}$$

$$v_R = 84 \alpha_{\rm ss}^{4/5} \bar{\mu}^{-3/4} M_1^{-3/14} \dot{M}_{13}^{13/35} \mu_{20}^{-1/7} \Lambda(r)^{-7/10} r^{-1/4} \,{\rm m\,s^{-1}} \tag{3.83}$$

$$B_{\phi,{\rm dyn}} = 12 \epsilon \gamma_{\rm dyn}^{1/2} \alpha_{\rm ss}^{1/20} \bar{\mu}^{3/16} M_1^{5/8} \dot{M}_{13}^{4/5} \mu_{20}^{-3/4} \Lambda(r)^{17/40} r^{-21/16} \,{\rm T} \tag{3.84}$$

$$B_{\phi,{\rm shear}} = 0.75 \gamma M_1^{3/7} \dot{M}_{13}^{6/7} \mu_{20}^{-5/7} r^{-3} \left(1 - \omega_s r^{3/2}\right) \,{\rm T} \tag{3.85}$$

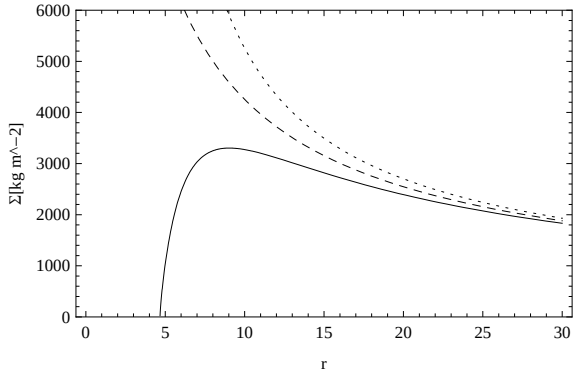

Figure 3.6: Σ as a function of r for the fiducial neutron star with a spin period of 7 s and $\epsilon = -1$ (solid line), $\epsilon = 0$ (dashed line), and $\epsilon = 1$ (dotted line).

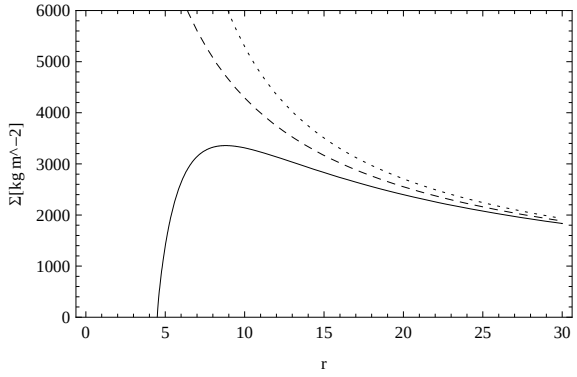

Figure 3.7: Σ, as a function of R for the fiducial neutron star with $\epsilon = 1$ (solid line below dashed line), $\epsilon = 0$ (dashed line), and $\epsilon = -1$ (solid line above dashed line) and spin period of 100s.

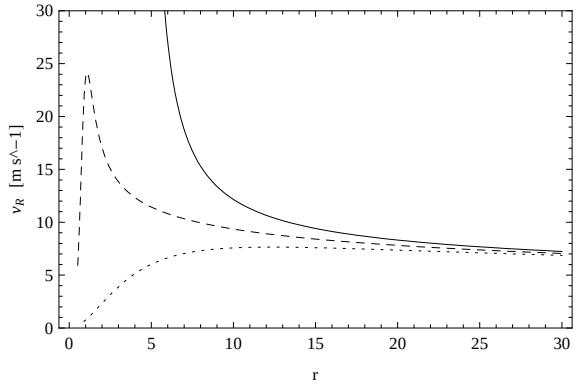

Figure 3.8: V_R as a function of r for the fiducial neutron star with a spin period of 7 s and $\epsilon = -1$ (solid line), $\epsilon = 0$ (dashed line), and $\epsilon = 1$ (dotted line).

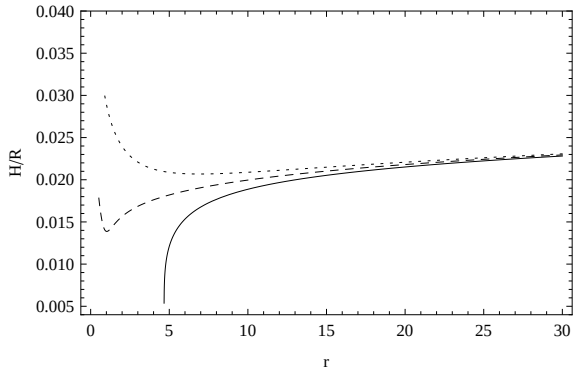

Figure 3.9: The aspect ratio, H/R, as a function of r, for the fiducial neutron star with $\epsilon = -1$ (solid line), $\epsilon = 0$ (dashed line), and $\epsilon = 1$ (dotted line) and a spin period of 7 s.

In Fig.3.6 we show the surface density as a function of radius for the fiducial neutron star with a spin period of 7 s and $\epsilon = -1$, 0, and 1, respectively. Note that for $\epsilon = -1$ the surface density attains a local maximum, while the other models have surface densities that are strictly decreasing functions of r. For $\epsilon = 1$ the surface density is maximum at small radii and decrease at large radii. Thus for a slow rotator the maximum occurs at smaller radius. Our model differs from the standard model in the presence of the numerical solution $\Lambda(r)$ found using Eq.(3.73) which results due to coupling of the magnetic field but at large radii approaches to Shakura-Sunyaev solution. When the magnetic field increases the surface density of the disc increases on the other hand as the spin period of the star increases the surface density decreases, these are related through the numerical solution of using Eq.(3.73). As the radius of the the accretion disc decreases the surface density increases that is the region where the magnetic stress and viscous stress are become comparable. In this region the magnetic stress is sufficiently influential to produce effects. As the accretion rate, mass, and $\Lambda(r)$ increase, so does the surface density. As expected, an increase accretion rate also pushes the disruption radii into smaller radii. Figure. 3.8 shows the radial velocity as a function of r. Since $v_R \propto \Sigma^{-1}$ it becomes infinite as the inner edge of the disc for $\epsilon = -1$, but it stays finite for $\epsilon = 0$ and 1 and eventually goes to 0 in the boundary layer. Increasing the spin period of the neutron star has a very marginal effect on the accretion disc, though $T_{\rm c}$, which is proportional to Σ^2, increases somewhat (Fig.3.10). The aspect ratio grows slowly with r throughout most of the disc, though it varies more rapidly at the inner edge of the disc. In Fig.3.9 the ratio of the disc scale height to radial distance follows an approximately linear relation with radial distance at large radii, slowly decreasing towards the inner edge of accretion disc and non-linear because of the effect of the magnetic field. As

ϵ increases from -1 to 1 the aspect ratio increases as in Fig. 3.6 and 3.10, however, disruption occurs some distance from the star in the same manner and at the same radii as with the surface density. The disc becomes thicker at strong magnetic field, higher accretion rates and $\Lambda(r)$ and the parameter $\frac{H}{R} \ll 1$ shows that the thin disc approximation appears to be justified with this ratio.

In Fig.3.11 the profile of density of the disc-mid plane is very similarly and approximately at the same position as surface density for different ϵ for a given spin period, as the radius increases the density decreases, but increase as the, magnetic field, accretion rate and $\Lambda(r)$ increase. The value indicates that it is very small and fits with Shakura-sunyaev solution at large radii for all values of ϵ.

Increasing the spin period 100 s makes the accretion disc hotter as seen in Figs. 3.7 and 3.10. When ϵ = -1, 0, 1 for spin period of 100 s.

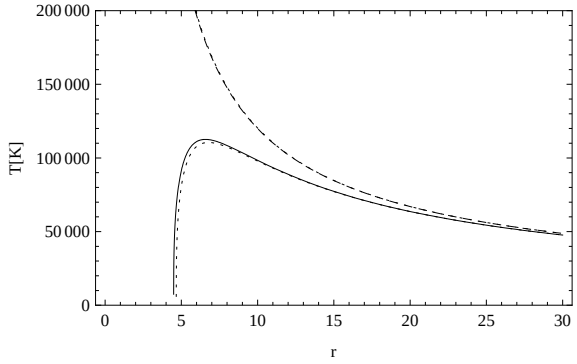

Figure 3.10: T_c as a function of r. The two lower curves show discs with $\epsilon = -1$ around neutron stars with spin periods of 7 s (dashed line) and 100 s (solid line), respectively. The two upper curves show discs with $\epsilon = 1$ around neutron stars with spin periods of 7 s (dashed line) and 100 s (dotted line), respectively.

We plot the magnetic fields for our fiducial model with varying ϵ and spin periods of 7 and 100 s, respectively, in Figs. 3.12 and 3.13, respectively. Note that the co-rotation radius, at which

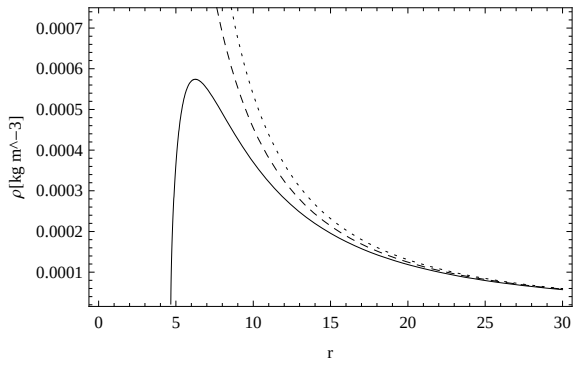

Figure 3.11: Midplane density, ρ_c, as a function of r, for the fiducial neutron star with $\epsilon = -1$ (solid line), $\epsilon = 0$ (dashed line), and $\epsilon = 1$ (dotted line) and a spin period of 7 s.

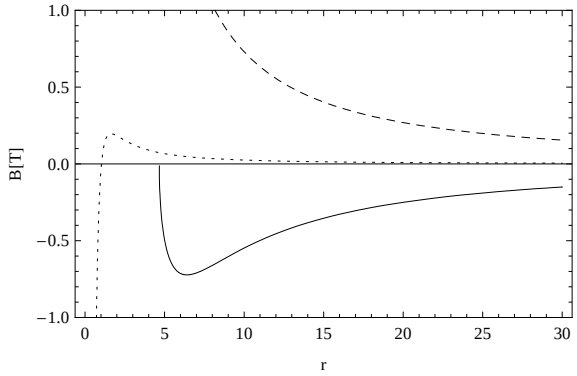

Figure 3.12: The toroidal magnetic field for the fiducial neutron star with a spin period of 7 s. The solid and dashed lines show the field generated by the dynamo for $\epsilon = -1$ and 1, respectively, while the dotted line shows the magnetic field generated by the shear

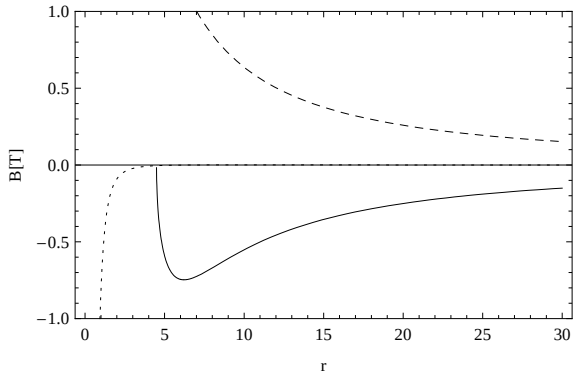

Figure 3.13: The toroidal magnetic field for the fiducial neutron star with a spin period of 100 s. The solid and dashed lines show the field generated by the dynamo for $\epsilon = -1$ and 1, respectively, while the dotted line shows the magnetic field generated by the shear

$B_{\phi\mathrm{shear}}$ changes sign, occurs inside of the inner edge of the accretion disc for $\epsilon = 1$ and -1, and that for these values of ϵ the dominant magnetic field everywhere inside the disc is $B_{\phi\mathrm{dyn}}$. In general the ratio of the magnetic field due to shear to that generated by the internal dynamo is

$$\frac{B_{\phi\mathrm{shear}}}{B_{\phi\mathrm{dyn}}} = 6.25 \times 10^{-2} \epsilon^{-1} \gamma \gamma_{\mathrm{dyn}}^{-1/2} \alpha_{\mathrm{ss}}^{-1/20} \bar{\mu}^{-3/16} M_1^{-11/56} \dot{M}_{13}^{2/35} \mu_{20}^{1/28} \left(1 - \omega_s r^{3/2}\right) \Lambda(r)^{-17/40} r^{-27/16}. \tag{3.86}$$

It is only during rather extreme conditions that the shear-induced field can dominate at small radii, and the dynamo is always dominant at large radii. So that the ratio of $\frac{B_{\phi,\mathrm{dyn}}}{B_{\phi,\mathrm{shear}}} > 1$ at large radii but $\frac{B_{\phi_{dyn}}}{B_{\phi_{shear}}} < 1$ at small radii, therefore, the magnetic field generated by the internal dynamo is strong component of the field.

3.6 Results and discussion

3.6.1 The inner edge of the accretion disc

We have shown that there are two different forms of inner disc boundaries that can be found among our solutions . We denote these as case D and V, respectively. Case D occurs only for sufficiently negative ϵ, while case V covers a larger part of the parameter domain that we have studied (Paper I). We summarise our values for the inner radius of the accretion disc in table. 3.2. We see that the inner radius can be significantly larger than the Alfvén radius when $|\epsilon|$ is close to unity. This is the result of that the dynamo enhances the coupling of the stellar magnetic field to the accretion flow, such that it dominates over the viscous torque at larger radii than would otherwise be the case.

3.6.2 The angular momentum balance

In order to understand the exchange of angular momentum between the accretion disc and its environment we multiply Eq. (3.37) by $2\pi R$ and integrate it from R_0 the inner radius of the disc to R_1 the outer edge of the disc

$$-\dot{M}\left(\sqrt{GMR_1} - \sqrt{GMR_0}\right) = \int_{R_0}^{R_1} 4\pi \frac{B_z B_{\phi,\mathrm{dyn}}}{\mu_0} R^2 \mathrm{d}R + \int_{R_0}^{R_1} 4\pi \frac{B_z B_{\phi,\mathrm{shear}}}{\mu_0} R^2 \mathrm{d}R - 3\pi \left(\nu\Sigma\right)_{R_1} \sqrt{GMR_1} + 3\pi \left(\nu\Sigma\right)_{R_0} \sqrt{GMR_0}. \tag{3.87}$$

The left-hand-side is the difference between the angular momentum that is advected out of the inner edge of the accretion disc and that which is fed into the disc at its outer edge and the right-hand-side describes the contribution of magnetic and viscous torques to the angular momentum balance. Notice that the term $3\pi(\nu\Sigma)_{R_1}\sqrt{GMR_1}$ describes the viscous tension at the outer edge of the disc, which will not be considered further in this paper. Rather we will consider the exchange of angular momentum between the accretion disc and the neutron star. Firstly we have the angular momentum which is advected from the disc to the star

$$N_{adv} = \dot{M}\sqrt{GMR_0} = 2.6 \times 10^{26}\mu_{20}^{2/7}M_1^{3/7}\dot{M}_{13}^{6/7}r_0^{1/2}. \tag{3.88}$$

Then we have the magnetic torques on the neutron star, which we divide into one part due to the shear

$$N_{\rm shr} = -\int_{R_0}^{R_1} 4\pi\frac{B_z B_{\phi,\rm shear}}{\mu_0}R^2{\rm d}R = 7.5 \times 10^{26}\gamma\mu_{20}^{2/7}M_1^{3/7}\dot{M}_{13}^{6/7}\int_{r_0}^{\infty}\left[r^{-4}\left(1-\omega_s r^{3/2}\right)\right]dr \tag{3.89}$$

and a second part due to the dynamo

$$N_{\rm dyn} = -\int_{R_0}^{R_1} 4\pi\frac{B_z B_{\phi,\rm dyn}}{\mu_0}R^2{\rm d}R = 1.2 \times 10^{28}\epsilon\gamma_{dyn}^{1/2}\alpha_{\rm ss}^{1/20}\bar{\mu}^{3/16}\mu_{20}^{1/4}M_1^{5/8}\dot{M}_{13}^{4/5}\int_{r_0}^{\infty}\Lambda^{17/40}r^{-37/16}dr. \tag{3.90}$$

Finally the viscous stress at the inner edge of the accretion disc transports angular momentum outwards away from the neutron star resulting in a torque

$$N_{\rm vis} = -3\pi\left(\nu\Sigma\right)_{R_0}\sqrt{GMR_0} = -2.46 \times 10^{27}\mu_{20}^{2/7}M_1^{3/7}\dot{M}_{13}^{6/7}\Lambda r_0^{1/2} \tag{3.91}$$

Notice that this torque vanishes for a case D inner boundary. We can now calculate the torques on our fiducial neutron star for our choices of spin periods and ϵ. These results are summarized in Tab. 3.2. Unless $\epsilon = 0$ we see that the magnetic torque due to the dynamo is always significantly stronger than the magnetic torque due to the shear, and are both stronger for $\epsilon = 0.1$ than for $\epsilon = 1$. The reason for the latter effect is that the central hole in the disc grows too large when $\epsilon = 1$. The dominant torque at $\epsilon = 1$ is therefore the viscous torque at the inner boundary, which has usually been ignored.

Let us now compare our results with the BATSE data (Bildsten et al. 1997). The 7.6 s X-ray pulsar 4U1626-67 was observed to spin down at a rate $\dot{\nu} \approx -7 \times 10^{-13}\,{\rm Hzs}^{-1}$ and spin up at $\dot{\nu} \approx +8.5 \times 10^{-13}\,{\rm Hz\,s}^{-1}$. These spin variations correspond to torques

$$N = 2\pi\dot{\nu}I = 6.3 \times 10^{25}\dot{\nu}_{-13}I_{38}\,{\rm Nm}, \tag{3.92}$$

where I is the moment of inertia of the neutron star, which we measure in $10^{38}\,\mathrm{kg\,m^2}$, and we measure the spin acceleration in units of $10^{-13}\,\mathrm{Hz\,s^{-1}}$. The required torque is significantly larger than that produced by $N_{\rm shear}$ in any of our models, but $N_{\rm dyn}$ is even an order of magnitude larger than this value if $|\epsilon| = 0.1$. This overestimate can be explained by that we have assumed a unidirectional $B_{\phi,\rm dyn}$ across the disc surface, while it might be more realistic to expect that the toroidal field is organized in magnetic annuli with opposite polarities, or that $|\epsilon|$ is significantly smaller fraction of the total turbulent magnetic field.

We explain the torque reversals in the same way as in (Torkelsson 1998), that the dynamo undergoes a field reversal, which in our model corresponds to that ϵ changes sign. One might speculate that during this field reversal the disc passes through a state corresponding to $\epsilon = 0$, in which the disc will have a smaller inner radius than during the states with an active dynamo. An accretion disc that extends closer to the surface of the neutron star might absorb and re-process more of the X-ray emission that is generated in the accretion columns. Dynamo theory should in principle provide us with an estimate of the interval between the torque reversals. Torkelsson & Brandenburg (1994a) found that an oscillatory dipolar dynamo has a period, $T_{\rm dyn}$, of about $10^{-2}t_\eta$, where $t_\eta = R^2/\eta$ is the diffusive time scale at $6R_0$. If we now assume that the $t_\eta = t_\nu = R^2/\nu$ and that $R_0 = R_A$, then we get that

$$T_{\rm dyn} = 7 \times 10^3 \alpha_{ss}^{-4/5} \bar{\mu}^{3/4} M_1^{1/14} \dot{M}_{13}^{-23/35} \mu^{5/7}\,\mathrm{s} \tag{3.93}$$

and assuming that $\alpha_{ss} = 0.01$, we get a time scale for the dynamo of about 3 days. This should be compared to the observed interval between the torque reversals, which is 10 to 100 days for Cen X-3 and OAO 1657-415, while the time between the torque reversals is several years in GX 1+4 and 4U 1626-67 (Bildsten et al. 1997). Thus the time scale of the oscillatory dipolar dynamo mode is too short to explain the torque reversals, but there is also a steady dipolar mode, which is stable for a finite range of dynamo numbers (Torkelsson & Brandenburg 1994b; Soward 1992). We speculate that this mode goes unstable due to some external perturbation. Assuming that this perturbation is due to an instability in the accretion flow through the disc we expect it to evolve on the global viscous time scale of the disc, which is comparable to the time scale between the torque reversals in Cen X-3, OAO 1657-415 and GX1+4, however 4U 1626-67 is a small system with a viscous time scale on the order of one day (Torkelsson 1998). Perhaps the torque reversals in the latter case are rather due to an instability in the mass transfer from the secondary (cf. Bath 1973).

Table 3.2: The inner edge of the accretion disc and its torque on the fiducial neutron star.

$P_{\rm spin}$ [s]	ϵ	Case	R_0	$N_{\rm shear}$	$N_{\rm dyn}$	$N_{\rm adv}$	$N_{\rm vis}$	$N_{\rm tot}$
7	1	V	$9.0R_A$	7.0×10^{24}	5.7×10^{26}	7.8×10^{26}	-1.2×10^{27}	2.6×10^{26}
	0.1	V	$2.0R_A$	5.3×10^{25}	4.3×10^{27}	3.7×10^{26}	-4.9×10^{26}	4.2×10^{27}
	0	V	R_A	5.9×10^{25}	0	2.6×10^{26}	-1.2×10^{26}	2.0×10^{26}
	-0.1	D	$1.62R_A$	6.34×10^{25}	-3.73×10^{27}	3.32×10^{26}	0	-3.33×10^{27}
	-1	D	$4.67R_A$	1.82×10^{25}	-9.06×10^{26}	5.64×10^{26}	0	-3.24×10^{26}
18.7	1	V	$9R_A$	2.44×10^{24}	5.72×10^{26}	7.83×10^{26}	-1.11×10^{27}	2.47×10^{26}
	0.1	V	$2R_A$	8.18×10^{24}	4.39×10^{27}	3.69×10^{26}	-5.43×10^{26}	4.23×10^{27}
	0	V	R_A	-6.74×10^{25}	0	2.61×10^{26}	-2.96×10^{26}	1.68×10^{26}
	-0.1	V	R_A	-6.74×10^{25}	6.05×10^{27}	2.61×10^{26}	-2.46×10^{25}	-5.87×10^{27}
	-1	D	$4.55R_A$	6.03×10^{24}	-9.31×10^{26}	5.56×10^{26}	0	-3.68×10^{26}
100	1	V	$10R_A$	2.89×10^{23}	4.89×10^{26}	8.25×10^{26}	-1.04×10^{27}	2.80×10^{26}
	0.1	V	$2.5R_A$	-5.45×10^{24}	3.2×10^{27}	4.12×10^{26}	-6.18×10^{26}	3.00×10^{27}
	0	V	$1.2R_A$	-7.06×10^{25}	0	2.86×10^{26}	-4.45×10^{26}	-2.30×10^{26}
	-0.1	V	R_A	-1.26×10^{26}	-7.08×10^{27}	2.61×10^{26}	-4.49×10^{25}	-6.86×10^{27}
	-1	D	$4.4R_A$	-1.41×10^{23}	-9.43×10^{26}	5.47×10^{26}	0	-3.96×10^{26}

3.7 Conclusions

We have investigated the interaction between a magnetic neutron star and its surrounding accretion disc in the case that the accretion disc is supporting an internal dynamo. The magnetic field that is produced by the dynamo can lead to a significant enhancement of the magnetic torque between the neutron star and the accretion disc, compared to what is seen in the model by Ghosh and Lamb (1979). This increase is not so important, but the fact that it naturally explains the torque reversals that have been observed in some disc-accreting X-ray pulsars (Bildsten et al. 1997) is important. This extra magnetic torque can explain the large variations in spin frequency Cen X-3 and OAO 1657-415 (Bildsten et al.1997). Further a reversal of the magnetic field that is generated by the dynamo, similar to the reversals that we see of the magnetic fields on the sun, could explain the torque reversals in theses objects.

From the way that we calculate the structure of the accretion disc we find two kinds of solutions with different behaviour at the inner edge. A few of our solutions have case D boundaries at which the density and temperature go to 0 at finite radius, while most of our solutions have case V boundaries at which the accretion is driven entirely by the magnetic tension between

the accreting matter and the neutron star. In the latter case there is a viscous stress between the accretion disc and the boundary layer, which can transfer angular momentum outwards at a rate that is comparable to the one at which it is advected inwards by the accreting matter itself.

We have also found that the dynamo leads to that the inner edge of the accretion disc occurs at a radius which is larger than the traditional Alfvén radius. For a realistic value of the dynamo-generated magnetic field this effect is small though.

Chapter 4

Accretion discs around millisecond X-ray pulsars

This chapter is adapted from the paper "Thin Accretion Discs Around Millisecond X-ray Pulsars" by Solomon Belay Tessema and Ulf Torkelsson has been submitted to **The Mon. Not.R.Astron.Soc. Journal**.

4.1 Introduction

One decade ago it was shown that neutron stars in low-mass X-ray binaries (LMXBs) are spinning at millisecond periods through the detection of 2.5 ms X-ray pulsations from SAX J1808.4-3658 (Wijnands and van der Klis 1998; Chakrabarty and Morgan 1998; Since then several other millisecond X-ray pulsars with spin periods between 1.7 and 5.4 ms have been discovered (e.g. SAX J1808.4-3658, XTE J0929-314, XTE J1751-305, XTE 1807-294 and XTE J1814-338; see Wijnands 2004 for a review). These neutron stars have considerably weaker magnetic dipole moments, $\sim 10^{16}\,\mathrm{T\,m^3}$, than the conventional X-ray pulsars. With such a weak magnetic field the accretion disc will extend much closer to the neutron star and reach such a high temperature that the opacity can be dominated by electron scattering and radiation pressure can grow stronger than the gas pressure. These situations have already been studied for accretion discs around black holes Shakura and Sunyaev (1973), which have found that there can be a middle region in which the electron scattering is important for the opacity, but the pressure is still dominated by gas pressure, and an inner region in which the structure is

determined by electron scattering and radiation pressure.

The purpose of this chapter is to extend our previous study of an accretion disc with an internal dynamo (Tessema & Torkelsson 2009, hereafter Paper I) to discs around millisecond X-ray pulsars. The most important result of the previous chapter was that the magnetic field that is generated by the disc dynamo can enhance the angular momentum exchange between the accretion disc and the neutron star by more than an order of magnitude (Tessema & Torkelsson 2010, hereafter Paper II) . Furthermore a strong magnetic field in the disc can lead to that the accretion disc is truncated by the stellar magnetic field at larger radius than in the standard model Paper II).

Millisecond X-ray pulsars have a great potential to test the neutron star structure. Because they are exceptional sources of laboratories to study the physics of accretion onto magnetized stars. The matter that accreting neutron stars pull off their companions often settles onto an accretion disc around the neutron star. How matter gets from the inner edge of the disc to the star's surface depends on the strength of the neutron star's magnetic field. For stars with weak magnetic fields, the disc can extend all the way to the surface (Reiun Hoshi 1984; Paper II). For accreting pulsars, which stronger field, the magnetic field stops the disc from getting to close. Accreting matter can only reach the star's surface by flowing along magnetic field lines onto the magnetic poles of the neutron star. The hot polar caps swing past us our lines of sight as the star rotates so that the neutron star as an accreting millisecond pulsars.

The standard model of a viscous accretion disc was formulated by Shakura and Sunyaev (1973). The disc is thin, the vertical scale height of density being much less than its radial length scale. They were able to find a self-consistent solution of the height-integrated hydrodynamic equations, after having introduced $\alpha-$ prescription for the turbulent stress, which transport the angular momentum outwards through the disc and considering the disc consists of three distinct regions. However this did not show the structure solution of accretion disc around millisecond pulsars for different regions.

In this chapter we will extend our previous work model in the spirit of (Shakura and Sunyaev 1973, Shakura and Sunyaev 1976), and divide the disc into an outer region with gas pressure and a free-free opacity, a middle region with gas pressure and electron scattering opacity, and an inner region with radiation pressure and electron scattering. We derive a single ordinary differential equation, which is generally applicable for the radial structure of the accretion disc independently of the equation of state and the form of opacity, we then present regional disc

structure equations, the numerical solutions in each regions, the properties of these solutions and their application to the millisecond X-ray pulsars and finally discuss and summarise our results at the end of this chapter.

4.2 Governing equations

4.2.1 The magnetohydrodynamic angular momentum balance

In the thin axisymmetric Keplerian disc approximation around a magnetized star discussed in the previous chapter, the structure of the thin accretion disc is governed by continuity equation, angular momentum balance, the vertical equilibrium, toroidal magnetic field and conservation of energy that have been derived from equations of magnetohydrodynamics. Here our approach is an extension of the standard model for a thin accretion disc (Shakura and Sunyaev 1973), and it follows closely the method that we introduced in (Paper I), though we will now consider free-free absorption and electron scattering opacity law and equation of state. For this reason we will concentrate on these parts of the derivation that are different from chapter 3 below, and otherwise only summarise the main results of equations derived in the previous chapter for our convenience.

The continuity equation gives us

$$\frac{1}{R}\frac{\partial}{\partial R}(R\Sigma v_R) = 0. \tag{4.1}$$

Now the surface density of the accretion disc is defined by

$$\Sigma = \int_{-\infty}^{\infty} \rho \mathrm{d}z = 2\rho H, \tag{4.2}$$

where ρ is the density, and H is the half-thickness of the disc. We can then write the accretion rate as

$$\dot{M} = -2\pi R\Sigma v_R, \tag{4.3}$$

which is independent of the radial coordinate R, and where v_R is the radial velocity.

From Eq. (3.17) we can derive the momentum equations. The radial component of the momentum is

$$\rho\left[v_R\frac{\partial v_R}{\partial R} - \frac{v_\phi^2}{R} + \frac{GM}{(R^2+z^2)^{3/2}}\right] = \left[\frac{B_z}{\mu_0}\left(\frac{\partial B_R}{\partial z} - \frac{\partial B_z}{\partial R}\right) - \frac{B_\phi}{\mu_0}\left(\frac{1}{R}\frac{\partial}{\partial R}(RB_\phi)\right)\right] - \frac{\partial P}{\partial R} + \frac{4}{3R^{3/2}}\frac{\partial}{\partial R}\left(R^{3/2}\nu\rho\frac{\partial v_R}{\partial R}\right) - \frac{2}{3R^3}\frac{\partial(R^2\nu\rho v_R)}{\partial R} \tag{4.4}$$

The momentum equation for a thin accretion disc is supported by the centrifugal force in the radial direction, so the dominant terms of the equation give us

$$v_\phi^2 - \frac{GM}{R} = 0, \tag{4.5}$$

The vertical component of momentum equation:

$$\begin{aligned} \rho\left[v_R\frac{\partial v_z}{\partial R} + v_z\frac{\partial v_z}{\partial z}\right] &= -\frac{B_\phi}{\mu_0}\frac{\partial B_\phi}{\partial z} - \frac{B_R}{\mu_0}\frac{\partial B_R}{\partial z} + \frac{B_R}{\mu_0}\frac{\partial B_z}{\partial R} \\ -\frac{\partial P}{\partial z} - \frac{\rho GM}{R^2} + \frac{1}{R}\frac{\partial}{\partial R}\left[\rho\nu R\left(\frac{\partial v_z}{\partial R} + \frac{\partial v_R}{\partial z}\right)\right] &+ \frac{4}{3}\frac{\partial}{\partial z}\left[\rho\nu\frac{\partial v_z}{\partial z} - \frac{\partial v_R}{\partial R} - \frac{v_R}{R}\right] \end{aligned} \tag{4.6}$$

The disc is in hydrostatic equilibrium in the vertical direction, which gives us that the pressure at the midplane of the disc is

$$P = \frac{1}{2}H\Sigma\frac{GM}{R^3} = \rho\frac{GMH^2}{R^3} \tag{4.7}$$

but the hydrostatic equilibrium can also be expressed as

$$\frac{H}{R} = \frac{c_\mathrm{s}}{v_\mathrm{kepl}} \tag{4.8}$$

The azimuthal component of Navier- Stoke's equation is:

$$\rho\left(\frac{v_R}{R}\frac{\partial}{\partial R}\left(Rv_\phi\right)\right) = \left[\frac{B_R}{\mu_0}\frac{1}{R}\frac{\partial}{\partial R}(RB_\phi) + \frac{B_z}{\mu_0}\frac{\partial B_\phi}{\partial z}\right] + \frac{1}{R^2}\frac{\partial}{\partial R}\left[R^3\rho\nu\frac{\partial}{\partial R}\left(\frac{v_\phi}{R}\right)\right], \tag{4.9}$$

After keeping the dominant terms of Eq. (4.9) and integrating vertically we obtain

$$\Sigma\left(v_R\frac{\partial l}{\partial R}\right) = \left[\frac{B_zB_\phi}{\mu_0}\right]_{-H}^{H}R + \frac{1}{R}\frac{\partial}{\partial R}\left[R^3\nu\Sigma\frac{\partial}{\partial R}\left(\frac{l}{R^2}\right)\right], \tag{4.10}$$

(see Tessema and Torkelsson 2009) where the specific angular momentum $l = Rv_\phi \propto R^{1/2}$ and ν is the viscosity.

As we pointed out in chapter 3 the magnetic term describes the exchange of angular momentum between the disc and the star via the magnetosphere. The vertical magnetic field is due to the dipolar field of the neutron star in the equatorial plane is

$$B_\mathrm{z} = -\frac{\mu}{R^3} \tag{4.11}$$

where μ is the magnetic dipole moment of the star. Since B_z is an even function of z this term will vanish if B_ϕ is also an even function of z, but the shear between the disc and the stellar magnetosphere generates an odd B_ϕ whose value in the upper half of the disc is

$$B_{\phi,\mathrm{shear}} = -\gamma B_\mathrm{z}\frac{(\Omega_\mathrm{k} - \Omega_\mathrm{s})}{\Omega_\mathrm{k}}, \tag{4.12}$$

where $\Omega_{\rm k} = v_\phi/R$, $\Omega_{\rm s}$ is the angular velocity of the star, and γ is a dimensionless parameter of the order of a few (Ghosh and Lamb 1979). We now add an extra large-scale toroidal field, that is generated by an internal dynamo in the accretion disc. Such a dynamo is a natural consequence of the magnetohydrodynamic turbulence in the accretion disc (e.g. Balbus and Hawley 1998). In order to estimate the size of $B_{\phi,\rm dyn}$ we will for the moment assume that the viscous stress in the accretion disc is due to the internal magnetic stress

$$f_{\rm r\phi} = \frac{B_{\rm R} B_{\phi,\rm dyn}}{\mu_0} = \alpha_{\rm ss} P(r) \tag{4.13}$$

where we use the Shakura and Sunyaev (1973) prescription for the viscosity and $\gamma_{\rm dyn}$ given by Eq. (3.36).

However this B_ϕ is the sum of the large-scale field and a small-scale turbulent field, which is also contributing to the stress $f_{\rm R\phi}$ through its correlation with a turbulent B_R-field. Since the large-scale field might be a small fraction of the total field we multiply B_ϕ with a factor ϵ to get an estimate for $B_{\phi,\rm dyn}$:

$$B_{\phi,\rm dyn} = \epsilon \left(\alpha_{ss}\mu_0\gamma_{dyn}P(r)\right)^{1/2}, \tag{4.14}$$

where $-1 \leq \epsilon \leq 1$, and a negative value describes a magnetic field which is pointing in the negativeϕ-direction at the upper disc surface.

With these preparations we can now re-express Eq. (4.10) as

$$\Sigma\left(v_{\rm R}\frac{\partial l}{\partial R}\right) = -2\epsilon\frac{B_{\rm z}}{\mu_0}\left(\alpha_{\rm ss}\mu_0\gamma_{\rm dyn}P(r)\right)^{1/2}R - 2\gamma\frac{B_{\rm z}^2}{\mu_0}\frac{(\Omega_{\rm k}-\Omega_{\rm s})}{\Omega_{\rm k}}R + \frac{1}{R}\frac{\partial}{\partial R}\left[R^3\nu\Sigma\frac{\partial}{\partial R}\left(\frac{\ell}{R^2}\right)\right]. \tag{4.15}$$

which can be formulated as an ordinary differential equation in $\nu\Sigma$ (Tessema and Torkelsson 2009):

4.2.2 Heating and radiative transport

For a slow inflow of matter through an optically thick disc the local viscous dissipation $\mathbf{v}\cdot\mathbf{f}_\nu$ is balanced by the radiative losses $\nabla\cdot\mathbf{F}_{\rm rad}$. This leads to the height-integrated equation

$$\frac{4\sigma T_{\rm c}^4}{3\tau} = \frac{9}{8}\nu\Sigma\frac{GM}{R^3} \tag{4.16}$$

where $T_{\rm c}$ is the temperature at the midplane of the disc, σ the Stefan - Boltzmann constant, and the optical depth of the disc is given by:

$$\tau = \int_0^z \kappa\rho dz = \rho H\kappa = \frac{1}{2}\Sigma\kappa \tag{4.17}$$

where the general opacity is

$$\kappa = \kappa_{\rm es} + \kappa_{\rm ff}, \tag{4.18}$$

the electron scattering opacity is

$$\kappa_{\rm es} = 0.04 \ {\rm m}^2 \, {\rm kg}^{-1}, \tag{4.19}$$

and the free-free absorption is given by Kramer's law

$$\kappa_{\rm ff} = \kappa_0 \rho T_c^{-7/2} {\rm m}^2 \, {\rm kg}^{-1} \tag{4.20}$$

with

$$\kappa_0 = 5 \times 10^{20} \ {\rm m}^5 \, {\rm kg}^{-2} \, {\rm K}^{7/2}. \tag{4.21}$$

4.2.3 Disc structure equations

The total pressure is the sum of gas and radiation pressure

$$P(\rho, T) = \frac{\rho k_{\rm B} T_{\rm c}}{m_{\rm p} \bar{\mu}} + \frac{4\sigma T_c^4}{3c} \tag{4.22}$$

where $k_{\rm B}$ is Boltzmann's constant, $\bar{\mu} = 0.62$ the mean molecular weight for fully ionised gas, $m_{\rm p}$ the mass of a proton, and c the speed of light, but the pressure can also be expressed using the equation (4.7) for hydrostatic equilibrium. We can thus express the scale height in terms of gas and radiation pressure

$$H = \left(\frac{k_B T_{\rm c} R^3}{m_{\rm p} \bar{\mu} G M} + \frac{4\sigma T_c^4 R^3}{3c\rho G M} \right)^{1/2}. \tag{4.23}$$

The viscosity model (Tessema & Torkelsson 2009) assumes that

$$\nu = \frac{4}{3} \alpha_{\rm ss} \frac{PH}{\Sigma} \left(\frac{GM}{R^3} \right)^{-1/2} = \frac{2}{3} \alpha_{\rm ss} \frac{P}{\rho} \left(\frac{GM}{R^3} \right)^{-1/2}, \tag{4.24}$$

where $\alpha_{\rm ss}$ is a parameter which describe the strength of the viscous stress. From Eq. (4.24) the internal pressure can be expressed as

$$P(r) = \frac{3}{2} \alpha_{\rm ss}^{-1} \nu \rho \left(\frac{GM}{R^3} \right)^{1/2} \tag{4.25}$$

which we solve for the density of the gas

$$\rho = \frac{3}{4\alpha_{\rm ss}} \frac{\nu \Sigma}{H^3} \left(\frac{GM}{R^3} \right)^{-1/2}. \tag{4.26}$$

Combining Eqs. (4. 16), (4.17), and (4.18) we get

$$T_c^4 = \frac{27}{32\sigma} \rho H (\kappa_R + \kappa_{es}) \nu \Sigma \frac{GM}{R^3} \tag{4.27}$$

Combining Eqs. (4.12),(4.13),(4.17) and (4.25) and solving for $y = \nu\Sigma$ we get

$$y' = \frac{\dot{M}}{6\pi R} - \frac{y}{2R} - \epsilon \left[\frac{4\mu^2\gamma_{dyn}y}{3\mu_0 H R^{3/2}}\right]^{1/2} (GM)^{-1/4} R^{-3/2} - \frac{4\mu^2\gamma}{3\mu_0\sqrt{GM}} R^{-9/2} \left[1 - \left(\frac{R}{R_c}\right)^{3/2}\right], \tag{4.28}$$

where R_c is the co-rotation radius given by Eq. (3.59).

As $R \to \infty$, the standard disc theory gives

$$y \to \frac{\dot{M}}{3\pi},$$

which we use as the outer boundary condition.

We now introduce the dimensionless variable Λ through

$$y = \Lambda\dot{M}, \tag{4.29}$$

and a dimensionless radial coordinate through

$$R = rR_{\rm A}, \tag{4.30}$$

where $R_{\rm A}$ is the Alfvén radius, which is given by putting the magnetic pressure equal to the ram pressure

$$R_A = \left(\frac{2\pi^2\mu^4}{GM\dot{M}^2\mu_0^2}\right)^{1/7} \simeq 1.4 \times 10^4 \dot{M}_{14}^{-2/7} M_1^{-1/7} \mu_{16}^{4/7} \mathrm{m}, \tag{4.31}$$

where $\dot{M}_{14}$ represents the mass transfer rate in units of $10^{14}\,\mathrm{kg\,s^{-1}}$, and μ_{16} is the stellar magnetic moment in units of $(\mu 10^{16})\mathrm{T\,m^3}$.

Furthermore we introduce the fastness parameter

$$\omega_s = \left(\frac{R_A}{R_c}\right)^{3/2} = 0.36 M_1^{-5/7} \dot{M}_{14}^{-3/7} \mu_{16}^{6/7} \left(\frac{P_{spin}}{4.8\mathrm{ms}}\right)^{-1}. \tag{4.32}$$

We can now write Eq. (4.28) as:

$$\Lambda' = \frac{1}{6\pi r} - \frac{\Lambda}{2r} - \epsilon \left[\frac{4\mu^2\gamma_{dyn}\Lambda}{3\mu_0 H\dot{M}}\right]^{1/2} (GM)^{-1/4} R_A^{-5/4} r^{-9/4} - \frac{4\mu^2\gamma}{3\mu_0\sqrt{GM}\dot{M}} R_A^{-7/2} r^{-9/2} \left[1 - \left(\frac{R}{R_c}\right)^{3/2}\right], \tag{4.33}$$

Note that the expression for H is different for different disc regions. In order to make further progress we have to specialise to a certain region of the disc.

With gas pressure and Kramer's opacity we get

$$H(r) = \left(\frac{243\kappa_0}{512\sigma}\right)^{1/20} \alpha_{\rm ss}^{-1/10} \left(\frac{k_{\rm B}R^3}{m_p\bar{\mu}GM}\right)^{3/8} (\nu\Sigma)^{3/20}, \tag{4.34}$$

and for the gas pressure and electron scattering opacity

$$H(r) = \left(\frac{81\kappa_{\rm es}}{128\sigma\alpha_{\rm ss}}\right)^{1/10}\left(\frac{k_{\rm B}}{m_p\bar{\mu}}\right)^{2/5}\left(\frac{R^3}{GM}\right)^{7/20}(\nu\Sigma)^{1/5}. \tag{4.35}$$

Finally with radiation pressure and electron scattering the scale height is

$$H = \frac{9\kappa_{\rm es}}{8c}\nu\Sigma \tag{4.36}$$

which is essentially independent of R. This comes from the fact that for radiation pressure $T_{\rm c}^4 \sim \nu\Sigma MR^{-3}$. Now Eq. (4.33) can then be solved numerically.

Since we divide the disc in to three regions such as the outer, the middle and the inner regions, then the structure equation for three regions are derived as follows:

4.2.4 The outer disc equations

Using Eq.(4.34) for the scale height, then the expression for the surface density of the outer disc becomes

$$\Sigma = \frac{3}{2}\left(\frac{243\kappa_0}{512\sigma}\right)^{-1/10}\left(\frac{m_p\bar{\mu}}{k_B}\right)^{-3/4}\alpha_{ss}^{-4/5}\left(\frac{GM}{R^3}\right)^{1/4}(\nu\Sigma)^{7/10} \tag{4.37}$$

The optical depth of the disc is

$$\tau = \frac{9\kappa_0}{16}\alpha_{ss}^{-2}\left(\frac{m_p\bar{\mu}}{k_B}\right)^{5/2}\left(\frac{GM}{R^3}\right)^{3/2}(\nu\Sigma)^2T_c^{-6} \tag{4.38}$$

where $\kappa_0 = 5\times10^{20}\,{\rm m}^5\ {\rm kg}^{-2}\,{\rm K}^{-7/2}$.

$$T_c = \alpha_{ss}^{-1/5}\left(\frac{243\kappa_0}{512\sigma}\right)^{1/10}\left(\frac{m_p\bar{\mu}}{k_B}\right)^{1/4}(GM)^{1/4}\,R^{-3/4}(\nu\Sigma)^{3/10} \tag{4.39}$$

We express the density as

$$\rho = \frac{3}{4}\left(\frac{243\kappa_0}{512\sigma}\right)^{-3/20}\left(\frac{m_p\bar{\mu}}{k_B}\right)^{9/8}\alpha_{ss}^{-7/10}\left(\frac{GM}{R^3}\right)^{5/8}(\nu\Sigma)^{11/20} \tag{4.40}$$

The pressure is then given by

$$P(r) = \frac{3}{4}\left(\frac{243\kappa_0}{512\sigma}\right)^{-1/20}\left(\frac{m_p\bar{\mu}}{k_B}\right)^{3/8}(GM)^{7/8}\,\alpha_{ss}^{-9/10}(\nu\Sigma)^{17/20}R^{-21/8} \tag{4.41}$$

Then we obtained the magnetic field generated by the internal dynamo :

$$B_{\phi_{dyn}} = \left(\frac{3}{4}\right)^{1/2}\left(\frac{243\kappa_0}{512\sigma}\right)^{-1/40}\left(\frac{m_p\bar{\mu}}{k_B}\right)^{3/16}(GM)^{7/16}\,\alpha_{ss}^{1/20}(\gamma_{dy}\mu_0)^{1/2}(\nu\Sigma)^{17/40}R^{-21/16} \tag{4.42}$$

4.2.5 The middle disc equations

Using Eq. (4.35) for the middle region some of the structure equations are given as follows

$$\Sigma = \frac{3}{2\alpha_{\rm ss}} \left(\frac{81\kappa_{\rm es}}{128\sigma\alpha_{\rm ss}}\right)^{-1/5} \left(\frac{m_p\bar{\mu}}{\kappa_B}\right)^{4/5} \left(\frac{GM}{R^3}\right)^{1/5} (\nu\Sigma)^{3/5} \tag{4.43}$$

Inserting equation (4.35) into (4.27) gives the midplane temperature as

$$T_c = \left(\frac{81\kappa_{\rm es}}{128\sigma\alpha_{\rm ss}}\right)^{1/5} \left(\frac{m_p\bar{\mu}}{\kappa_B}\right)^{1/5} \left(\frac{GM}{R^3}\right)^{3/10} (\nu\Sigma)^{2/5} \tag{4.44}$$

$$P = \frac{3}{4\alpha_{\rm ss}} \left(\frac{81\kappa_{\rm es}}{128\sigma\alpha_{\rm ss}}\right)^{-1/10} \left(\frac{m_p\bar{\mu}}{\kappa_B}\right)^{7/5} \left(\frac{GM}{R^3}\right)^{17/20} (\nu\Sigma)^{4/5} \tag{4.45}$$

$$\rho = \frac{3}{4\alpha_{\rm ss}} \left(\frac{81\kappa_{\rm es}}{128\sigma\alpha_{\rm ss}}\right)^{-3/10} \left(\frac{m_p\bar{\mu}}{\kappa_B}\right)^{6/5} \left(\frac{GM}{R^3}\right)^{11/20} (\nu\Sigma)^{2/5} \tag{4.46}$$

$$\tau = \frac{3}{\alpha_{\rm ss}} \left(\frac{81\kappa_{\rm es}}{128\sigma\alpha_{\rm ss}}\right)^{-1/5} \left(\frac{m_p\bar{\mu}}{\kappa_B}\right)^{4/5} \left(\frac{GM}{R^3}\right)^{1/5} (\nu\Sigma)^{3/5} \tag{4.47}$$

The equation for the magnetic field generated by an internal dynamo is

$$B_{\phi,\rm dyn} = \left(\frac{3\mu_0\gamma_{\rm dyn}}{4}\right)^{1/2} \left(\frac{81\kappa_{\rm es}}{128\sigma\alpha_{\rm ss}}\right)^{-1/20} \left(\frac{m_p\bar{\mu}}{\kappa_B}\right)^{7/10} \left(\frac{GM}{R^3}\right)^{17/40} (\nu\Sigma)^{2/5} \tag{4.48}$$

4.2.6 The inner disc equations

Similarly using scale height for the radiation pressure dominated disc we obtain the inner disc equations

$$\Sigma = \frac{32c^3}{27\kappa_{\rm es}\alpha_{\rm ss}} \left(\frac{GM}{R^3}\right)^{1/2} (\nu\Sigma)^{-1} \tag{4.49}$$

$$T_c = \left(\frac{c^2}{2\kappa_{\rm es}\alpha_{\rm ss}}\right)^{1/4} \left(\frac{GM}{R^3}\right)^{1/8} \tag{4.50}$$

The temperature depend mass, radius and α in the inner region of the disc.

$$P = \frac{2c}{3\kappa_{\rm es}\alpha_{\rm ss}} \left(\frac{GM}{R^3}\right)^{1/2} \tag{4.51}$$

This pressure is independent of dynamical viscosity in the inner regions of the disc.

$$\rho = \frac{128c^3}{243\kappa_{\rm es}^3\alpha_{\rm ss}} \left(\frac{GM}{R^3}\right)^{1/2} (\nu\Sigma)^{-2} \tag{4.52}$$

The optical depth the inner region is

$$\tau = \frac{16c^3}{27\kappa_{\rm es}\alpha_{\rm ss}} \left(\frac{GM}{R^3}\right)^{1/2} (\nu\Sigma)^{-1} \tag{4.53}$$

Finally dynamo component of the magnetic field is

$$B_{\phi,\mathrm{dyn}} = \left(\frac{2c\gamma_{\mathrm{dyn}}\mu_0}{3\kappa_{\mathrm{es}}\alpha_{\mathrm{ss}}}\right)^{1/2}\left(\frac{GM}{R^3}\right)^{1/4} \tag{4.54}$$

Now will continue to find the structure solutions for regional disc in terms of the required parameters.

4.3 Regional disc structure equations

Several regions in the accretion flows have been identified (Shakura and Sunyaev, 19973, 1976; Novikov and Thorne, 1973; Kafatos, 1998). These are: i) an outer region where gas pressure dominates over radiation pressure and where the opacity is predominantly free-free absorption; ii) a middle region where gas pressure again dominates but the opacity is primarily due to electron scattering; and iii) an inner region where radiation pressure dominates over gas pressure and the opacity is due to electron scattering. We can now write down the self similar structure of the different regions of the accretion disc in terms of the function $\Lambda(r)$. The toroidal magnetic field is given by the same expression:

$$B_{\phi,\mathrm{sh}} = -3.64\times10^3\gamma M_1^{3/7}\dot{M}_{14}^{6/7}\mu_{16}^{-5/7}\left(1-\omega_s r^{3/2}\right)r^{-3}\mathrm{T} \tag{4.55}$$

everywhere in the disc, but for all the other relevant quantities we have to handle the different regions of the disc separately.

In the outer disc where $P_{\mathrm{g}} \gg P_{\mathrm{rad}}$, and $\kappa_{\mathrm{ff}} \gg \kappa_{\mathrm{es}}$ we have that:

$$\Sigma = 1.58\times10^6\bar{\mu}^{3/4}\alpha_{ss}^{-4/5}M_1^{5/14}\dot{M}_{14}^{32/35}\mu_{16}^{-3/7}\Lambda(r)^{7/10}r^{-3/4}\mathrm{kg\,m^{-2}} \tag{4.56}$$

$$T_c = 8.12\times10^7\bar{\mu}^{1/4}\alpha_{ss}^{-1/5}M_1^{5/14}\dot{M}_{14}^{18/35}\mu_{16}^{-3/7}\Lambda(r)^{3/10}r^{-3/4}\mathrm{K} \tag{4.57}$$

$$\frac{H}{R} = 8.09\times10^{-3}\bar{\mu}^{-3/8}\alpha_{ss}^{-1/10}M_1^{-11/28}\dot{M}_{14}^{4/35}\mu_{16}^{1/14}\Lambda(r)^{3/20}r^{1/8} \tag{4.58}$$

$$\rho_c = 7.06\times10^3\bar{\mu}^{9/8}\alpha_{ss}^{-7/10}M_1^{25/28}\dot{M}_{14}^{38/35}\mu_{16}^{-15/14}\Lambda(r)^{11/20}r^{-15/8}\mathrm{kg\,m^3} \tag{4.59}$$

$$\tau_{ff} = 5.86\times10^2\alpha_{ss}^{-4/5}\bar{\mu}\dot{M}_{14}^{1/5}\Lambda(r)^{1/5} \tag{4.60}$$

$$\nu = 6.35\times10^7\bar{\mu}^{-3/4}\alpha_{ss}^{4/5}M_1^{-5/14}\dot{M}_{14}^{3/35}\mu_{16}^{3/7}\Lambda(r)^{3/10}r^{3/4}\mathrm{m^2\,s^{-1}} \tag{4.61}$$

$$v_R = -7.36 \times 10^2 \bar{\mu}^{-3/4} \alpha_{ss}^{4/5} M_1^{-3/14} \dot{M}_{14}^{13/35} \mu_{16}^{-1/7} \Lambda(r)^{-7/10} r^{-1/4} \mathrm{m\,s^{-1}} \tag{4.62}$$

$$P_c = 2.74 \times 10^{18} \bar{\mu}^{3/8} \alpha_{ss}^{-9/10} M_1^{5/4} \dot{M}_{14}^{8/5} \mu_{16}^{-3/2} \Lambda(r)^{17/20} r^{-21/8} \mathrm{N\,m^{-2}} \tag{4.63}$$

$$B_{\phi,\mathrm{dyn}} = 7.66 \times 10^4 \epsilon \bar{\mu}^{3/16} \gamma_{\mathrm{dyn}}^{1/2} \alpha_{ss}^{1/20} M_1^{5/8} \dot{M}_{14}^{4/5} \mu_{16}^{-3/4} \Lambda(r)^{17/40} r^{-21/16} \mathrm{T} \tag{4.64}$$

The transition from the outer to the middle region occur where $\kappa_{\mathrm{es}} = \kappa_{\mathrm{ff}}$. Assuming that $\Lambda \simeq 1/3\pi$ at this point we have that the transition radius is

$$r_{OM} = 46.7 \bar{\mu}^{-1/3} M_1^{10/21} \dot{M}_{14}^{20/21} \mu_{16}^{-4/7},$$

which is independent of α_{ss}.

In the middle disc where $P_{\mathrm{g}} \gg P_{\mathrm{rad}}$, and $\kappa_{\mathrm{es}} \gg \kappa_{\mathrm{ff}}$ the solution in this region is:

$$\Sigma = 7.08 \times 10^5 \bar{\mu}^{4/5} \alpha_{ss}^{-4/5} M_1^{2/7} \dot{M}_{14}^{27/35} \mu_{16}^{-12/35} \Lambda(r)^{3/5} r^{-3/5} \mathrm{kg\,m^{-2}} \tag{4.65}$$

$$T_c = 1.79 \times 10^8 \bar{\mu}^{1/5} \alpha_{ss}^{-1/5} M_1^{3/7} \dot{M}_{14}^{23/35} \mu_{16}^{-18/35} \Lambda(r)^{2/5} r^{-9/10} \mathrm{K} \tag{4.66}$$

$$\frac{H}{R} = 1.25 \times 10^{-2} \bar{\mu}^{-2/5} \alpha_{ss}^{-1/10} M_1^{-5/14} \dot{M}_{14}^{13/70} \mu_{16}^{1/14} \Lambda(r)^{1/5} r^{1/20} \tag{4.67}$$

$$\rho_c = 2.03 \times 10^3 \bar{\mu}^{6/5} \alpha_{ss}^{-7/10} M_1^{11/14} \dot{M}_{14}^{61/70} \mu_{16}^{-33/35} \Lambda(r)^{2/5} r^{-33/20} \mathrm{kg\,m^{-3}} \tag{4.68}$$

$$P_g = 3.2 \times 10^{15} \bar{\mu}^{2/5} \alpha_{ss}^{-9/10} M_1^{17/14} \dot{M}_{14}^{107/70} \mu_{16}^{-51/35} \Lambda(r)^{4/5} r^{-51/20} \mathrm{N\,m^{-2}} \tag{4.69}$$

$$\tau = 1.42 \times 10^4 \bar{\mu}^{13/10} \alpha_{ss}^{-4/5} M_1^{2/7} \dot{M}_{14}^{27/35} \mu_{16}^{3/35} \Lambda(r)^{3/5} r^{-3/5} \tag{4.70}$$

$$\nu = 1.48 \times 10^8 \bar{\mu}^{-4/5} \alpha_{ss}^{4/5} M_1^{-2/7} \dot{M}_{14}^{8/35} \mu_{16}^{12/35} \Lambda(r)^{2/5} r^{3/5} \mathrm{m^2\,s^{-1}} \tag{4.71}$$

$$v_R = -1.61 \times 10^3 \bar{\mu}^{-4/5} \alpha_{ss}^{4/5} M_1^{-1/7} \dot{M}_{14}^{18/35} \mu_{16}^{-8/35} \Lambda(r)^{-3/5} r^{-2/5} \mathrm{m\,s^{-1}} \tag{4.72}$$

$$B_{\phi,\mathrm{dyn}} = 6.27 \times 10^4 \epsilon \bar{\mu}^{1/5} \gamma_{\mathrm{dyn}}^{1/2} \alpha_{ss}^{1/20} M_1^{17/28} \dot{M}_{14}^{107/140} \mu_{16}^{-51/70} \Lambda(r)^{2/5} r^{-51/40} \mathrm{T} \tag{4.73}$$

The disc structure changes drastically in the inner disc where $P_{\rm rad} \gg P_{\rm g}$ and $\kappa_{\rm es} \gg \kappa_{\rm ff}$, for instance the disc thickness is independent of radius. The complete solution in this region is

$$\Sigma = 9.56 \times 10^{1} \alpha_{ss}^{-1} M_1^{-5/7} \dot{M}_{14}^{-10/7} \mu_{16}^{6/7} \Lambda(r)^{-1} r^{3/2} \mathrm{kg\,m^{-2}} \tag{4.74}$$

$$T_c = 1.93 \times 10^{7} \alpha_{ss}^{-1/4} M_1^{5/28} \dot{M}_{14}^{3/28} \mu_{16}^{-3/14} r^{-3/8} \mathrm{K} \tag{4.75}$$

$$\frac{H}{R} = 1.07 M_1^{1/7} \dot{M}_{14}^{9/7} \mu_{16}^{-4/7} \Lambda(r) r^{-1} \tag{4.76}$$

$$\rho_c = 3.19 \times 10^{-3} \alpha_{ss}^{-1} M_1^{-5/7} \dot{M}_{14}^{-17/7} \mu_{16}^{6/7} \Lambda(r)^{-2} r^{3/2} \mathrm{kg\,m^{-3}} \tag{4.77}$$

$$P = 3.49 \times 10^{13} \alpha_{ss}^{-1} M_1^{5/7} \dot{M}_{14}^{3/7} \mu_{16}^{-6/7} r^{-3/2} \mathrm{N\,m^{-2}} \tag{4.78}$$

$$\tau_{es} = 1.92 \alpha_{ss}^{-1} M_1^{-5/7} \dot{M}_{14}^{-10/7} \mu_{16}^{6/7} \Lambda(r)^{-1} r^{3/2} \tag{4.79}$$

$$\nu = 1.05 \times 10^{12} \alpha_{ss} M_1^{5/7} \dot{M}_{14}^{17/7} \mu_{16}^{-6/7} \Lambda(r)^{2} r^{-3/2} \mathrm{m^2\,s^{-1}} \tag{4.80}$$

$$v_R = -1.19 \times 10^{7} \alpha_{ss} M_1^{6/7} \dot{M}_{14}^{19/7} \mu_{16}^{-10/7} \Lambda(r) r^{-5/2} \mathrm{m\,s^{-1}} \tag{4.81}$$

$$B_{\phi,\rm dyn} = 6.62 \times 10^{3} \epsilon \gamma_{\rm dyn}^{1/2} M_1^{5/14} \dot{M}_{14}^{3/14} \mu_{16}^{-3/7} r^{-3/4} \mathrm{T} \tag{4.82}$$

$$B_{\phi,\rm sh} = -3.64 \times 10^{3} \gamma M_1^{3/7} \dot{M}_{14}^{6/7} \mu_{16}^{-5/7} \left(1 - \omega_s r^{3/2}\right) r^{-3} \mathrm{T} \tag{4.83}$$

It is of particular significance here that $\Sigma \propto \Lambda^{-1}$.

The transition radius between the middle and the inner region is estimated by equating the gas and radiation pressures in the middle region and approximating Λ with $1/3\pi$

$$r_{IM} = 12.5 \bar{\mu}^{8/21} \alpha_{\rm ss}^{2/21} M_1^{10/21} \dot{M}_{14}^{22/21} \mu_{16}^{-4/7}$$

We then see that the accretion disc right outside of the Alfvén radius is dominated by radiation pressure only if

$$\mu_{16} < 83.1 \bar{\mu}^{2/3} \alpha_{\rm ss}^{1/6} M_1^{5/6} \dot{M}_{14}^{11/6} \tag{4.84}$$

This condition is not fulfilled for a conventional X-ray pulsar with a magnetic dipole moment of $\sim 10^{20}\,\mathrm{T\,m^3}$ (White & Stella 1988). Rather for a neutron star accreting at $\sim 5\%$ of the Eddington limit it requires a magnetic field as weak as $10^4 - 10^5\,\mathrm{T}$ as in the millisecond X-ray pulsars.

4.4 Global solutions

During the numerical iteration the two quantities R_A and R_c are very important because they determine how and when the accretion disc terminates. According to the conventional picture, the Alfvén radius is supposed to lie with in the corotation radius, in order for accretion to take place (e.g. Lamb, Pethian, and Pines 1973, Ghosh and Lamb 1979). Otherwise, the material of the disc which couples to the magnetic field is forced to rotate faster than the local Keplerian velocity and may be expelled from the system (Illarionov and Sunyaev, 1975). If the accretion rate is too large, then the value of the Alfvén radius could drop below a value of $\sim$ 10kms, the approximate radius of the accreting neutron star. For typical system parameter values associated with accreting millisecond pulsars, Alfvén radius might have to lie with a rather restricted range, e.g. 10 - 35 km. Thus selecting the magnetic field values and accretion would have to be in just the correct range to allow accretion to continue through out (see also Burderi and King 1998; Psaltis and Chakrabarty 1999). With appropriate selection of the magnetic field and accretion rate, then the regional solution is found below. We write Eq. (4.33) for the different regimes of the disc using the expression of scale height for each regions. We integrate these equations for outer, middle and inner regions inwards from the large radius usually $1000R_A$ for outer region, small radius $\sim$ 8.5 for the middle region and very small radius $\sim$ 12.5 for the inner regions of the disc at which we impose the boundary conditions that $\Lambda = \frac{1}{3\pi}$, which is close to the approach by Paper I and Brandenburg and Campbell (1998). For our fiducial model we take a neutron star of $M = 1.4M_\odot$ and a magnetic moment of $10^{16}\mathrm{T\,m^3}$. We set the dimensionless parameters γ and $\gamma_{\rm dyn}$ to 1 and 10, respectively, while $\alpha_{ss} = 0.01$. γ, $\gamma_{\rm dyn}$, and α_{ss} appear only in combinations with other parameters, and thus their values do not carry any special significance, but the parameters ϵ and $\dot{M}$ appear on their own in the equation, and therefore influence the solution directly.

Firstly, we find the numerical solution for the outer regions of the disc with in the limit of integration in which $R_A > R_{0M}$.
Secondly, in the range of $R_{IM} < R < R_{OM}$, and thirdly, we consider the radiation pressure and electron scattering dominated disc (the inner region) in which $R_A < R_{IM}$ by increasing accretion rate.

4.4.1 Regional solutions

Case I: $R_A > R_{OM}$

The accretion disc consists of only the outer region when $r_{OM} < 1$, which corresponds to that $\dot{M} \leq 1.4 \times 10^{12}\mathrm{kg\,s^{-1}}$ for our fiducial model (Paper II). Assuming the accretion rate $\dot{M}= 0.012\dot{M}_{14}$ for our calculation we get the solutions from the top to the bottom Fig.4.1 for $\epsilon = 0.1, 0.05, 0, -0.05$, and -0.1 . We see here that $\Lambda \to 0$ for a finite r for $\epsilon = -0.1,$ and -0.05, which we called case D in (paper I), while in the other cases Λ grows without a bound for decreasing r, which we called V in Paper I, since then the viscous stress becomes 0 at a finite radius (Fig. 4.2). The surface density becomes infinite at the inner radius of the disc in case V, while it goes to 0 in case D (Fig. 4.1). As we see from the solution the large portion of the disc is the gas pressure and Kramer's opacity dominated part unless the accretion rate is increased. In Figure. 4.1 we get solutions in which $\Lambda = 0$ for $\epsilon = -0.1$ at the inner boundary, which case D, while for $\epsilon = 0, 0.05$ and 0.1, solutions have case V of Paper I (see Fig.4.2) inner boundaries. In Fig.4.3 we show the surface density as a function of radius for the fiducial neutron star with a spin period of 4.8ms and $\epsilon = 0.1, 0$ and -0.1 from the top to the bottom for the outer region. For $\epsilon = -0.1$ the surface density attains a local maximum, while the other models have surface densities that are strictly decreasing functions of r. Figure.4.4 shows the radial velocity as a function of r. Since $v_R \propto \Sigma^{-1}$ it becomes infinite as the inner edge of the disc for $\epsilon = -0.1$, but it stays finite for $\epsilon = 0$ and 0.1 (compared with Figs.4.11 & 4.18). In Fig.4.5 we get the midplane temperature for the outer disc region which is proportional to Σ^2.

In Fig.4.22 we have the toroidal magnetic field generated by the internal dynamo and by the shear for our fiducial model in the outer disc region. In our model the dominant magnetic field everywhere inside the disc is $B_{\phi\mathrm{dyn}}$.

Case II: $R_{IM} < R_A < R_{OM}$

In the limit of integration in which $R_A > R_{OM}$, that is at large radii the gas pressure and Kramer's opacity are dominating and the disc has only the outer region. If the accretion rate is increased the disc has both an outer and a middle region when $1.4 \times 10^{12}\mathrm{kg\,s^{-1}} \leq \dot{M} \leq 1.4 \times 10^{13}\mathrm{kg\,s^{-1}}$. We then use analytical solution with $\Lambda = \frac{1}{3\pi}$ for the outer region and solve Eq. (4.29) numerically for the middle region. For our calculation we take $\dot{M} = 1.2 \times 10^{13}\mathrm{kg\,s^{-1}}$, which yields $r_{OM} \simeq 8.5$. At $R = R_{OM}$ the outer disc region is replaced by middle region in which the gas pressure and electron scattering are started to dominate. The numerical solutions for

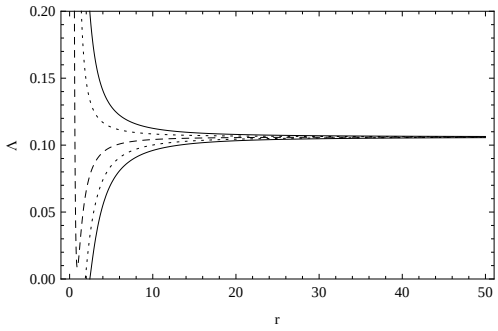

Figure 4.1: $\Lambda(r)$ for our fiducial neutron star with a spin period of 4.8 ms and $\epsilon = 0.1,\ 0.05,\ 0,\ -0.05,\ -0.1$ for the gas pressure and Kramer's opacity dominated region (outer region) from the top to the bottom.

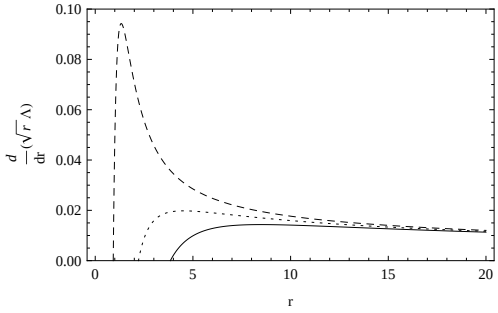

Figure 4.2: $\frac{d}{dr}\left(\sqrt{r}\Lambda\right)$ as a function of r for the fiducial neutron star with a spin period of 4.8 ms and with $\epsilon = 0.1,\ 0.05,$ and 0 for the gas pressure and Kramer's opacity dominated region (outer region) from the bottom to the top.

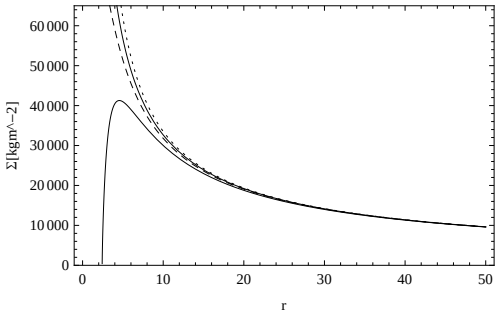

Figure 4.3: Σ as a function of r for our fiducial neutron star with a spin period of 4.8 ms and $\epsilon = 0.1,\ 0,$ and -0.1 for the gas pressure and Kramer's opacity dominated region (outer region) from the top to the bottom.

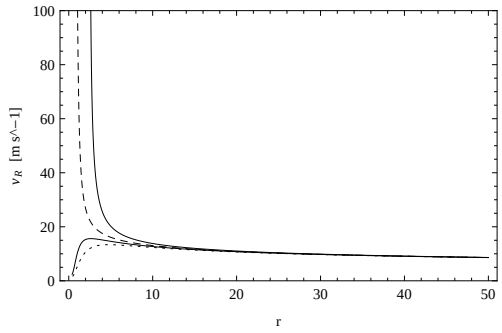

Figure 4.4: V_R as a function of r for the fiducial neutron star with a spin period of 4.8 ms and $\epsilon = 0.1, 0$ and -0.1 for the gas pressure and Kramer's opacity dominated region (outer region) from the top to the bottom.

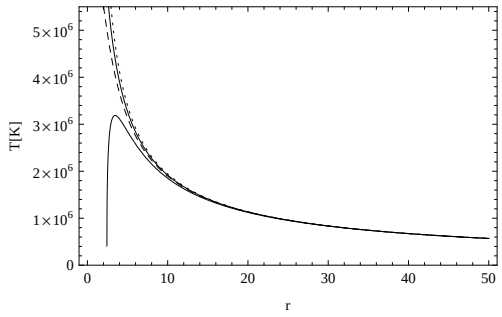

Figure 4.5: T_c as a function of r for our fiducial neutron star with a spin period of 4.8 ms and $\epsilon = 0.1, 0,$ and -0.1 for the gas pressure and Kramer's opacity dominated region (outer region) from the top to the bottom.

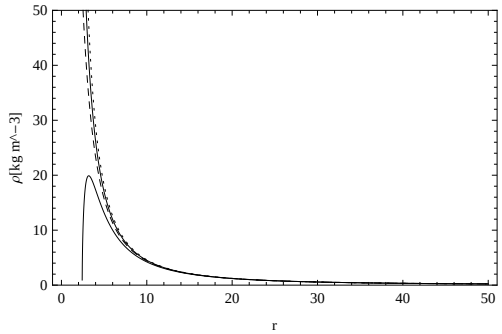

Figure 4.6: ρ as a function of r for our fiducial neutron star with a spin period of 4.8 ms and $\epsilon = 0.1, 0,$ and -0.1 for the gas pressure and Kramer's opacity dominated region (outer region) from the top to the bottom.

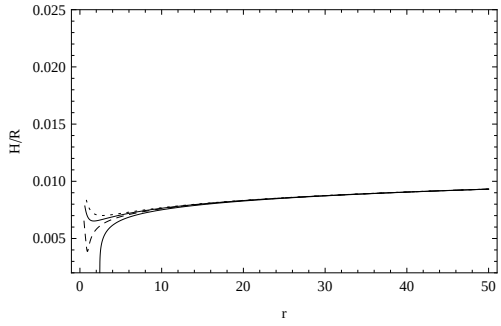

Figure 4.7: H/r as a function of r for our fiducial neutron star with a spin period of 4.8 ms and $\epsilon = 0.1,\ 0,$ and -0.1 for the gas pressure and Kramer's opacity dominated region (outer region) from the top to the bottom.

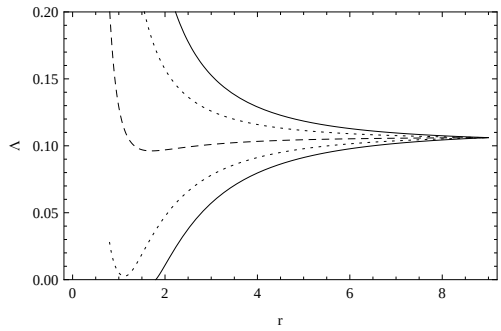

Figure 4.8: $\Lambda(r)$ for our fiducial neutron star with a spin period of 4.8 ms and $\epsilon = 0.1,\ 0.05,\ 0,\ -0.05,\ -0.1$ and -1 for the gas pressure and electron scattering opacity dominated region (Middle region) from the top to the bottom.

the middle region are shown in Fig.4.8 for our fiducial neutron star with a spin period of 4.8 ms and with $\epsilon = 0.1,\ 0.05,\ 0,\ -0.05$ and -0.1. Here our solution gives that $\Lambda \to 0$ for -0.1 which corresponds to case D in Paper I, while other solutions have case V inner boundaries in this case.

We show the numerical solution for the middle region in Fig.4.8 for our fiducial neutron star for $\epsilon = 0.1,\ 0.05,\ 0,\ -0.05,$ and -0.1 with spin period of 4.8ms and the solutions are terminated with in the respective transition radius.

In Fig.4.9 for $\epsilon = 0.1,\ 0.05,\ 0$ our solutions have case V of (Paper I) in the inner boundaries, while for $\epsilon = -0.1,\ -0.05$ corresponds to case D. We show the surface density as a function of radius for our fiducial neutron star for $\epsilon = 0.1,\ 0,$ and -0.1. As we see in the figure the value of the surface density in this region is greater than the outer region. Figs. 4.11 and 4.18 show

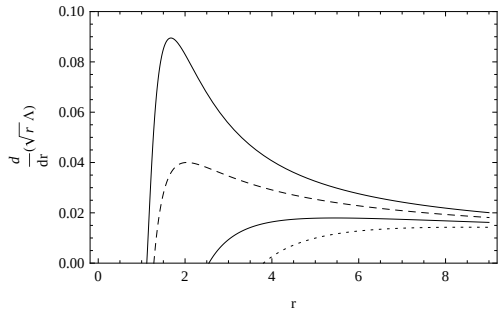

Figure 4.9: $\frac{d}{dr}(\sqrt{r}\Lambda)$ as a function of r for the fiducial neutron star with a spin period of 4.8 ms and with $\epsilon = 0.1, 0.05, 0,$ for the gas pressure and electron scattering opacity dominated region (middle region) from the bottom to the top.

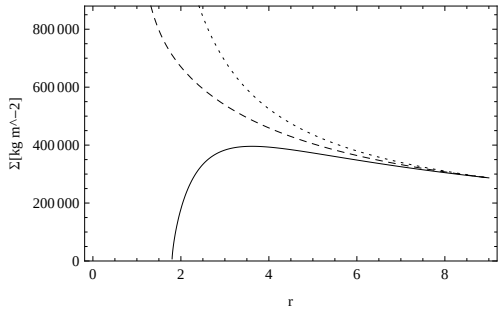

Figure 4.10: Σ as a function of r for our fiducial neutron star with a spin period of 4.8 ms and $\epsilon = 0.1, 0,$ and -0.1 for the gas pressure and electron scattering opacity dominated region (middle region) from the top to the bottom.

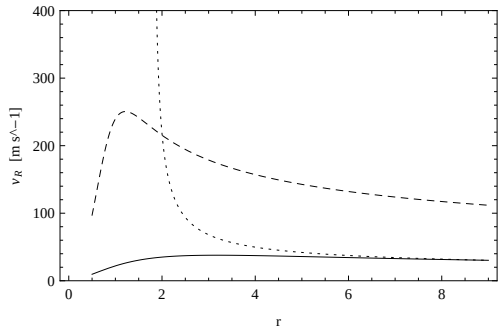

Figure 4.11: V_R as a function of r for the fiducial neutron star with a spin period of 4.8 ms and $\epsilon = 0.1, 0$ and -0.1 for the gas pressure and electron scattering opacity dominated region(middle region) from the top to the bottom.

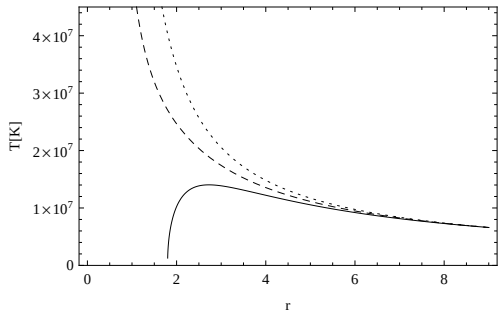

Figure 4.12: T_c as a function of r for our fiducial neutron star with a spin period of 4.8 ms and $\epsilon = 0.1,\ 0,$ and -0.1 for the gas pressure and electron scattering opacity dominated region (middle region) from the top to the bottom.

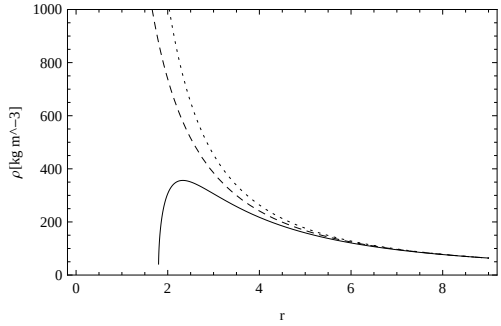

Figure 4.13: ρ as a function of r for our fiducial neutron star with a spin period of 4.8 ms and $\epsilon = 0.1,\ 0,$ and -0.1 for the gas pressure and electron scattering opacity dominated region (middle region) from the top to the bottom.

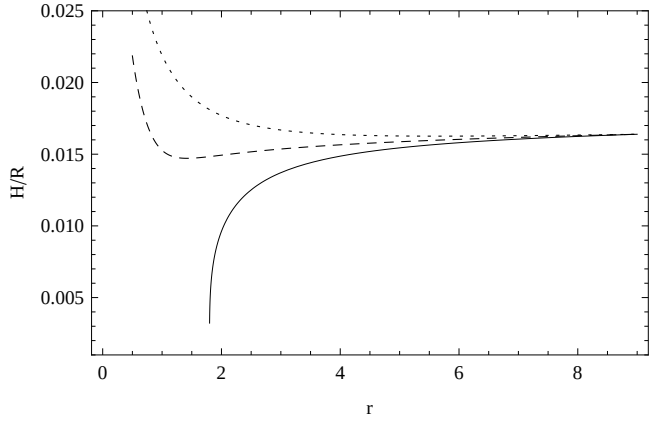

Figure 4.14: H/r as a function of r for our fiducial neutron star with a spin period of 4.8 ms and $\epsilon = 0.1,\ 0,$ and -0.1 for the gas pressure and electron scattering opacity dominated region (middle region) from the top to the bottom.

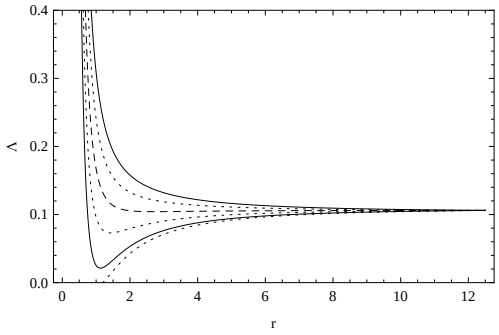

Figure 4.15: $\Lambda(r)$ for our fiducial neutron star with a spin period of 4.8 ms and $\epsilon = 0.1$, 0.05, 0, -0.05, -0.1 and -0.12 for the radiation pressure and electron scattering opacity dominated region(inner region) from the top to the bottom.

the radial velocity as a function of r in the middle and inner regions respectively. As the inner edge of the accretion disc approaches to the surface of the star the radial velocity either goes to zero or infinite (see Figs. 4.11 & 4.18). In Figs.4.12 and 4.19 show the mid plane temperature as a function of radius in the middle and inner regions of the disc respectively. In the inner region of the disc the mid-plane temperature is independent of Λ, however, the disc is hotter in the inner region than middle region. For $\epsilon = -0.1$, -0.05 in the middle region the surface density, the central density and the mid-plane temperature approaches to zero.
In Fig. 4.13 we get the density in the middle region which is the same manner as the surface density and in Fig. 4.14 we show the aspect ratio as a function of r in the middle region for $\epsilon = 0.1$, 0, and -0.1. We plot the toroidal magnetic field generated by the internal dynamo and the shear in Fig.4.23. We found the numerical values for both components, but both components of the magnetic field increases in this region compared to the outer disc region, while the shear increases.

Case III : $R_A < R_{IM}$

The innermost region of the disc is dominated by the radiation pressure and electron scattering opacities. From Eqs.(4.27) and (4.84) this region exists when the accretion rate increases that is when $\dot{M} > 1.4 \times 10^{13} \mathrm{kg\,s^{-1}}$. It is reasonable to use the accretion rate up to Eddington limit, so that we take $\dot{M} = 1.5\dot{M}_{14}$ for our calculation and we use the analytical solutions with $\Lambda = 1/3\pi$ for the outer and the middle regions of the disc , and solve Eq. (4.33) for the inner region starting from $r_{IM} \sim 12$.

Using a similar approach as the other two cases, our solutions for the inner disc region for

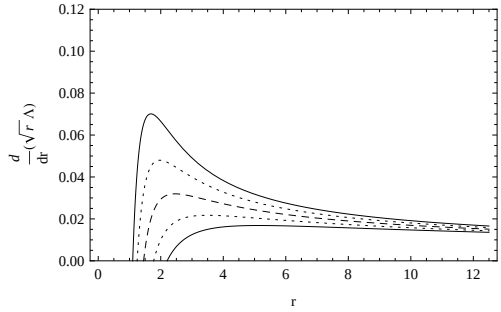

Figure 4.16: $\frac{d}{dr}(\sqrt{r}\Lambda)$ as a function of r for the fiducial neutron star with a spin period of 4.8 ms and with $\epsilon = 0.1,\ 0.05,\ 0,\ -0.05,$ and -0.1 for the radiation pressure and electron scattering opacity dominated region (inner region) from the bottom to the top.

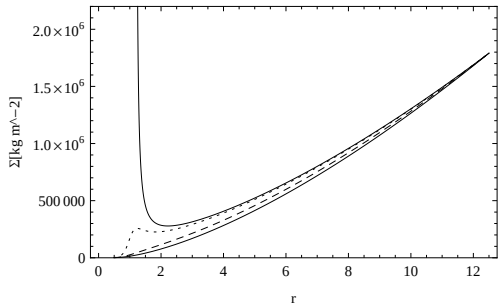

Figure 4.17: Σ as a function of r for the fiducial neutron star with spin period of 4.8 ms , an accretion rate of $1.5 \times 10^{14}\mathrm{kg\,s^{-1}}$ and with $\epsilon = 0.1,\ 0,\ -0.1,$ and -0.12 for radiation pressure and electron scattering opacity dominated disc region (inner disc) from the bottom to the top.

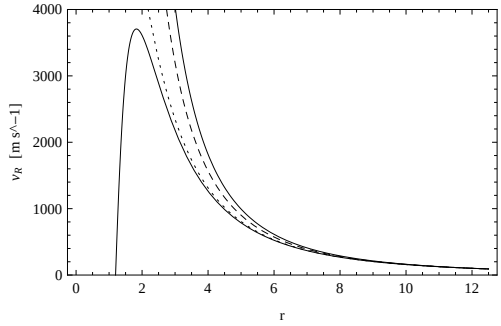

Figure 4.18: V_R as a function of r for the fiducial neutron star with a spin period of 4.8 ms and $\epsilon = 0.1,\ -0.1,\ 0,$ and -0.12 for the radiation pressure and electron scattering opacity dominated region (inner region) from the top to the bottom and for the accretion rate of $1.5 \times 10^{14}\mathrm{kg\,s^{-1}}$.

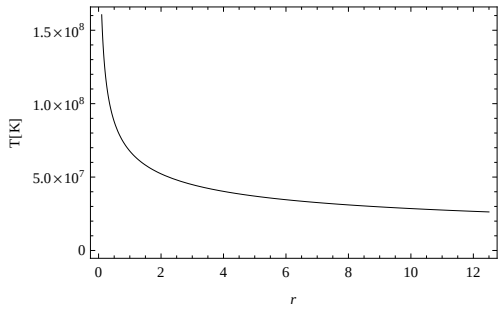

Figure 4.19: T_c as a function of r for the fiducial neutron star with spin period of 4.8 ms for the radiation pressure and electron scattering opacity dominated disc region (inner region) for the accretion rate of $1.5 \times 10^{14}\mathrm{kg\,s^{-1}}$.

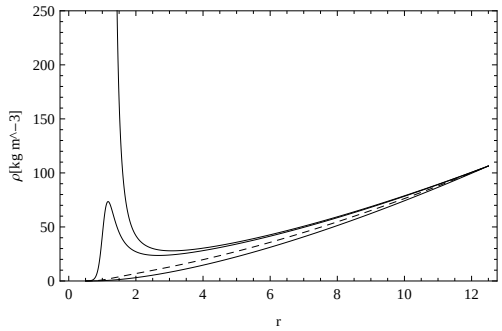

Figure 4.20: ρ as a function of r for our fiducial neutron star with a spin period of 4.8 ms and $\epsilon = 0.1,\ 0,\ -0.1,$ and -0.12 for the radiation pressure and electron scattering opacity dominated region (inner region) from the top to the bottom for the accretion rate of $1.5 \times 10^{14}\mathrm{kg\,s^{-1}}$.

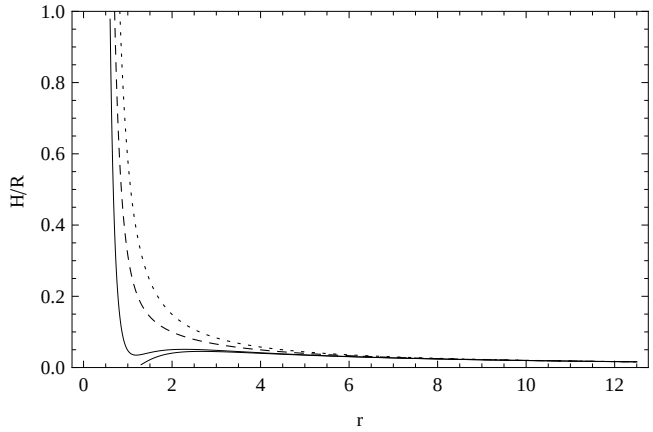

Figure 4.21: The aspect ratio,H/r, as a function of r for our fiducial neutron star with a spin period of 4.8 ms and $\epsilon = 0.1,\ 0,\ -0.1,$ and -0.12 for the radiation pressure and electron scattering opacity dominated region (inner region) from the top to the bottom for the accretion rate of $1.5 \times 10^{14} \mathrm{kg\,s^{-1}}$.

our fiducial neutron star with $\epsilon = 0.1,\ 0.05,\ 0,\ -0.05,\ -0.1$ are shown in Fig. 4.15. All these solutions have case V inner boundaries except for $\epsilon = -0.12$. It is characteristic for a disc that is dominated by radiation pressure that the surface density decreases with decreasing radius (Fig. 4.17), since the scale height is independent of the radius, and the magnetic stress due to the dynamo is independent of Λ. In this region the inner radius extends down to the surface of the star, dependence of the solution on the ϵ and accretion rate can be better seen in Fig. 4.15 with different values of ϵ, Λ has approximately a local minimum for $\epsilon = -0.1$ and -0.05 , while the other three solutions have shown in Fig. 4.16. As ϵ is increased the local minimum grows and the solution develops a case V inner boundary. When the minimum becomes positive , Λ increases as radius decreases. In Fig.4.16 the inner edge of accretion disc in this region is less than middle region. In Fig. 4.17 we show the surface density as a function of radius in the radiation pressure and electron scattering dominated region, decreasing with decreasing radius which is different from the middle and outer regions and the nature of the central density follows same character as the surface density because the scale height is independent of radius and magnetic stress due to dynamo also does not depend on Λ in this region which is the typical behavior of radiation pressure dominated accretion disc that differ from the other two regions. As we see in the figure the surface density in the inner region of the disc is growing without limit for $\epsilon = -0.12$. In Fig.4.21 we show the aspect ratio in the innermost regions of the disc. From this solution we understand that in the inner disc region the aspect ratio increases.

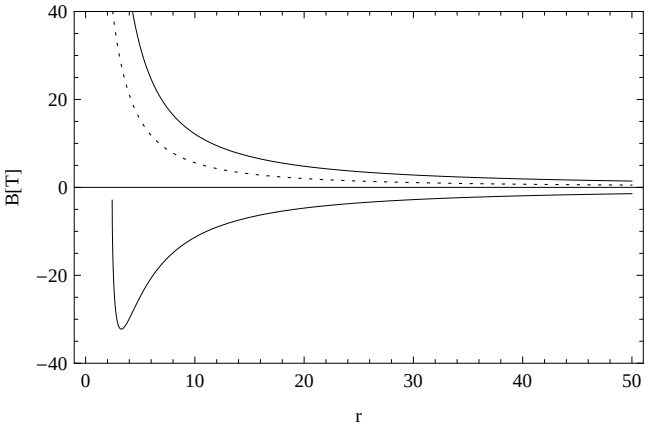

Figure 4.22: The toroidal magnetic field for our fiducial neutron star with a spin period of 4.8 ms and $\epsilon = 0.1,$ and -0.1 for the gas pressure and Kramer's opacity dominated region (outer region) from the top to the bottom, while the dotted line shows the magnetic field generated by the shear and for accretion rate of $0.012\dot{M}_{14}$.

In the inner disc region the mid-plane temperature is independent of Λ so that as radius decreases the temperate increases which is the same as the outer and the middle disc region. As we see from the three regions the magnetic field increases as the accretion rate increases, but the magnetic field generated by the internal dynamo is stronger in the radiation pressure dominated disc than the other two (see fig.4.24) because at small distance the magnetic field due to internal dynamo decreases and the magnetic field arise due to shear increases.

4.5 Results and discussion

4.5.1 The inner edge of the accretion disc

In this chapter we have studied the disc interaction of a rapidly rotating magnetised star, in particular with an accretion disc around magnetised millisecond X-ray pulsars by dividing the disc into three distinct regions. The inner edge of accretion disc can be found by similar case as (Paper I & II) for different regions of the disc. The inner radius of the disc in each region mainly depends on the accretion rate and the internal magnetic field generated due to dynamo. In the inner regions of the disc the action of the magnetic field leads to enhanced accretion rate, while in the outer regions to reduce the accretion or even to outflow of matter. In the model studied here the location of the inner edge of the inner radius varies with the accretion

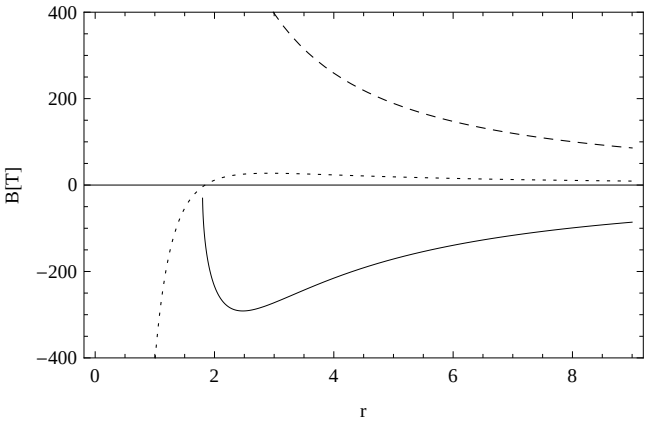

Figure 4.23: The toroidal magnetic field for our fiducial neutron star with a spin period of 4.8 ms and $\epsilon = 0.1, -0.1$ for the gas pressure and electron scattering opacity dominated region (middle region) from the top to the bottom, while the dotted line shows the magnetic field generated by the shear and for accretion rate of $0.12\dot{M}_{14}$.

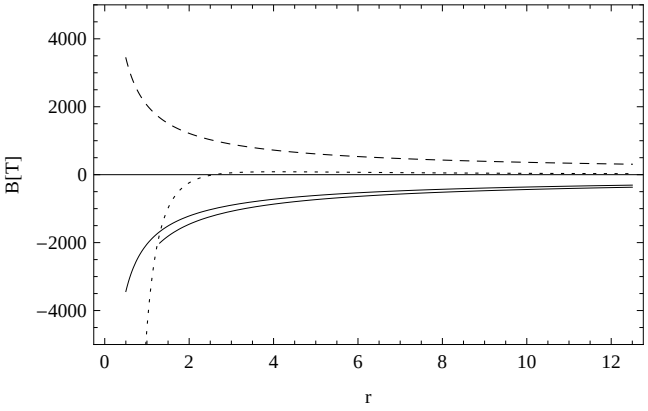

Figure 4.24: The toroidal magnetic field for fiducial neutron star with a spin period of 4.8 ms. The solid and dashed lines show the field generated by the dynamo for ϵ =-1, -0.1, and 0.1 from bottom to top, respectively, while the dotted line shows the magnetic field generated by the shear in the inner disc region and for accretion rate of $1.5\dot{M}_{14}$.

rate. For low accretion rate (see Table.4.1) we have only the outer region and for different ϵ we calculate different values of R_0. At transition radius, R_{OM}, the outer disc region is started to replace by the middle region. At intermediate accretion rate (see Table. 4.1) we get the outer and the middle region in which the outer disc region is replaced by the middle region which will be terminated at transition radius from middle to the inner region, R_{IM}. For sufficiently large negative values of ϵ the inner edge of the accretion disc in the middle increases. At higher accretion rate we get the three region i.e. outer, middle and inner regions at which the middle region is replaced by the inner region at transition radius R_{IM}. In this region electron scattering and radiation pressure dominates and accretion disc extends down into the surface of the neutron star. Therefore, it is interesting to determine the inner edge of the accretion disc in this region, we find that the inner edge of accretion disc in this region is greater than the Alfvén radius (see Table. 4.1). For large value of ϵ the inner edge of the accretion disc in the inner region also increases. The advection and and viscous stress are dominant in the inner region compared to magnetic stress but they are opposite sign, however, the magnetic stress generated by the internal dynamo still influences the location of the inner edge of the accretion disc in this region too.

4.5.2 Accretion Torque

To understand the nature of the torque and the exchange of angular momentum between the accretion disc and its environment we multiply Eq. (4.13) by $2\pi R$ and integrate it from R_0 the inner radius of the disc to R_1 the outer edge of the disc for each region which relates the radial advection of material angular momentum to the viscous and magnetic torque yields

$$\begin{aligned} -\dot{M}\left(\sqrt{GMR_1}-\sqrt{GMR_0}\right) = \\ \int_{R_0}^{R_1} 4\pi\frac{B_z B_{\phi,\mathrm{dyn}}}{\mu_0}R^2\mathrm{d}R + \int_{R_0}^{R_1} 4\pi\frac{B_z B_{\phi,\mathrm{shear}}}{\mu_0}R^2\mathrm{d}R \\ -3\pi\left(\nu\Sigma\right)_{R_1}\sqrt{GMR_1}+3\pi\left(\nu\Sigma\right)_{R_0}\sqrt{GMR_0}. \end{aligned} \tag{4.85}$$

The left-hand-side is the difference between the angular momentum that is advected out of the inner edge of the accretion disc and that which is fed into the disc at its outer edge and the right-hand-side describes the contribution of magnetic and viscous torques to the angular momentum balance. Notice that the term $3\pi(\nu\Sigma)_{R_1}\sqrt{GMR_1}$ describes the viscous tension at the outer edge of the disc in the outer region, which will not be considered further in this work and the transition radius for middle and inner disc regions in which the viscous stress is zero. The limit of

integration in our model for the three disc regions are $R_{OM} \longrightarrow R, R_{MI} \longrightarrow R_{OM}, R_0 \longrightarrow R_{MI}$, for the outer, middle and inner regions of the disc respectively.

Now it is meaningful to discuss the accretion torque arising from the inner edge of the disc at R_0. For this case the inner disc region has relatively smaller inner edge, then we will give attention to accretion torque in this region. For a neutron star with a weak magnetic field (a typically millisecond pulsars) radiation pressure will be important for accretion a few percent of the Eddington rate. In fact, that thin-disc model is unstable in a region where the radiation pressure dominates the gas pressure was suggested along time by Lightman and Eardly (1974) describing systems accreting below the critical rate. For faster accretors, there will exist an inner region inside r_{MI} where the disc is no longer thin. The fact that radiation pressure will affect accretion disc structure, and hence the spin period of the neutron stars in LMXBs, has previously been discussed by several authors (White & Stella 1988; see also Miller, Lamb & Psaltis 1998; Psaltis & Chakrabarty 1999).

The material torque at the inner edge of the disc is usually approximated by

$$N_{adv} = \dot{M}\sqrt{GMR_0} = 1.37 \times 10^{26} \mu_{16}^{2/7} M_1^{3/7} \dot{M}_{14}^{6/7} r_0^{1/2}. \tag{4.86}$$

The material torque increases as accretion rate increases (see Tab.4.1) it is dominant at the inner region of the disc than the other two regions. Then we have the magnetic torques on the neutron star, which we divide into one part due to the shear

$$N_{\rm shr} = -\int_{R_0}^{R_1} 4\pi \frac{B_z B_{\phi,\rm shear}}{\mu_0} R^2 {\rm d}R = 3.64 \times 10^{26} \gamma \mu_{16}^{2/7} M_1^{3/7} \dot{M}_{14}^{6/7} \int_{r_0}^{\infty} \left[r^{-4} \left(1 - \omega_s r^{3/2} \right) \right] dr \tag{4.87}$$

and a second part due to the dynamo

$$N_{\rm dyn} = -\int_{R_0}^{R_1} 4\pi \frac{B_z B_{\phi,\rm dyn}}{\mu_0} R^2 {\rm d}R \tag{4.88}$$

which yields for three regions

$$\begin{aligned} N_{\rm dyn,outer} &= 7.66 \times 10^{27} \epsilon \gamma_{dyn}^{1/2} \alpha_{\rm ss}^{1/20} \bar{\mu}^{3/10} \mu_{16}^{1/4} M_1^{5/8} \dot{M}_{14}^{4/5} \int_{r_0}^{r} \Lambda^{17/40} r^{-37/16} dr, \\ N_{\rm dyn,Mid} &= 6.27 \times 10^{27} \epsilon \gamma_{dyn}^{1/2} \alpha_{\rm ss}^{1/20} \bar{\mu}^{1/5} \mu_{16}^{3/10} M_1^{17/28} \dot{M}_{14}^{107/140} \int_{r_{0M}}^{r_{MO}} \Lambda^{2/5} r^{-91/40} dr, \\ N_{\rm dyn,inner} &= 6.62 \times 10^{26} \epsilon \gamma_{dyn}^{1/2} \mu_{16}^{4/7} M_1^{5/14} \dot{M}_{14}^{3/14} \int_{r_{0i}}^{r_{MI}} r^{-7/4} dr. \end{aligned} \tag{4.89}$$

where $r_1 = R_1/R_{\rm A}$, $r_{\rm MO} = R_{\rm MO}/R_{\rm A}$, $r_{\rm IM} = R_{\rm IM}/R_{\rm A}$, $r_{0,\rm out}$ is either $R_0/R_{\rm A}$ or $r_{\rm MO}$, if this exists, $r_{0,\rm mid}$ is either $R_0/R_{\rm A}$ or $r_{\rm IM}$, if this exists, and $r_{0,\rm in} = R_0/R_{\rm A}$ when the inner region exists. Finally the viscous stress at the inner edge of the accretion disc transports angular momentum outwards away from the neutron star resulting in a torque

$$N_{\rm vis} = -3\pi \left(\nu\Sigma\right)_{R_0} \sqrt{GMR_0} = \\ -1.29 \times 10^{27} \mu_{16}^{2/7} M_1^{3/7} \dot{M}_{14}^{6/7} \Lambda r_0^{1/2} \tag{4.90}$$

After integrating all the components of the torque, the total torque acting on the neutron star is given

$$N_{\rm total} = N_{\rm dyn,outer} + N_{\rm dyn,middle} + N_{\rm dyn,inner} + N_{\rm sh,outer} + N_{\rm sh,middle} + N_{\rm sh,inner} + N_{\rm adv} + N_{\rm visc} \tag{4.91}$$

We report all the components and the total sum of the torques acting on our fiducial neutron star in Tab.4.1 for our choice of spin period and ϵ for different accretion rate Unless $\epsilon = 0$ we see that the magnetic torque due to the dynamo in the three regions are the dominant component if the accretion rate increases. For low accretion rate the dominant torque for our choice of accretion rate in all models is the magnetic torque due to internal dynamo. As we see in Tab.4.1 magnetic stress due to internal dynamo is dominant than the shear in the three distinct disc regions. At higher accretion rate the magnetic torque is dominated by either viscous or material torque.

4.5.3 Observed properties of millisecond X-ray Pulsars

There is a large variation in the accretion rates among the millisecond X-ray pulsars. The well-studied system IGR J00291+5934 is accreting at a rate of at least $\sim 10^{14}\,{\rm kg\,s^{-1}}$ based on its X-ray flux (Burderi et al., 2007),, while in some other systems, for instance SAX J1808.4-3658 Bildsten and Chakrabarty (2001), the neutron star is accreting at a rate below $10^{12}\,{\rm kg\,s^{-1}}$ from a brown dwarf companion. The latter accretion rate is so low that the disc can be susceptible to a dwarf-nova like instability (King, 2000), which means that even if the mass transfer rate is fairly stable the accretion rate through the accretion disc can vary significantly over time, if a description based on a steady disc is at all applicable.

There are large uncertainties in the spin variations that have been reported for the millisecond X-ray pulsars. For instance (Burderi et al., 2006) reported $\dot{\nu}$s between -7.6×10^{-14} and $4.4 \times 10^{-13}\,{\rm Hz\,s^{-1}}$ for SAX J1808.4-3658, but (Hartman et al. 2008) noted that the measurements

Table 4.1: The inner edge of the accretion disc and its torque on the fiducial neutron star in different regions of the disc for different accretion rate. For comparison, (Alfvén radius: $R_A = 4.72 \times 10^4$m, $R_{OM} = 1.33 \times 10^4$m when ($\dot{M} = 0.012\dot{M}_{14}$) ; $R_A = 2.45 \times 10^4$m, $R_{OM} = 1.20 \times 10^5$m, $R_{IM} = 20.9 \times 10^3$m, when ($\dot{M} = 0.12\dot{M}_{14}$) ; $R_A = 1.20 \times 10^4$, when $\dot{M} = 1.5\dot{M}_{14}$, and $R_{IM} = 14.33 \times 10^4$m) .

$\dot{M}_{14}$	ϵ	R_0 [m]	$N_{\rm dyn}$ [Nm]	$N_{\rm sh}$ [Nm]	$N_{\rm adv}$ [Nm]	$N_{\rm vis}$ [Nm]	$N_{\rm total}$ [Nm]
$0.012\dot{M}_{14}$	0.1	1.8×10^5	3.4×10^{24}	-7.8×10^{23}	7.0×10^{24}	-7.4×10^{24}	2.2×10^{24}
	0.05	9.9×10^4	3.7×10^{24}	-1.7×10^{24}	5.2×10^{24}	-6.7×10^{24}	5.0×10^{23}
	0	4.7×10^4	0	-3.1×10^{24}	3.6×10^{24}	-3.4×10^{22}	4.7×10^{23}
	-0.05	8.8×10^4	-2.9×10^{24}	-1.9×10^{24}	4.9×10^{24}	0	1.0×10^{23}
	-0.1	1.2×10^5	-4.1×10^{24}	-1.4×10^{24}	5.6×10^{24}	0	1.0×10^{23}
$0.12\dot{M}_{14}$	0.1	9.4×10^4	9.8×10^{25}	-2.1×10^{24}	5.1×10^{25}	-1.0×10^{26}	4.7×10^{25}
	0.05	6.0×10^4	5.6×10^{25}	-3.2×10^{24}	4.1×10^{25}	-7.7×10^{25}	1.7×10^{25}
	0	3.0×10^4	0	-7.4×10^{23}	2.9×10^{25}	-2.4×10^{25}	-4.3×10^{24}
	-0.05	3.2×10^4	-6.6×10^{25}	-2.0×10^{24}	2.9×10^{25}	-6.7×10^{22}	-3.9×10^{25}
	-0.1	4.8×10^4	-1.1×10^{26}	-3.7×10^{24}	3.6×10^{25}	0	-7.7×10^{25}
$1.5\dot{M}_{14}$	0.1	2.6×10^4	1.4×10^{26}	-5.6×10^{24}	3.3×10^{26}	-4.5×10^{26}	1.2×10^{25}
	0.05	2.1×10^4	8.5×10^{25}	4.8×10^{24}	2.9×10^{26}	-4.2×10^{26}	-4.0×10^{25}
	0	1.8×10^4	0	1.7×10^{25}	2.7×10^{26}	-3.2×10^{26}	-3.3×10^{25}
	-0.05	1.6×10^4	-1.1×10^{26}	3.7×10^{25}	2.6×10^{26}	-3.2×10^{26}	-1.3×10^{26}
	-0.1	1.5×10^4	-2.3×10^{26}	5.5×10^{25}	2.5×10^{26}	-1.1×10^{25}	6.7×10^{25}
	-0.12	1.3×10^4	-2.7×10^{26}	5.8×10^{25}	2.5×10^{26}	0	3.6×10^{25}

of this source are plagued by large variations in the pulse shape, and put an upper limit of $2.5 \times 10^{-14}\,\mathrm{Hz\,s^{-1}}$ on the spin variations and in found a long-term spin down with $\dot{\nu} = -5.6 \times 10^{-16}\,\mathrm{Hz\,s^{-1}}$. On the other hand (Burderi et al., 2007) report that IGR J00291+5934 is spinning up at $\sim 10^{-12}\,\mathrm{Hz\,s^{-1}}$ during the December 2004 outburst. These spin variation correspond to torques

$$N = 2\pi\dot{\nu}I = 6.3 \times 10^{25}\dot{\nu}_{13}I_{38}\,\mathrm{Nm}, \tag{4.92}$$

where I_{38} is the moment of inertia of the neutron star measured in $10^{38}\,\mathrm{kg\,m^2}$, and $\dot{\nu}_{13}$ is the spin derivative in units of $10^{-13}\,\mathrm{Hz\,s^{-1}}$. Some of the reported spin variations are so large that they become difficult to explain in the Ghosh and Lamb (1979) model, but our Tab. 4.1 shows that the internal disc dynamo can significantly enhance the torque, though we have not attempted to model any particular system.

4.6 Conclusion

We have studied the interaction between millisecond X-ray pulsars and its surrounding accretion disc in the three regions of the disc in the case that the accretion disc is supporting an internal dynamo, and the highest accretion rates are sufficient to make the innermost part of the accretion disc to be dominated by radiation pressure and electron scattering. For these reasons we have followed the approach by Shakura & Sunyaev (1973) and divide our disc model into in three regions, an outer region dominated by the gas pressure and Kramer's opacity, and a middle region dominated by gas pressure and electron scattering, and an inner region dominated by radiation pressure and electron scattering.The magnetic field that is produced by the dynamo can lead to a significant enhancement of the magnetic torque between the neutron star and the accretion disc, compared to what is seen in the model by Ghosh & Lamb (1979). But the magnetic torque generated by the internal dynamo is dominant in gas pressure dominated disc and dominated by viscous torque in the radiation pressure disc (inner disc region).

We calculate the structure of the accretion disc in the three regions we find two kinds of solutions with different behaviour at the inner edge most parts of the disc is gas pressure and free-free opacity dominated disc. When the accretion rate increases the solution of the disc behavior is changed. A few of our solutions in the outer region have case D boundaries at which the density and temperature go to 0 at finite radius, while most of our solutions have case V boundaries at which the accretion is driven entirely by the magnetic tension between

the accreting matter and the neutron star (Paper I). In the inner region of the disc the latter case is applied to find the solution there is a viscous stress between the accretion disc and the boundary layer, which can transfer angular momentum outwards at a rate that is comparable to the one at which it is advected inwards by the accreting matter itself.

We have also found that the dynamo leads to that the inner edge of the accretion disc occurs at a radius which is larger than the traditional Alfvén radius in the outer regions of the disc which is in good agreement with Paper I, II and greater or equal to Alfvén radius in the inner disc region that is the inner radius extends towards the surface of the neutron star. The nature of the solution and the inner radius varies with varying accretion rate and ϵ in addition to internal dynamo.

We have found that at higher accretion rate (inner region of the disc) the inner edge of the accretion disc is greater than the radius of the neutron star for all values of ϵ. We have found that magnetic field, and spin derivatives for different accretion rate in any of our model are in good agreement with RXTE observed data in millisecond X-ray pulsars and also the solution of the structure of accretion disc around magnetised millisecond X-ray pulsars are consistently explained by this model.

Chapter 5

Time-Dependent Accretion disc

In the previous chapters we solved the set of steady state disc equations including both magnetic and viscous torques and gas and radiation pressure for the whole disc. Now, we are interested in using the time-dependent equations for the accretion disc to do a linear stability analysis of our steady disc solutions in the presence of strong magnetic field and we can see how the disc evolves in time. We do this by expressing the surface density as a function of time and position in the conservation of mass, momentum and energy.
This chapter is adapted from the paper "The Time-dependent Accretion Discs Around Magnetised Stars" by Solomon Belay Tessema and Ulf Torkelsson, which is in preparation for submission to **The Mon. Not.R.Astron.Soc. Journal**.

5.1 Introduction

According to the widely adopted standard solutions (Shakura & Sunyaev 1973), luminous accretion discs close to the Eddington rate should be radiation pressure dominated and therefore unstable to perturbations of both mass flow (Lightman & Eardley 1974) and heating rate (Pringle, Rees & Pacholczyk 1973) for the commonly adopted assumption that viscous stresses within the disc are proportional to the total (gas plus radiation) pressure (α-viscosity prescription). Taking into account the stabilizing effect of radial advection near the Eddington rate, often modelled with the slim disc solutions (Abramowicz et al. 1988), a limit-cycle-type behaviour should be expected, which has been confirmed by numerical simulations of time-dependent discs (Taam & Lin 1984; Honma, Matsumoto & Kato 1991; Szuszkiewicz & Miller 1997) which will not be treated in this work for the moment. But we will concentrate on stability time-dependent

accretion disc around magnetised stars.

Two physically reasonable ways to make luminous accretion discs stable are well known. First of all, the discs may be cooling much faster than the standard solution assumes due to an additional rapid energy transfer from the disc mid-plane into a corona, a jet or a wind, so that the radiation pressure simply never dominates in the disc (e.g. Svensson & Zdziarski 1994). Secondly, the anomalous viscosity of accretion discs, now understood to be due to magnetorotational instability (MRI), may not scale with the total disc pressure (e.g. Lightman & Eardley 1974). Numerical magnetohydrodynamics (MHD) simulations of turbulent accretion flows are the most promising tools for differentiating between these possibilities from first principles (see, in particular, Sano et al. 2004, and references therein). However, due to immense numerical challenges, one will have to wait until global 3D radiative simulations are performed over a large enough range of parameter space before a clear answer will emerge.

The Balbus - Hawley (magnetorotational) instability (Velikhov 1959; Chandrasekhar 1961) of weak magnetic fields in accretion discs drives MHD turbulence which transports angular momentum radially outwards (Balbus & Hawley 1991; Hawley & Balbus 1991; Stone et al. 1996), and is thought to play an important role in the evolution and dynamics of astrophysical accretion discs. The instability has also been invoked as a component of a disc dynamo model, in which the instability creates radial field from vertical field, the shear in the disc creates azimuthal field from the radial component, and the Parker instability creates vertical from azimuthal field and expels flux from the disc (Tout & Pringle 1992).

In this chapter, we investigate the time-dependent evolution of magnetized accretion discs by means of analytic techniques for steady state and non-steady state discs by linearizing nonlinear equations considering the small perturbation of the surface density and analyzing the stability conditions. We perform a local viscous disc stability analysis and present a linear analysis of the stability of the accretion disc and, later check with time-dependent disc models. We find that the stability properties of accretion disc around magnetized star for gas pressure dominated and radiation pressure dominated disc and timescale analysis are given and explained.

5.2 Time-dependent equations

In order to solve the equations of the time-dependent disc between an accretion disc and accreting star, we use the Navier-Stoke's equations, including gravity of the star (gravity of the

accreting gas is negligible), turbulent viscosity and radiative transfer treated in the diffusion approximation. The effect of radiation pressure is included in the equation of state when the gas pressure is less dominant than radiation pressure but the magnetic pressure is excluded . The treatment is one-dimensional and the equations are written in cylindrical coordinates (R, ϕ, z). Axisymmetry is assumed around the z-axis, thus $\frac{\partial}{\partial \phi} = 0$. The problem is solved at the mid-plane of the disc and we assume that the disc is optically thick, geometrically thin. We also assume that the disc is in hydrostatic equilibrium in the vertical direction and we integrate the quantities in the vertical direction from -H to + H, where H is the half-thickness of the disc in the vertical direction.

5.2.1 Conservation of mass

The equations governing a thin accretion disc with surface density profile can be obtained from the Navier-Stoke's equations in cylindrical symmetry integrating over the height of the disc. The equation of mass conservation are given by Eq. (2.29) and in general it is written as

$$\frac{\partial \rho}{\partial t} + \nabla \cdot (\rho \mathbf{v}) = 0. \tag{5.1}$$

The surface density Σ has been defined by vertically integrating ρ over the disc thickness H, and in the thin disc approximation given by Eq. (3.16). The continuity equation in the cylindrical coordinates, in terms of the surface density Σ, in the disc approximation, is thus given by

$$\frac{\partial \Sigma}{\partial t} + \frac{1}{R}\frac{\partial (R\Sigma v_R)}{\partial R} = 0, \tag{5.2}$$

The variation in the surface density $\Sigma(R, t)$ at radius R in the equation for non steady disc accretion conforms to the equation of continuity

$$\frac{\partial \Sigma}{\partial t} = -\frac{1}{R}\frac{\partial (R\Sigma v_R)}{\partial R}, \tag{5.3}$$

where $\dot{M}$ represents the mass transfer rate at each radius given by

$$\dot{M} = 2\pi R\Sigma(-v_R) \tag{5.4}$$

in which Σ and v_R are now allowed to be functions of t, we can rewrite the mass conservation equation (5.3) as

$$2\pi R\frac{\partial \Sigma}{\partial t} = \frac{\partial \dot{M}}{\partial R} \tag{5.5}$$

Here and throughout this thesis $\dot{M}$ is the mass crossing a cylindrical surface density in unit time and constant.

5.2.2 Conservation of momentum

Using Eqs. (2.20)- (2.22) the momentum equations for a fluid in general expressed by the Navier-Stoke's equations can be rewritten for the time- dependent thin disc as:

$$\rho\frac{\partial \mathbf{v}}{\partial t} + \rho\left(\mathbf{v}\cdot\nabla\right)\mathbf{v} = -\nabla P - \rho\nabla\Phi + \mathbf{J}\times\mathbf{B} + \rho\nu\nabla^{\mathbf{2}}\mathbf{v} \tag{5.6}$$

Applying Eqs. (2.20)- (2.22) we find the component of the momentum equations for the time-dependent disc. Assuming that v_R is very small, the radial component of the Navier-stoke's equation is

$$\rho\left[\frac{\partial v_R}{\partial t} + v_R\frac{\partial v_R}{\partial R} - \frac{v_\phi^2}{R} + \frac{GM}{(R^2+z^2)^{3/2}}\right] = \frac{B_z}{\mu_0}\left(\frac{\partial B_R}{\partial z} - \frac{\partial B_z}{\partial R}\right) - \frac{B_\phi}{\mu_0}\left(\frac{1}{R}\frac{\partial}{\partial R}(RB_\phi)\right)$$
$$-\frac{\partial P}{\partial R} + \frac{4}{3R^{3/2}}\frac{\partial}{\partial R}\left(R^{3/2}\nu\rho\frac{\partial v_R}{\partial R}\right) - \frac{2}{3R^3}\frac{\partial(R^2\nu\rho v_R)}{\partial R} \tag{5.7}$$

To a first approximation matter in the disc flows in Keplerian orbits with velocity

$$v_\phi = \sqrt{\frac{GM}{R}} \tag{5.8}$$

The Keplerian rotation law (5.8) is not that of a rigid body as $\frac{\partial\Omega}{\partial R} \neq 0$, and so frictional forces between neighbouring layers, which are assumed to be much smaller than the centrifugal force $\frac{v_\phi^2}{R}$ and the gravitational force $-\frac{GM}{R^2}$, should redistribute angular momentum. Consequently a radial velocity component $v_r \ll v_\phi$ will appear in the disc.

In similar manner the vertical component of momentum equation for time -dependent disc gives

$$\rho\left[\frac{\partial v_z}{\partial t} + v_R\frac{\partial v_z}{\partial R} + v_z\frac{\partial v_z}{\partial z}\right] = -\frac{B_\phi}{\mu_0}\frac{\partial B_\phi}{\partial z} - \frac{B_R}{\mu_0}\frac{\partial B_R}{\partial z} + \frac{B_R}{\mu_0}\frac{\partial B_z}{\partial R}$$
$$-\frac{\partial P}{\partial z} - \frac{\rho GM}{R^2} + \frac{1}{R}\frac{\partial}{\partial R}\left[\rho\nu R\left(\frac{\partial v_z}{\partial R} + \frac{\partial v_R}{\partial z}\right)\right] + \frac{4}{3}\frac{\partial}{\partial z}\left[\rho\nu\frac{\partial v_z}{\partial z} - \frac{\partial v_R}{\partial R} - \frac{v_R}{R}\right] \tag{5.9}$$

We assume that motions in the disc along the z-direction are subsonic, then the disc is in the hydrostatic equilibrium in the vertical direction and the magnetic field is weak. In the direction perpendicular to the plane of the disc the gas and radiation pressure gradient is balanced by the component of the gravitational attraction of the central body normal to the disc (the self-gravitation of the disc is being negligible), we have the reduced equation

$$\frac{1}{\rho}\frac{\partial P}{\partial z} = -\frac{GM}{R^3}z, \tag{5.10}$$

where ρ is the density, P is the pressure, G is the gravitational constant and M is the mass of the accreting star. Following the usual procedure, we integrate the quantities in the z direction from -H to + H, where 2H is the thickness of the disc in the vertical direction. From the equation of hydrostatic equilibrium we obtain

$$H \approx \frac{c_{\rm s}}{v_{\rm kep}} R, \tag{5.11}$$

where $c_{\rm s}$ is the velocity of the sound and given by $c_{\rm s}^2 = \frac{P}{\rho}$ and $V_{\rm kepl} = \frac{GM}{R^2}$ is the Keplerian velocity

Similarly the azimuthal component of Navier- Stoke's equation for time-dependent disc gives the transfer of the angular momentum:

$$\rho\left(\frac{\partial v_\phi}{\partial t} + \frac{v_R}{R}\frac{\partial}{\partial R}\left(R v_\phi\right)\right) = \left[\frac{B_R}{\mu_0}\frac{1}{R}\frac{\partial}{\partial R}(R B_\phi) + \frac{B_z}{\mu_0}\frac{\partial B_\phi}{\partial z}\right] + \frac{1}{R^2}\frac{\partial}{\partial R}\left[R^3\rho\nu\frac{\partial}{\partial R}\left(\frac{v_\phi}{R}\right)\right], \tag{5.12}$$

Integrating vertically both sides of Eq.(5.12) and assuming that the smallness of the changes in angular velocity allows the possibility of ignoring the first term in equation (5.12) $\frac{d\Omega_{\rm k}}{dt} = 0$, we obtain

$$\left(\Sigma R v_{\rm R}\frac{\partial \ell}{\partial R}\right) = 2\frac{B_{\rm z}B_\phi}{\mu_0}R^2 + \frac{\partial}{\partial R}\left[R^3\nu\Sigma\frac{\partial}{\partial R}\left(\frac{\ell}{R^2}\right)\right]. \tag{5.13}$$

It is clear from this equation that the direction of overall mass-flow (the sign of $\dot{M}$) is given by the dependence of viscous and magnetic stress on radius and also Eq.(5.13) relates the radial advection of material angular momentum to the viscous and magnetic torque.

The expression for the radial component of velocity can be obtained

$$v_{\rm R} = -\frac{3}{R^{1/2}\Sigma}\frac{\partial}{\partial R}\left(R^{1/2}\nu\Sigma\right) + \frac{4B_{\rm z}B_\phi R^{3/2}}{\mu_0\Sigma\sqrt{GM}} \tag{5.14}$$

Inserting Eq.(5.14) into continuity equation [Eq.(5.3)] the equation for the evolution of the surface density $\Sigma(r,t)$ of the accretion disc for the disc around the magnetized star can be found as

$$\frac{\partial\Sigma}{\partial t} = \frac{3}{R}\frac{\partial}{\partial R}\left\{R^{1/2}\frac{\partial}{\partial R}\left(R^{1/2}\nu\Sigma\right) - \frac{4B_{\rm z}B_\phi R^{5/2}}{\mu_0\sqrt{GM}}\right\} \tag{5.15}$$

Equation (5.15) is an integral of the mass and angular momentum equations (5.2) and (5.12) which is more general, and relies on the assumptions: conservation of mass, conservation of angular momentum, and that the potential is Keplerian. Since the time-dependence enters only through Eq. (5.15), it is essential to try to express the other quantities in terms of Σ as far as possible, as they depend on t only through Σ and not explicitly.

5.3 Transport of energy in the disc

The Navier- Stoke's equation for the conservation of internal energy can be written as:

$$\frac{\partial}{\partial t}(\rho e) + \nabla \cdot [(\rho e + P)\,\mathbf{v}] = \mathbf{v} \cdot \mathbf{f}_\nu + \frac{\mathbf{J^2}}{\sigma} - \nabla \cdot \mathbf{F_{rad}} - \nabla \cdot \mathbf{q}, \tag{5.16}$$

Here the second term on the left describes the variations in the internal energy $e = E/\rho$, while the first and third terms in the right-hand-side describes viscous heating and radiative cooling respectively and the second and fourth terms are respectively ohmic heating and heat conduction. Neglecting very small terms and retaining the dominant terms, then the energy equation gives

$$\frac{\partial E}{\partial t} = \mathbf{v} \cdot \mathbf{f}_\nu - \nabla \cdot \mathbf{F_{rad}}, \tag{5.17}$$

Integrating Eq.(5.17) vertically over the disc we have

$$\frac{\partial E}{\partial t} H = \frac{9}{8}\nu\Sigma\frac{GM}{R^3} - \frac{8\sigma T_{\rm c}^4}{3\Sigma\kappa} \tag{5.18}$$

This is the conservation of energy equation which can be used to analayse the thermal instability of the disc.

5.3.1 Equation of state

The total pressure is the sum of gas pressure and radiation pressure and then given by the equation of state:

$$P = P_{\rm gas} + P_{\rm radiation}, \tag{5.19}$$

$$P_{\rm gas} = \frac{\rho k_{\rm B} T_{\rm c}}{m_{\rm p}\bar{\mu}},\ P_{\rm rad} = \frac{aT_c^4}{3} \tag{5.20}$$

In equation (5.19), $m_{\rm p}$, $k_{\rm B}$, $\bar{\mu}$, and a are the mass of a proton, Boltzmann constant, the mean molecular weight for ionized gas, and familiar radiation constant, respectively. But the pressure can also be expressed using the equation of hydrostatic equilibrium

$$\frac{1}{2}\Sigma\Omega^2 H = \frac{\Sigma k_{\rm B} T_{\rm c}}{2H m_{\rm p}\bar{\mu}} + \frac{aT_c^4}{3} \tag{5.21}$$

This is the conservation of energy equation which can be used to explain the thermal stability of the disc.

5.3.2 Viscous stress

In our model the viscous stress tensor is related according to

$$f_{r\phi} = \frac{3}{4}\Sigma\nu\left(\frac{GM}{R^3}\right)^{1/2} H^{-1} = \frac{3}{4}\Sigma\nu\Omega H^{-1} = \alpha_{\rm ss}P(r) \tag{5.22}$$

The conventional $\alpha_{\rm ss}$ model assumes that

$$\nu = \frac{4}{3}\alpha_{\rm ss}\frac{PH}{\Sigma}\left(\frac{GM}{R^3}\right)^{-1/2} = \frac{2}{3}\alpha_{\rm ss}\Omega H^2, \tag{5.23}$$

where $\alpha_{\rm ss}$ is a parameter which describe the strength of the viscous stress. From Eq. (5.23) the internal pressure can be expressed as

$$P(r) = \frac{3}{4}\alpha_{\rm ss}^{-1}\nu\Sigma\left(\frac{GM}{R^3}\right)^{1/2} H^{-1} = \frac{3}{2}\alpha_{\rm ss}^{-1}\nu\rho\left(\frac{GM}{R^3}\right)^{1/2} \tag{5.24}$$

which we solve for the density of the gas

$$\rho = \frac{3}{4\alpha_{\rm ss}}\frac{\nu\Sigma}{H^2}\left(\frac{GM}{R^3}\right)^{-1/2}. \tag{5.25}$$

5.4 Viscous stability

Viscous stability of geometrically thin, optically thick, Keplerian accretion disc is described by the evolution of the discs surface density which is obtained by combining the conditions of conservation of mass and angular momentum. In our model this is the equation for the evolution of the surface density Σ of an accretion disc around a magnetized star

$$\frac{\partial\Sigma}{\partial t} = \frac{3}{R}\frac{\partial}{\partial R}\left[R^{1/2}\frac{\partial}{\partial R}\left(R^{1/2}\nu\Sigma\right)\right] - \frac{4}{R}\frac{\partial}{\partial R}\left(\frac{RB_zB_\phi}{\mu_0\Omega}\right), \tag{5.26}$$

where B_ϕ is the sum of the magnetic field generated by the internal dynamo and due to shear. This is a diffusion equation giving the evolution of the surface density function, due to the spreading of material controlled by viscous and magnetic stresses. It is clear that in order to solve non-linear equation (5.13) and subsequently find all the other disc variables is in general a formidable task which must be solved numerically. However, we can draw important conclusions relating different equations and the form of equation (5.13) alone. Suppose the viscous ν varies as given power of radius the equation can be solved analytically. Assuming that the viscosity at a given radius depend on local parameters in the disc. In its simplest form we may write $\nu = \nu(R, \Sigma)$. For convenience we write

$$y\left(R, \Sigma\right) = \nu\Sigma. \tag{5.27}$$

The explicit R-dependent in ν, and hence y, arises from the magnetic and viscous stress. We further assume that the surface density in a steady disc is perturbed axisymmetrically at each radius R, so that

$$\Sigma(R,t) \rightarrow \Sigma_0(R) + \delta\Sigma(R,t) \tag{5.28}$$

where $\Sigma_0(R)$ is the steady- state distribution and let the corresponding perturbation for y be δy, then

$$y \rightarrow y + \delta y, \quad \delta y = \left(\frac{\delta y}{\partial \Sigma}\right) \delta\Sigma \tag{5.29}$$

Taking similar perturbations in the toroidal magnetic field generated by the internal dynamo $B_{\phi,\mathrm{dyn}}$ and substituting in diffusion equation yields the linear equation

$$\frac{\partial(\delta\Sigma)}{\partial t} = \frac{3}{R}\frac{\partial}{\partial R}\left[R^{1/2}\frac{\partial}{\partial R}\left(R^{1/2}\delta y\right)\right] + \frac{4}{R}\frac{\partial}{\partial R}\left(\frac{RB_z\delta B_{\phi,\mathrm{dyn}}}{\mu_0\Omega_k}\right), \tag{5.30}$$

where

$$\delta B_{\phi,\mathrm{dyn}} = \left(\frac{\partial B_\phi}{\partial\Sigma}\right)_0 \left(\frac{\partial y}{\partial\Sigma}\right)_0^{-1} \delta y \text{ and } \delta\Sigma = \left(\frac{\partial \mathrm{y}}{\partial\Sigma}\right)_0^{-1} \delta \mathrm{y}. \tag{5.31}$$

Here the shear component of the magnetic field is very small and dropped. Thus a small perturbation δy satisfies the linear equation

$$\frac{\partial(\delta y)}{\partial t} = \frac{3}{R}\left(\frac{\partial y}{\partial\Sigma}\right)\frac{\partial}{\partial R}\left[R^{1/2}\frac{\partial}{\partial R}\left(R^{1/2}\delta y\right)\right] + \frac{4}{R}\left(\frac{\partial y}{\partial\Sigma}\right)\frac{\partial}{\partial R}\left(b\delta y\right), \tag{5.32}$$

where

$$b = \frac{RB_z}{\mu_0\Omega_k}\left(\frac{\partial B_\phi}{\partial\Sigma}\right)_0\left(\frac{\partial y}{\partial\Sigma}\right)_0^{-1} \tag{5.33}$$

Eq. (5.32) is a linear modified diffusion equation for δy, which describes the evolution of a perturbation in y and well behaved if and only if the modified diffusion coefficient is positive. When the coefficient $\frac{\partial y}{\partial\Sigma}$ is positive we have the evolution equation of the type of diffusion equation behaviour including magnetic stress. However, if $\frac{\partial y}{\partial\Sigma}$ is negative, more material will be fed into those regions of the disc that are denser than their surroundings and material will be removed from those regions that are less dense so that the disc will tend to break up into rings and this breakup of on viscous time scale constitutes the viscous instability; steady disc flow is only possible provided that $\frac{\partial y}{\partial\Sigma} > 0$. Thus the criterion for viscous instability is

$$\text{Instability} \Leftrightarrow \frac{\partial}{\partial\Sigma}(\mathrm{y}) < 0 \tag{5.34}$$

where the derivative is taken under the assumptions of vertical hydrostatic equilibrium and of thermal balance. If a disc is viscously unstable, a region that is locally under dense (over dense)

evolves faster (slower) than its surroundings and thus becomes even more under dense (over dense). Thus Eq.(5.32) is the fundamental equation of non-stationary disc accretion. Stability analysis can be made based on these equations. We shall look for solutions to Eq. (5.30) and (5.32) of the form which represents the perturbations considering short-wavelength modes of the form,

$$\delta y = A \exp\left[\imath(\omega \mathrm{t} - \mathrm{kR})\right], \tag{5.35}$$

where A is a constant, ω the angular frequency and k the wavenumber and $kR \gg 1$. For such modes, variations in disc quantities can be ignored over a wavelength $kR \gg 2\pi$ and have the decay/growth rate ω principally determined by the first term on the right-hand side of Eq. (5.32) (Paper III). Viscous instability then follows when $\left(\frac{\partial y}{\partial \Sigma}\right)_0 < 0$, with y being influenced by the magnetic field.

Since the magnetic diffusivity is fixed the we drop subscribe zero and the shear part of the magnetic stress from Eq. (5.32) and we obtain

$$\frac{\partial(\delta y)}{\partial t} = \frac{3}{R}\left(\frac{\partial y}{\partial \Sigma}\right)\frac{\partial}{\partial R}\left[R^{1/2}\frac{\partial}{\partial R}\left(R^{1/2}\delta y\right)\right] + \frac{4}{R}\left(\frac{\partial y}{\partial \Sigma}\right)\frac{\partial}{\partial R}\left(b\delta y\right) \tag{5.36}$$

Substitution of Eq.(5.35) into (5.36) gives an expression for ω. The viscous diffusion term dominates the magnetic term in (5.36) in determining ω, since it contains a term in $(kR)^2$, while the magnetic term is only linear in kR. It follows that the sign of $\left(\frac{\partial y}{\partial \Sigma}\right)_0$ determines the sign of ω and hence the stability of the perturbation. The magnetic field affects the viscous stability by influencing the form of $y(R, \Sigma)$. The increase in $\nu\Sigma$ due to the the effect of the magnetic field. The magnetic field generated due to internal dynamo is dominant in our model (Paper I, II & III) as a result the disc is stable in the presence of strong magnetic field in the gas pressure dominated disc. Because the magnetic field due to the internal dynamo may maintain sufficient angular momentum transport through out in such type of disc. But in the radiation pressure dominated disc the toroidal magnetic field generated by an internal dynamo is independent of dynamical viscosity as well as the magnetic field is weak compared to the gas pressure dominated disc (Paper II), then the the innermost disc region is unstable.

From the perturbation equations we can find the dispersion relation, which will give solutions that are stable and unstable in addition to the stability condition which have already used above (Paper III). Substituting Eq. (5.35) into (5.36)

$$\omega^2 = \chi^2\left(\frac{-1}{4R^{3/2}} - \frac{3k\imath}{2R^{3/2}} + \frac{3(k\imath)^2}{2R^{1/2}} - \frac{4bk\imath}{R}\right)\left(\frac{-1}{4R^{3/2}} + \frac{3k\imath}{2R^{3/2}} + \frac{3(k\imath)^2}{2R^{1/2}} + \frac{4bk\imath}{R}\right), \tag{5.37}$$

where $\chi = \frac{\partial y}{\partial \Sigma}$. After squaring Eq. (5.37) we get

$$\omega^2 = \chi^2 \left(\frac{9k^4}{4R} + \frac{9k^2}{4R^3} + \frac{3k^2}{4R^2} + \frac{1}{16R^3} \right) + \chi^2 \left(\frac{12bk^2}{R^{5/2}} + \frac{16b^2k^2}{R^2} \right) + \chi^2 \left(\frac{12k^3b}{R^{3/2}} - \frac{2bk}{R^{5/2}} \right) \imath \tag{5.38}$$

We can obtain approximate values of ω

$$\omega \approx \pm \frac{\chi}{4} \sqrt{\frac{1 + 36k^2 + 192bk^2\sqrt{R} + 12k^2R + 256b^2k^2R + 192b^2k^3R^{3/2} + 36k^4R^2 - 32bk\sqrt{R}\imath}{R^3}} \tag{5.39}$$

For $k \longrightarrow \infty$ Eq. (5.39) gives

$$\omega \approx \pm \frac{3k^2\chi}{2} \frac{1}{\sqrt{R}} \tag{5.40}$$

Equation (5.38) is the general dispersion relation and will help us to investigate the stability of our disc model. The first term in equation (5.38) is due to viscous stress, which is the fourth and the second orders of k the leading term in k is the fourth order, the second and the third terms are due to magnetic field generated by the internal dynamo. For the short wavelength limit $k \longrightarrow \infty$, we obtain real roots from Eq. (5.38). When the real part of $\omega > 0$, then it satisfies the stability condition and when the real part of $\omega < 0$ then the disc is unstable (see Eq. 5.40). Weakly magnetised accretion discs are subject to a powerful axisymmetric instability. The instabilities lead to electron scattering and acceleration of fast particles leading to enhancement in radiation pressure. Strongly magnetised the accretion discs are subjected to stability conditions. The dispersion relation (5.38) indicates that the most rapidly growing wave numbers in a thin discs have growing rates. The growing rate is dependent on the strength of the magnetic field. For imaginary of ω the instability criterion is most easily satisfied than the real part of it but the azimuthal component of the strong magnetic field (dynamo field) tends to stabilize. Generally the dispersion relation is used to investigate the stability properties of the accretion disc by considering the local perturbation of the disc.

5.5 Results and Discussion

5.5.1 Timescales and Stability

The time-dependent accretion discs with α-parameter viscosity were constructed by Lightman(1974a,b) and its flow is controlled by the size of the viscosity. Hence observations of time-dependent disc behaviour offer one of the few sources of quantitative information , it is

important to consider the relative magnitudes of the various timescales over which accretion discs form and evolve and the effect of magnetic field is observed on timescales. We begin by identifying the typical timescales on which the disc structure may vary.

Dynamical Time Scale($t_{\rm dyn}$): a timescale in which pressure forces adjusts to combine gravitational and centrifugal force and which is simply related as

$$t_{\rm dyn} \sim \frac{R}{v_\phi} \sim \Omega_k^{-1}. \tag{5.41}$$

This is the shortest time scale present in the disc, which is the Keplerian period, that ranges very small in the inner region and increases to outer disc and also the typical growth time of some important instabilities, such as the magneto-rotational instability. Using steady state equations we can write this as

$$t_{\rm dyn} \sim 8.66 \times 10^{-11} M_1^{-1/2} R^{3/2}\,{\rm s} \tag{5.42}$$

We see that the dynamical timescale depends on mass of the accretor and radius. Clearly, inhomogeneities, such as flares on the disc surface, would cause quasi-periodic variations in the disc light at some wavelengths with this time scale. A second important timescale is the vertical timescale, needed to reach hydrostatic balance in the vertical direction. This is given by the isothermal sound speed crossing time across the disc thickness H. Deviations from hydrostatic equilibrium in the z-direction are smoothed out on a timescale

$$t_z = \frac{H}{c_s} \tag{5.43}$$

But from the relations

$$H \sim \mathtt{M}^{-1} R, \;\; \mathtt{M} = \frac{v_\phi}{c_s} \quad \text{, Mach number}$$

$$v_\phi \sim \alpha \mathtt{M}^{-1} c_s$$

We see that

$$t_z \sim \frac{R}{\mathtt{M} c_s} = \frac{R}{v_\phi} \sim t_\phi \sim 8.66 \times 10^{-11} M_1^{-1/2} R^{3/2}\,{\rm s}$$

Interestingly, this timescale is equal to the dynamical one. So that the dynamical timescale also measures the speed with which hydrostatic equilibrium in the vertical direction is established.

Thermal Time Scale ($t_{\rm th}$): is the time needed by the disc to modify its thermal structure, and its temperature. In general, we will have a cooling timescale $t_{\rm cool}$ which is set by the specific cooling processes in the disc, and a heating timescale $t_{\rm heat}$ which is determined by energy release

due to accretion. In thermal equilibrium, clearly these two timescales are equal. The heating timescale is simply given by the ratio between the heat content at a given radius and the power produced by accretion disc.

We thus see that $t_{\rm th} \sim t_{\rm dyn}\alpha_{ss} \gg t_{\rm dyn}$.

Mathematically we can define the thermal timescale:

$$t_{\rm th} = \frac{\text{heat content per unit disc area}}{\text{dissipation rate unit disc area}},$$

which gives the timescale for re-adjustment to thermal equilibrium , if, say, the dissipation rate is altered. Since the heat content per unit volume of a gas is $\sim \frac{\rho k_B T_c}{m_p \bar{\mu}} \sim \rho c_s^2$, this gives

$$t_{\rm th} \sim \frac{\Sigma c_s^2}{W(R)} \tag{5.44}$$

The relation $W_\nu(R) = \frac{9}{8}\nu\Sigma\frac{GM}{R^3}$ and $\nu\Sigma$ means that $t_{\rm th}$ can be re-expressed in terms of the viscous timescale; for a Keplerian disc, we have ($\Omega = \Omega_k$)

$$t_{\rm th} \sim \frac{R^3 c_s^2}{GM\nu} \simeq \mathtt{M}^{-2} t_{\rm visc} \tag{5.45}$$

Viscous Time Scale ($t_{\rm visc}$): a time in which angular momentum distribution changes due to torque caused by dissipative stresses. The viscous timescale sets the scale for the evolution of the surface density. From the analysis of time dependent models above, we have seen that this timescale is given by the viscous timescale

$$t_{\rm visc} \sim \frac{R^2}{\nu} \sim \frac{R}{v_R} \sim 9.63 \times 10^3 \alpha_{ss}^{-4/5} \bar{\mu}^{3/4} M_1^{1/14} \dot{M}_{13}^{17/35} \mu_{20}^{5/7} \Lambda^{-3/10} r^{11/4} \tag{5.46}$$

which gives the timescale on which matter diffuses through the disc under the effect of viscous torques. The viscosity has the effect of spreading the original ring in radius on a typical time scale, assuming that the typical length scale for surface density gradients in the disc is $\sim R$. Which is an order of magnitude longer than other time scales.

Using the $\alpha-$ parametrization we can also write

$$t_{\rm visc} \sim \frac{R^2}{\nu} \sim \frac{1}{\alpha}\frac{R}{H}\frac{R}{v_\phi}.\frac{v_\phi}{c_s}$$

which, for a thin disc, gives

$$t_{\rm visc} \sim \alpha^{-1}\mathtt{M}^2 t_\phi \tag{5.47}$$

Collecting results we have

$$t_{\rm dyn} \sim t_{\rm z} \sim \alpha_{\rm ss} t_{\rm th} \sim \alpha_{\rm ss} \left(\frac{H}{R}\right)^2 t_{\rm visc} \tag{5.48}$$

Then from Eq.(5.48) the thermal time scale is

$$t_{\rm th} \sim 1.4\alpha^{3/5} M_1^{-11/14} \dot{M}_{13}^{-3/35} \mu_{20}^{6/7} r^{3/2} \tag{5.49}$$

If we assume $\alpha \leq 1$ there is thus a well-defined hierarchy of timescales

$$t_{\rm dyn} \sim t_{\rm z} \leq t_{\rm th} \ll t_{\rm visc}$$

As long as the disc is thin, we thus see that the various timescales are ordered in the following way::

$$t_{\rm vis} \gg t_{\rm th} \gg t_{\rm z} \sim t_{\rm dyn}, \tag{5.50}$$

which then shows that the centrifugal balance in the radial direction and hydrostatic balance in the vertical direction are very rapidly achieved, while the disc temperature generally evolves on a longer timescale, and finally, on an even longer timescale, one can see some evolution in the surface density profile.

Finally, note that all of the above timescales are a function of radius. In particular, if H/R are constant which is not our case (which is not generally true), then they all scale in the same way, and for a Keplerian disc, they increase with radius as $R^{3/2}$. Thus the evolution of the inner disc is generally much more rapid than the evolution of the outer disc. Suppose now that a small perturbation is made to a generally considered equilibrium solution and that this perturbation continues to grow rather than being damped. Then the supposed steady solution is said to be unstable and cannot occur in reality. The sharp difference we have found in the various timescales means we can distinguish different types of instability. If for example the energy balance is distributed in the disc, any instability will grow on a timescale $t_{\rm th}$, which is much less than $t_{\rm visc}$. Since $t_{\rm visc}$ is the timescale for different changes in the surface density Σ to occur, we can assume that Σ is fixed during the growth time $t_{\rm th}$. We refer to this as a thermal instability. For $\alpha < 1$ we also have $t_{\rm th} > t_\phi \sim t_{\rm z}$, so the vertical structure of the disc can respond rapidly, on a timescale $t_{\rm z}$, to changes due to the thermal instability, and keep the vertical structure close to hydrostatic equilibrium.

Another condition for instabilities arise when the local cooling rate Q^- with in the disc can no longer cope with the heating rate Q^+ due to viscous dissipation. In equilibrium we must have $Q^+ = Q^-$.

But if, when the central temperature T_c is increased by a small perturbation ΔT_c which is not be the case here, Q^+ increases faster than Q^-, T_c will rise further because the cooling rate is in adequate. In other words, steady state is impossible in a parameter regime where the instability would grows, despite the fact that formally an "equilibrium" solution can be found.

5.5.2 Stability Analysis

In the previous two chapters we calculated the solution of Σ numerically by writing the relations in the form $\Sigma = \Sigma(\Lambda)$ because we know Λ numerically. To investigate the viscous stability of the solution we calculate the derivatives of $\frac{\partial\Sigma}{\partial\Lambda}$. We calculate this derivatives using the results of the previous chapters for a slightly perturbed value of Λ. When this derivative is positive the solution is viscously stable, other wise it is viscously unstable.

Eq.(5.27) gives the viscosity integral $y = \nu\Sigma$ for given $\dot{M}$, μ and other parameters as a function of r. In more general situation when the system is time-dependent, there is no fixed $\dot{M}$ but in our work we use accretion rate in steady state, and time-independent equation has to be replaced by an explicitly time-dependent diffusion type equation for Σ. In any case, in order to close the system of equations we need another equation that relates Λ with Σ. In the time-dependent case the sign of $\frac{\partial\Lambda}{\partial\Sigma}$ determines whether the solution is viscously stable (positive sign) or unstable (negative sign). In the steady case we calculate $\Sigma = \Sigma(\Lambda)$, where Λ has been calculated in the previous chapters. In paper I equations (40) and (41) we have the relations $y = \Lambda\dot{M}$, $R = rR_A$, use of these relations Eq. (5.32) gives

$$\frac{\partial(\delta\Lambda)}{\partial t} = \frac{3\dot{M}}{R_A^2 r}\left(\frac{\partial\Lambda}{\partial\Sigma}\right)_0 \frac{\partial}{\partial r}\left[r^{1/2}\frac{\partial}{\partial r}\left(r^{1/2}\delta\Lambda\right)\right] + \frac{4\dot{M}}{R_A r}\left(\frac{\partial\Lambda}{\partial\Sigma}\right)_0 \frac{\partial}{\partial r}\left(b\delta\Lambda\right) - \frac{4}{\dot{M}R_A r}\left(\frac{\partial\Lambda}{\partial\Sigma}\right)_0 \frac{\partial}{\partial r}\left(\frac{rB_z B_{\phi,\mathrm{sh}}}{\mu_0\Omega_k}\right), \tag{5.51}$$

With similar reason given in section 5.4 we drop the subscript zero and the shear component of the magnetic stress Eq. (5.51) can be rewritten as

$$\frac{\partial(\delta\Lambda)}{\partial t} = \frac{3\dot{M}}{R_A^2 r}\left(\frac{\partial\Lambda}{\partial\Sigma}\right)\frac{\partial}{\partial r}\left[r^{1/2}\frac{\partial}{\partial r}\left(r^{1/2}\delta\Lambda\right)\right] + \frac{4\dot{M}}{R_A r}\left(\frac{\partial\Lambda}{\partial\Sigma}\right)\frac{\partial}{\partial r}\left(b\delta\Lambda\right) \tag{5.52}$$

In the gas pressure dominated disc when the accretion rate increases the magnetic field due to dynamo increases (strong field is generated) as result sufficient angular momentum is transported which lead to stability of the disc properties. But in the radiation pressure dominated disc the inner edge of accretion disc close to the surface of the neutron star and the magnetic field due

to dynamo decrease which cannot shut off the instability. From paper I Eq. (47) Λ and Σ were related as

$$\frac{\partial \Sigma}{\partial \Lambda} = 5285.7 \alpha_{\rm ss}^{-4/5} M_1^{5/14} \dot{M}_{13}^{32/35} \mu_{20}^{-3/7} \Lambda^{3/7} r^{-3/4} > 0 \tag{5.53}$$

this is the case for steady-disc which shows the disc is stable.

For the time-dependent disc we have

$$\Lambda = C_1 \Sigma^{10/7} r^{15/14}, \tag{5.54}$$

where

$$C_1 = \left(3.7 \times 10^3 \alpha_{\rm ss}^{-4/5} M_1^{5/14} \dot{M}_{13}^{32/35} \mu_{20}^{-3/7}\right)^{-10/7}$$

And hence

$$\left(\frac{\partial \Lambda}{\partial \Sigma}\right)_0 = \frac{10}{7} C_1 \Sigma^{3/7} r^{15/14} > 0 \tag{5.55}$$

which gives that

$$\left(\frac{\partial \Lambda}{\partial \Sigma}\right)_0 = 5.6 \times 10^{-6} \alpha_{\rm ss}^{8/7} M_1^{-25/49} \dot{M}_{13}^{-64/49} \mu_{20}^{30/49} \Sigma^{3/7} r^{15/14} > 0$$

In this case steady disc flow is possible and which satisfies stability condition. Therefore, steady state model is stables against small perturbation in the gas pressure and free-free absorption dominated disc. That is positive slope. Since in the gas pressure dominated disc the magnetic field is strong than the radiation pressure dominated disc, the strong magnetic field generated by internal dynamo helps the disc to be stable.

We can also show stability of the disc using the derivatives of temperature with respect to the surface density

$$\frac{\partial T}{\partial \Sigma} = 33112.3 \bar{\mu}^{1/4} \alpha_{ss}^{1/7} M_1^{10/49} \dot{M}_{13}^{6/49} \mu_{20}^{-12/49} \Sigma^{-4/7} r^{-3/7} > 0 \tag{5.56}$$

the disc is stable. When $\frac{\partial T}{\partial \Sigma} < 0$, and a viscous instability, this time known as the Lightman-Eardley instability.

The time-dependent disc give us an information to explain the torque reversal of X-ray pulsars by reversing the magnetic field in the disc with similar magnitude of spin-up and spin-down torques which depends on the inner and corotation radii. In linearly stable disc we can observe the stable torques, and it is non-linearly unstable because otherwise no torque reversal would occur. Since in the star disc interacting system presence of a disc dynamo produces a significant enhancement of the torque between the magnetic field of the neutron star and the accretion disc.

5.5.3 Thermal Stability

The general stability criteria of accretion discs were explained by different authors (for example Piran 1978; Shakura and Sunyaev 1976; Frank, King and Raine 2002). These criteria can be used as a prior check if some choice of cooling mechanisms gives rise to a stable disc even before the complete disc structure equation are solved. Thermal instability criterion can be expressed as

$$\left(\frac{dQ^-}{dT_c}\right)_\Sigma < \left(\frac{dQ^+}{dT_c}\right)_\Sigma$$
$$\left(\frac{dlnQ^-}{dlnT_c}\right)_\Sigma < \left(\frac{dlnQ^+}{dlnT_c}\right)_\Sigma, \tag{5.57}$$

where Q^+, Q^-, and T are the viscous heating rate, radiative cooling rate and temperature, respectively; such a criteria is identical to (Piran 1978) if we replace T with H. The thermal instability can be understood according to this criterion. Considering a small temperature increase and assuming that the surface density does not change with in the thermal timescale, if the viscous heating rate increases more rapidly than radiative cooling rate does, it will lead to a further increase of temperature and the thermal instability sets in. If the standard viscosity law is adopted, Piran (1978) has pointed out that the inner region of accretion disks is always thermally unstable no matter what kind of cooling mechanism is involved. Because in the inner most regions of the disc opacity due to electron scattering is dominant than Kramer's opacity and there is no enough radiative cooling which balance viscous heating rate as well as the disc is truncated near the surface of the neutron with magnetic field generated due dynamo.
For optically thick discs the effective volume cooling rate is approximately given by

$$Q^- \approx \frac{\sigma T_c^4}{\kappa_R \rho H^2}.$$

For Kramer's opacity this can be written as:

$$Q^- \sim \frac{T_c^{15/2}}{\Sigma^2} \sim T_c^{15/2}$$

In the gas pressure dominated disc α_{ss} decreases more rapidly than T_c^{-7}, optically thick parts of the disc will be thermally stable. Since Kramer's opacity is dominant than over opacity due to electron scattering and the magnetic field generated due to dynamo is stronger than the inner most disc.

The equation that obtained from the equation of energy conservation in section 5.3 can relate Σ and H which describe thermal stability after linearization:

$$\frac{\partial E}{\partial t} H = \frac{3\alpha_{ss}}{4} \Sigma H^2 \Omega^3 - \frac{8\sigma T_c^4}{3\Sigma\kappa} \tag{5.58}$$

The total energy density is related with pressure by

$$E = \frac{3}{2}(I+\beta)p,$$

where $\beta = p_r/p,\ (p = p_r + p_g)$ describes the contribution of radiation to the total pressure. Note that in the limit of dominant radiation pressure ($\beta_0 = p_r/p \simeq I$). Using the relations

$$P = \frac{1}{2}\Omega^2 \Sigma H$$

gives

$$E = \frac{3}{4}(I+\beta)\Sigma H \Omega^2 \tag{5.59}$$

Then equation (5.59) becomes

$$\frac{3}{4}\frac{\partial}{\partial t}(I+\beta)\Sigma H^2\Omega^2 = \frac{3\alpha_{ss}}{4}\Sigma H^2\Omega^3 - \frac{2\beta\Omega^2 H}{\kappa_{es}} \tag{5.60}$$

We linearize Eq. (5.58) substituting into a perturbation solution of the form

$$\begin{aligned} \Sigma &= \Sigma_0 + \delta\Sigma = \Sigma_0\left(1+\frac{\delta\Sigma}{\Sigma_0}\right) = \Sigma_0(1+u) \\ H &= H_0 + \delta H = H_0\left(1+\frac{\delta H}{H_0}\right) = H_0(1+h) \end{aligned} \tag{5.61}$$

Thus neglecting the higher order terms and retaining only the linear one we get

$$(4I\beta_0 + 4\beta_0^2)\frac{\partial u}{\partial t} + (4I\beta_0 + 4\beta_0^2)\frac{\partial h}{\partial t} = \alpha_{ss}\beta_0(u+2h)\Omega - \frac{8\beta_0 H_0(1+h)}{\kappa_{es}} \tag{5.62}$$

From the linearization Eq. (5.62) if β_0 is greater or equal to one the disc is thermally unstable and if β_0 is less or equal to unity then the disc is stable that is the cooler accretion disc is expected.

5.5.4 Instabilities in the radiation pressure dominated disc

Accretion discs have been extensively examined in relation to binary X-ray sources, quasars and galactic nuclei. Theoretical investigations of stationary disc models have revealed that some models are secularly unstable (Lightman and Eardley 1974) or thermally unstable (Pringle, Rees & Pacholczyk 1973; Shibazaki and Hoshi 1975 ; Shakura and Sunyaev 1976; Pringle 1976). The presence of instabilities is of interest because periodic, quasi-periodic or Chaotic variability have been observed in some binary X-ray sources and quasars.

The fate of these instabilities are, however, still open to question at this moment ; Shapiro et

al. (1976) argued that the instabilities may lead to the formation of two-temperature, optically thin discs, while the slim disc model by Abramowicz et al. (1988) asserts that a third branch is realized by efficient advective cooling in the relativistic discs, so that the disc can undergo limit cycles. Note that the accretion rate in slim disc is higher than thin disc but will not discuss the stability of slim disc in our thesis.

In our work we assume that disc is optically thick geometrically thin and we found that the derivative of y with respect Σ gives us the information about the instabilities of the disc.

The steady angular momentum balance can then only be satisfied by viscous and magnetic stress increasing, via an increase in $\nu\Sigma = y$ and the increase in $\nu\Sigma$ leads to enhanced viscous dissipation and an increased central temperature. The radiation pressure becomes dominant and the disc is disturbed vertically, with viscous instability ensuring. When the coefficient of $\frac{\partial y}{\partial \Sigma}$ becomes negative.

In steady-state disc the inner regions of the disc where the radiation pressure and an electron scattering opacity is dominant, then Λ and Σ are related as (see paper II Eq. (5.51))

$$\Lambda = C_2 \Sigma^{-1} r^{3/2}, \tag{5.63}$$

where

$$C_2 = 9.56 \times 10^1 \alpha_{ss}^{-1} M_1^{-5/7} \dot{M}_{14}^{-10/7} \mu_{16}^{6/7}.$$

Thus

$$\left(\frac{\partial \Lambda}{\partial \Sigma}\right)_0 = -C_2 \Sigma^{-2} r^{3/2} < 0 \tag{5.64}$$

which is the condition for viscous instability (negative slope) and also $\frac{\partial \Sigma}{\partial \Lambda} < 0$. Thus viscous instability also appears in another case, namely when the disc is dominated the radiation pressure, with a pure scattering opacity $\kappa_R =$ constant. These conditions hold in the central regions of disc around neutron stars and black holes. But the disc is stable in the other two regions. From Eq. (5.27) follows that

$$\frac{\partial y}{\partial \Sigma} = \nu + \Sigma \frac{\partial \nu}{\partial \Sigma} \tag{5.65}$$

To understand why the instability exists in the inner regions of the disc, we first understand the relation between Σ and Λ. In this region Λ decreases as surface density increases. Physically, low stress in high- Σ regions and high stress in low-Σ regions means that matter is pushed into regions of low stress thus density contrast grows, forming rings of gas.

5.6 Conclusion

We investigated a theory for the time-dependent behaviour of a stationary thin accretion around magnetized star. A linear stability analysis of the thin accretion disc solutions in the presence of a strong external magnetic field gives an information about the behaviour of stationary disc. The time-dependent behaviour of the accretion disc around magnetised stars will give us Simple analytical arguments show that a Keplerian accretion disc ought to be hydrodynamically stable, but Balbus and Hawley showed in 1991 that it is unstable in the presence of a weak magnetic field because a strong magnetic field can shut off the instability.

However,the perturbation of surface density helps us to linearize steady state equation and the coefficient of equations is still diffusion equation if the slope is positive with no problem which gives the information of stability and instability of the disc. According to our model the thin disc model resulting from the generation of the magnetic field generated by the internal dynamo is stable in the gas pressure dominated disc region and unstable in the radiation pressure dominated disc.

The presence of magnetic field due an internal dynamo makes the disc more stable in the gas pressure dominated region.

Chapter 6

General Summary and Future Prospects

We have presented a model for the interaction between a magnetic neutron star and its surrounding steady-state of an axisymmetric thin accretion disc with an internal dynamo around a magnetised star. Our model is based on the case where the accretion disc is supporting an internal dynamo. From the vertically integrated equations of magnetohydrodynamics we derive a single ordinary differential equations for a thin accretion disc around a massive magnetic dipole field which can be applicable for different regions of the disc. The differential equation is integrated numerically from the outside inwards for all cases. The numerical result indicates that the torque between the star and the accretion disc is dominated by the contribution from the dynamo in the disc. The location of the inner edge of the accretion disc depending mainly on the strength and direction of the magnetic field generated by the dynamo in the disc.

The magnetic field that is produced by the dynamo can lead to a significant enhancement of the magnetic torque between the neutron star and the accretion disc, compared to what is seen in the model by Ghosh & Lamb (1979a,b). This extra magnetic torque can explain the large variations in spin frequencies of Cen X-3 and OAO 1657-415 (Bildsten et al. 1997).

From our model we have calculated the fundamental solution for the structure of a steady state thin accretion disc a self-similar form similar to the classical solutions by (Shakura & Sunyaev 1973) in terms of radius, mass of the accretor, accretion rate and magnetic moment, we have found two kinds of solutions with different behaviours at the inner edge. A few of our solutions have case D boundaries at which the density and temperature go to 0 at finite radius,

while most of our solutions have case V boundaries at which the accretion is driven entirely by the magnetic tension between the accreting matter and the neutron star. In this case there is a viscous stress between the accretion disc and the boundary layer, which can transfer angular momentum outwards at a rate that is comparable to the one at which it is advected inwards by the accreting matter itself.
We have also found that the dynamo leads to that the inner edge of the accretion disc occurs at a radius that is larger than the traditional Alfvén radius.

The accretion rates that have been observed in millisecond X-ray pulsars cover several orders of magnitude, and the highest accretion rates are sufficient that the innermost part of the accretion disc is dominated by radiation pressure and electron scattering. For these reasons we have followed the approach by Shakura & Sunyaev (19973) and divided our disc model in three regions, an outer region dominated by gas pressures and Kramer's opacity, a middle region dominated by gas pressure and electron scattering, and an inner region dominated by radiation pressure and electron scattering.

The large spin changes that have been observed in some of the accreting millisecond X-ray pulsars are difficult to explain in the model by Ghosh & Lamb (1979), but the inclusion of a disc dynamo produces a significant enhancement of the torque between the accretion disc and the neutron star. This increase is not only due to the coupling between the magnetic fields of the neutron star and the accretion disc as such, but also to the fact that the accretion disc is truncated at a larger radius thus increasing the lever arm between the edge of the disc and the neutron star.

We have derived the time-dependent equations for an accretion disc in the small perturbation of the surface density to examine a linear stability analysis of our steady disc models in the presence of magnetic field due to an internal dynamo. The linearization of dynamical equations indicates that the radiation pressure dominated disc is unstable in the innermost part of the disc because the magnetic field generated by the internal dynamo is weak compared to the outer disc region.

One of the applications of our model is that it can help us to understand the rotational evolution of both neutron stars and T Tauri-stars based on the magnetic interaction between the disc and the star. It can also help us to understand the structure and the properties of millisecond X-ray pulsars. When it comes to neutron stars an important issue is the formation of millisecond pulsars from what most probably must have been ordinary neutron stars in binaries.

The interesting results in our work is the discovery of the inner edge of the accretion disc is greater than the Alfvén radius, and the magnetic field /or/and torque generated due to dynamo is stronger than the magnetic field/ or/and torque generated due to shear in all of our models.

There is still much work to be done in the future. We consider accretion disc around magnetised star, by including effects of mass loss from the disc to funnel flow onto the star and/ or to make a slim disc model that includes the effects of advection, radial pressure gradients, and a deviations from Keplerian rotation; or rather involve.

We also consider the time-dependent accretion disc theory further to develop a numerical code for studying the nonlinear time evolution of the accretors to see whether or the model can reproduce the observed behaviours of disc-accreting X-ray pulsars. A more detail model of viscosity is needed particularly strongly. Such a model must await a better understanding of turbulence and chaotic magnetic field.

Bibliography

Abramowicz, M. A., Czerny, B., Lasota, J. P., & Szuszkiewicz, E. 1988, ApJ, 332, 646

Alpar M.A., et al. 1982, Nat., 300, 728

Aly, J.J., 1986, A & A, 143, 19

Anzer U. and Börner G., 1980, ApJ, 83, 133

Arson et al. 1984, in Highe Energy Transients in Astrophysics (AIP conf. Proc. 115) ed. S. Wooselley,215

Balbus S. A., & Hawley J. F. 1991, ApJ, 376, 214

Balbus S. A., & Hawley J. F. 1995, ApJ, 467, 76

Balbus S.A., & Hawley J. F., Rev. of modern Physics, 1998.

Bardou, A., and Heyvaerts, J. 1996, A&A, 307, 1009

Bath, G. T., 1973, Nat. Phys. Sci., 246, 84

Bildsten, L., Chakrabarty, D., Chiu, J., et al. 1997, ApJS, 113, 367

Bildsten, L., Chakrabarty, D., Chiu,J.,Finger, M.H., and Nelson,R.W., 1997, ApJ. 481. L101

Brandenburg, A., Nordlund, A.A ., Stein, R. F. and Torkelsson U., 1995, ApJ, 446, 741

Brandenburg, A., and Campbell C.G., 1998, MNRAS, 298, 223

Burderi,L.,Di Salvo,T., Menna.M.T, Riggio, A., & Papitto A., 2006, ApJ, 653, L133

Burderi et al., 2007, ApJ, 657, 961

Campbell, C. G., 1997, Magnetohydrodynamics in binary stars, Kluwer, Dordrecht

Campbell, C.G., 1998, MNRAS, 301, 754

Campell C.G.,Heptinstall P.M.,1998,MNRAS.

Campbell, C.G., and Heptinstall P.M., 1998b, MNRAS,299, 301

Campbell, C.G., and Heptinstall, P.M., 1998, MNRAS, 299, 31 & MNRAS, 301, 558

Chadrasekhar, 1961, Proc. Nat. Acad. Sci. 46, 253

Chakrabarty,D., & Morgan, E.H., 1998, Nature, 394, 346

Chapman,S., and Cowling, T.G., 1939. The Mathematical Theory of Nonuniform Gases,

Cambridge, Univ. Press

Crawford and Kraft, 1956

Erkut, M., and Alpar, M., 2004, ApJ, 617, 461

Falanga et al., 2005, A& A, 444, 15

Frank, J., King A.R., & Raine D. 2002, Accretion power in astrophysics, Cambridge University Press

Ghosh P. Lamb F.K.,1978, ApJ,223,L83- L87

Ghosh P. Lamb F.K.,1979a, ApJ,232,259

Ghosh P. Lamb F.K.,1979b, ApJ,234,296

Ghosh, P., and Lamb, F.K.,1979, ApJ,232, 259 & ApJ, 234, 296

Giacconi, R., et al. 1971, ApJ, 167, L67.

Hartman, J. M. et al. 2008, ApJ, 675, 1468

Hawley, J. F., Gammie, C. F. & Balbus, S. A., 1995, ApJ. 440, 742

Honma, Matsumoto and Kato, 1991

Hoshi, R., 1984, PASJ. 36, 785

Illarionov, A. F., and, Sunyaev, R. A., 1975,A& A, 39, 185

Katos et al, MNRAS, 1988,231,37

King, A. R. 2000, MNRAS, 315, L33

Kuiper G.P., 1939, ApJ, 89, 548 ; 91, 269, and 1940, 92, 126, reference there.

Königl 1991

Landau, L.D., Lifshitz, E.M., 1959. Fluid Mechanics. Pergamon Press, New York.

Landau, L.D., Lifshitz, E.M., 1987. Fluid Mechanics. Pergamon Press, New York.

Li J., Wickramasighe D.T., Rüdiger G.,1997, MNRAST Lett.,286,L85

Li J., Wickramasighe D.T., Rüdiger G.,1998, Lightman, A. P., and Eardley, D. M., 1974, ApJ, 187,L1

Lynde-Bell, 1969, Nature 223, 690.

Lynde-Bell D., & Pringle, J.E., 1974, MNRAS, 168, 6030.

Markwardt C.B, 2003,BAAS, 35, 657

Matthews, O.M., Speith, R., and Wynn, G.A., 2004, MNRAS, 356, 66

Mayer M.and Wolfgang J. Duschl,2005, Mon.Not.R. Astron.Soc. 356, 1.

Miller, M.C., Lamb,F.K., & Psaltis,D., 1998, ApJ, 508, 791

Morgan et al., 2003,BAAS, 35, 629

Nagase, F., 1989, PASJ, 41,1

Nelson R. W., et al., 1997, ApJ, 488, L117

Ostriker and Shu 1995

Paczyński, B. and Bisnovatyi-Kogan, G. 1981,Acta Astron., 31, 283

Parmar, A. N., White, N. E., Stella, L., Izzo, C., Ferri, P., 1989, ApJ, 338, 359

Piran T., Astrophys. J. 221 (1978) 652.

Popham R.and Sunyaev R.A,2001,ApJ,547,355-383

Popham, R., & Narayan, R. 1992, ApJ, 394, 255

Pringle J.E., Rees M.J., Pacholoczyk, A.G., 1973, Astr. Astrophys. 29, 179

Pringle J.E., 1976, MNRAS. 177, 65

Psaltis,D.,& Chakrabarty, D., 1999, ApJ, 521, 332

Radhakrishnan V., and Srinivasan G., 1982. On the origin of the recently discovered ultra-rapid pulsar-current science 51, 1096.

Rappaport S.A., Fregeau J.M., & Spruit H., 2004, ApJ, 606, 436

Santo, T., et al. 2004, ApJ, 605,321

Scharlemann, E.T.: 1998,APJ, 219,617

Sean Matt, and Ralph E. Pudritz, 2005,Mon.Not.R. Astron.Soc. 356, 167- 182.

Shadmehri M., 2004, ApJ, 612,1000-1005

Shakura N.I.,Sunyaev R.A., 1973, A and A,24,337

Shakura N.I., & Sunyaev R.A., 1976, MNRAS, 175, 613

Shapirio S.L., et al. 1976, Astrophys. J 204, 187

Shibazaki,N., and Hoshbi, R. 1975, Prog. Theor.Phys. 54, 706

Soward, A. M. 1992, GAFD, 64, 163

Spitzer L., 1962, Physics of Fully Ionized Gases, Second ed, New York, Interscience

Spruit, H., & Taam, R. E. 1993, ApJ, 402, 593

Svensson R., and Zdziarski, A.A., 1994, ApJ, 436, 599

Szuskiiiewicz and Mill 1997

Taam, R.E.,& Lin D.N.C., 1984, ApJ, 287,76

Tauris T.M., & van den Heuvel E.P.J., 2006, In compact stellar X-ray sources, 623, New York, Combridge University Press

Tessema, S.B., & Torkelsson, U., 2010, A& A, 509, A45

Tessema, Solomon., & Torkelsson, U., 2010, MNRAS, submitted

Tessema, Solomon., & Torkelsson, U., 2010, in preparation for submission to the Mon. Not.R.Astron.Soc. Journal.

Tjemkes S.A.et al. 1986, A & A,154,77

Tokelsson U., Brandenburg A.,1994a, A & A,283,677

Tokelsson U., Brandenburg A.,1994b,A & A,292,341

Torkelsson U.,, Mon.Not.R.Astro.Soc, 1998

Tout, C.A., and Pringle, J.E., 1992, MNRAS, 259,599

Truss M.R.,Wynn G.A.,Murray J.R. and King A.R,2002, Mon.Not.R. Astron.Soc. 337, 1329-1339.

Van Kerkwijk, M.H., Chakrabarty, D & Pringle J.E., et al. 1998, 499, L27

Valdimir M. Lipunov, Astrophysics of Neutron stars,1992.

Velikhov, E.P., J.Exp. Theoret.Phys., 36, 1398 Yi I.,Wheel J.C., and Vishniac E.T.,1997, ApJ, 481,L51

YI, I., & Wheeler, J.C., 1998, ApJ., 498, 802

Wang, Y.M., 1987, ApJ, 183, 257

Wang, Y.M., 1995, ApJ, 449, L153

Wang, Y.M., 1997, ApJ, 487, L85

Warner, 1990

White, N.E., & Stella,L., 1988,MNRAS, 231, 325

Wijnands,R., & van der Klis, M., 1998, Nature, 394, 344

Wijnands, R., 2004, Nucl. Phys. B Proc. Suppl., 132, 496

Chapter 7

Appendix

7.1 Tensor T

$$\sigma_{\imath k} = 2\eta T_{\imath k} + \eta_B \frac{\partial v_\ell}{\partial x_\ell}\delta_{\imath k},$$
$$T_{\imath k} = \frac{1}{2}\Big(\frac{\partial v_\imath}{\partial x_k} + \frac{\partial v_k}{\partial x_\imath} - \frac{2}{3}\frac{\partial v_\ell}{\partial x_\ell}\delta_{\imath k}\Big). \tag{7.1}$$

7.2 Transformation of cylindrical coordinates

$$\mathbf{A} = \begin{pmatrix} A_{RR} & A_{R\phi} & A_{rz} \\ A_{\phi R} & A_{\phi\phi} & A_{\phi z} \\ A_{zr} & A_{z\phi} & A_{zz} \end{pmatrix} \tag{7.2}$$

The gradient of a scalar is defined as

$$\nabla A = \left(\frac{\partial A}{\partial R}, \frac{1}{R}\frac{\partial A}{\partial \phi}, \frac{\partial A}{\partial z}\right). \tag{7.3}$$

and also the divergence a vector is:

$$\nabla.\mathbf{A} = \frac{1}{R}\frac{\partial (RA)}{\partial r} + \frac{1}{R}\frac{\partial A_\phi}{\partial \phi} + \frac{\partial A_z}{\partial z}. \tag{7.4}$$

The curl of a vector is defined as follows:

$$\nabla \times \mathbf{A} = \left(\frac{1}{R}\frac{\partial A_z}{\partial \phi} - \frac{\partial A_\phi}{\partial z}, \frac{\partial A_R}{\partial z} - \frac{\partial A_z}{\partial r}, \frac{\partial A_\phi}{\partial R} + \frac{A_\phi}{R} - \frac{1}{R}\frac{\partial A_R}{\partial \phi}\right). \tag{7.5}$$

The gradient of a vector is:

$$\nabla \mathbf{A} = \begin{pmatrix} \frac{\partial A_R}{\partial R} & \frac{\partial A_\phi}{\partial r} & \frac{\partial A_z}{\partial z} \\ \frac{1}{R}\frac{\partial A_R}{\partial \phi} - \frac{A_\phi}{R} & \frac{1}{R}\frac{\partial A_\phi}{\partial \phi} + \frac{A_R}{R} & \frac{1}{R}\frac{\partial A_z}{\partial \phi} \\ \frac{\partial A_R}{\partial z} & \frac{\partial A_\phi}{\partial z} & \frac{\partial A_z}{\partial z} \end{pmatrix}. \tag{7.6}$$

The divergence of a tensor is:

$$\nabla . \mathbf{A} = \begin{bmatrix} \frac{\partial A_{RR}}{\partial R} + & \frac{1}{R}\frac{\partial A_{\phi r}}{\partial \phi} + & \frac{\partial A_{zR}}{\partial z} + & \frac{A_{RR} - A_{\phi\phi}}{R} \\ \frac{\partial A_{R\phi}}{\partial R} + & \frac{1}{R}\frac{\partial A_{\phi\phi}}{\partial \phi} + & \frac{\partial A_{z\phi}}{\partial z} + & \frac{A_{R\phi} + A_\phi R}{R} \\ \frac{\partial A_{Rz}}{R} + & \frac{1}{R}\frac{\partial A_{\phi z}}{\phi} + & \frac{\partial A_{zz}}{\partial z} + & \frac{A_{Rz}}{R} \end{bmatrix} \tag{7.7}$$

The Laplacian of a scalar is:

$$\begin{aligned} \nabla^{\mathbf{2}} \mathbf{A} &\equiv (\nabla . \nabla) A \\ &= \frac{\partial^2 A}{\partial R^2} + \frac{1}{R}\frac{\partial A}{\partial R} + \frac{1}{R^2}\frac{\partial^2 A}{\partial \phi^2} + \frac{\partial^2 A}{\partial Z^2}. \end{aligned} \tag{7.8}$$

The Laplacian of a vector is:

$$\nabla^{\mathbf{2}} \mathbf{A} \equiv (\nabla . \nabla) A = \begin{bmatrix} \frac{\partial^2 A_R}{\partial R^2} + \frac{1}{R}\frac{\partial A_R}{\partial R} - \frac{A_R}{R^2} + & \frac{1}{R^2}\frac{\partial^2 A_R}{\partial \phi^2} - & \frac{2}{R^2}\frac{\partial A_\phi}{\partial \phi} + \frac{\partial^2 A_R}{\partial z^2} \\ \frac{\partial^2 A_\phi}{\partial R^2} + \frac{1}{R}\frac{\partial A_\phi}{\partial R} - \frac{A_\phi}{R^2} + & \frac{1}{R^2}\frac{\partial^2 A_\phi}{\partial \phi^2} + \frac{2}{R^2}\frac{\partial A_R}{\partial \phi} + & \frac{\partial^2 A_\phi}{\partial z^2} \\ \frac{\partial^2 A_z}{\partial R^2} + \frac{1}{R}\frac{\partial A_z}{\partial R} + & \frac{1}{R^2}\frac{\partial^2 A_z}{\partial \phi^2} + & \frac{\partial^2 A_z}{\partial z^2} \end{bmatrix}. \tag{7.9}$$

7.3 For axisymmetric disc the expression for the Lorenz force acting on the disc

$$\begin{aligned} \mathbf{J} \times \mathbf{B} = &\left[\frac{B_z}{\mu_0}\left(\frac{\partial B_R}{\partial z} - \frac{\partial B_z}{\partial R}\right) - \frac{B_\phi}{\mu_0}\left(\frac{1}{R}\frac{\partial}{\partial R}(RB_\phi)\right)\right]\mathbf{R} \\ &+ \left[\frac{B_R}{\mu_0}\frac{1}{R}\frac{\partial}{\partial R}(RB_\phi) + \frac{B_z}{\mu_0}\frac{\partial B_\phi}{\partial z}\right]\phi \\ &\left[-\frac{B_\phi}{\mu_0}\frac{\partial B_\phi}{\partial z} - \frac{B_R}{\mu_0}\frac{\partial B_R}{\partial z} + \frac{B_R}{\mu_0}\frac{\partial B_z}{\partial R}\right]\mathbf{z} \end{aligned} \tag{7.10}$$

7.4 Summary of Papers

Paper I

In Paper I, we make the first comprehensive study of the interaction between a magnetic neutron star and its surrounding accretion disc in the case where the accretion disc is supporting an internal dynamo and we work in the spirit of Shakura & Sunyaev (1973) and assume that the disc is geometrically thin and develop a model for such accretion discs around magnetised star . We determine the steady-state of an axisymmetric thin accretion disc with an internal dynamo around a magnetised star. Starting from the vertically integrated equations of magnetohydrodynamics we derive a single ordinary differential equation for a thin accretion disc around a massive magnetic dipole and integrate this equation numerically from the outside inwards. Our global numerical solution shows that the torque between the star and the accretion disc is dominated by the contribution from the dynamo in the disc. The location of the inner edge of the accretion disc varies between R_A and $10R_A$ depending mainly on the strength and direction of the magnetic field generated by the dynamo in the disc. A self-similar solution for the structure of the accretion disc around magnetised stars is calculated.

Paper II

The purpose of Paper II is a continuation of paper I of an accretion disc with an internal dynamo around a magnetised star to the discs around millisecond pulsars. In the spirit of Shakura & Sunyaev (1973, 1976) we divide the disc into an outer region with gas pressure and free-free opacity, a middle region with gas pressure and electron scattering opacity, and an inner region with radiation pressure and electron scattering. Millisecond x-ray pulsars have weak magnetic dipole moments compared to ordinary X-ray pulsars. For this reason a surrounding accretion disc can extend closer to the neutron star, and thus reach a higher temperature, at which the opacity is dominated by electron scattering and radiation pressure is strong. Starting from the vertically integrated equations of magnetohydrodynamics we find the global numerical solution for the three regions of the disc taking different values of accretion rate. We compute the self-similar structure of such a geometrically thin axisymmetric accretion disc with an internal dynamo for three regions of the disc. Such models indicates that significantly stronger torques on the neutron star can produce than models without dynamos, and can explain the strong spin

variations in some millisecond X-ray pulsars.

Paper III

In Paper I it is noted that we study the accretion disc around magnetised stars in steady state. In addition, we find the global numerical solution to the location of the inner edge of the accretion disc, the total torque produced in such disc and the self-similar solution of the structure of the disc. In Paper III, we study the time-dependent behaviour of accretion disc around magnetised stars in general by means of analytical techniques for steady state and non-steady state discs by linearizing nonlinear equations considering the small perturbation of the surface density and analyzing the stability conditions. We find that the stability properties of accretion disc around magnetized star for gas pressure dominated and radiation pressure dominated disc and timescale analysis for our model. According to our model the thin disc model resulting from the generation of the magnetic field generated by the internal dynamo is stable in the gas pressure dominated disc region and unstable in the radiation pressure dominated disc. The presence of magnetic field due to an internal dynamo makes the disc more stable in the gas pressure dominated region.

Declaration

I hereby declare that the investigation presented in this dissertation titled "Accretion Discs around Magnetized Stars, in particular Neutron Stars" is entirely original and has been carried out by me independently in the department of Physics Addis Ababa university in collaboration with department of Physics University of Gothenburg, Sweden, under the supervision of Dr. Ulf Torkelsson, department of Physics, University of Gothenburg, Sweden, this dissertation has not be reported either in published form in a journal or in a thesis by anyone (other than me), to the best of my knowledge. I further declare that this dissertation has not been considered by any University or institute, for the award of a degree, diploma, associateship or fellowship whatsoever.

Solomon Belay Tessema(PhD Candidate)————————————————

This PhD dissertation has been submitted for examination with my approval as University supervisor

Ulf Torkelsson (Research Supervisor)————————————————

Place : Department of Physics Addis Ababa University, February 2010.